



# **RPG-MWSC-160**

## **Microwave Scintillometer**

### **Operation & Software Guide**

Version 2.11





## Document Change Log

Date	Issue/Rev	Change
17.03.2014	00/01	Work
03.07.2014	00/02	Work (Technical Description and Installation added)
23.07.2014	01/00	Release
12.01.2015	01/01	Update: installation chapter, saturation correction
20.05.2015	01/02	Update: Sections: 2.1, 2.2 (back panel), 4.3 (coordinates), 3.3.4 (power level display), 5.4.1 (text log variances)
16.01.2016	01/03	Update Section 3.3.4 (display + alignment)
24.02.2016	01/04	Addition of RAW file storage and ASCII conversion
14.06.2016	01/05	- Update recommendation signal level (Section 3.3) - Update Section 4.3 (setup): RAW file storage on Host-PC - Update Section 5.4 (data processing), incl. corr. formula
11.10.2016	01/06	- Section 4.8: Add description of Postprocessor Settings - Section 5.4.6: Add zero displacement height - Section 5.4.7: Def. wind speed height as separate param.
11.09.2017	01/07	- Section 5.4.1: corrected formula (9)-(11) – $\ln(I/I_0)$
11.11.2017	01/20	Splitting installation guide from instrument manual
31.01.2018	01/21	Update including photos/fuses/labeling/editorial changes
28.02.2018	01/30	- Section 3.3: Introduction of separate running mean periods for LAS and MWS (Auto-Mode), adjusted to path length and effective height - Section 3.8: Added description of post processor extension with full parameter control. - Appendix: Introduction of FLX file version 2, containing LAS / MWS saturation flags and evapo-transpiration - Introduction of measurement start trigger time grid
14.05.2018	02/00	- Section 3.3: Adapted instrument list (+X-LAS) and re-arranged data file description - Section 3.4: Added description of archiving with local time shift and data storage on external USB-stick - Section 3.7: Re-arranged text, added new screenshots, added foot note on Hill method, introduced evapo-transpiration display - Section 3.13: Included SW restart in update process
31.03.2020	02/10	- Section 3.2: Updated to new TCP/IP interface - Section 3.3: Re-arranged and updated - Section 3.3.1: updated Data Storage Options - Section 3.3.2: added Automatic Gain Control
25.08.2020	02/11	- Section 3.12: changed e-mail address for license inquiries



## Table of Contents

RPG-MWSC-160.....	1
Microwave Scintillometer .....	1
Operation & Software Guide .....	1
Document Change Log .....	2
1. Scope of this Document .....	4
2. Technical Description .....	4
3. Software Description .....	6
3.1 Installation of Host Software .....	6
3.1.1 Hardware Requirements for Host-PC .....	6
3.1.2 Directories .....	6
3.2 Getting Started.....	8
3.2.1 Interfacing via Ethernet.....	9
3.3 Configuration .....	14
3.3.1 Measurement Setup .....	14
3.3.2 Automatic Gain Control .....	19
3.3.3 Spectral Filters & Weighting Functions .....	21
3.3.4 LAS Saturation Check .....	24
3.4 Data Storage Configuration .....	25
3.5 Exchanging Data Files.....	26
3.6 Starting Measurements .....	28
3.7 The Data Processing Chain.....	29
3.8 Data Post Processing .....	32
3.9 Inspecting Data Files .....	34
3.10 Transform Data Files to ASCII Format .....	35
3.11 File Concatenation.....	36
3.12 The License Manager .....	37
3.13 Software Updates .....	38
3.14 Automatic E-Mail Warning Messages .....	39
3.15 Changing the Application Size on the Screen .....	41
3.16 Shutting Down the Scintillometer PC .....	41
4. Scientific Background.....	42
4.1 Turbulent Fluxes in the Surface Layer .....	42
4.2 The Scintillation Signal .....	44
4.3 Sensible and Latent Heat Fluxes from Scintillometry.....	46
4.4 The Data Processing Chain.....	47
4.4.1 From Signal Variances to Structure Parameters.....	48
4.4.2 Structure Parameters of Temperature and Humidity .....	52
4.4.3 MOST– from Structure Parameters to Heat Fluxes .....	53
4.4.4 Signal Saturation .....	56
4.4.5 Absorption Fluctuations .....	57
4.4.6 Effective Height.....	57
4.4.7 Roughness Length and Zero-Displacement Height .....	58
4.4.8 References .....	60
5. Appendix A (File Formats) .....	62
5.1 A1a: Heat Flux Files (*.FLX), Version 1 .....	62
5.2 A1b: Heat Flux Files (*.FLX), Version 2 .....	63
5.3 A2: Variance-Files (*.VAR) .....	65
5.4 A3: Raw Data Files (*.RAW).....	67
5.5 A4: Housekeeping Data Files (*.HKD) .....	68
6. Appendix B (Instrument Dimensions) .....	70



## 1. Scope of this Document

This document contains:

- A description of scientific background of scintillometry and deduction of the equations used in the instrument software to calculate sensible heat and latent heat fluxes
- A technical description of the RPG-MWSC-160 with details about its principle of operation
- A Complete software description with details on data formats (binary).

For detailed information on installation and maintenance of the RPG-MWSC-160 and combined optical LAS systems please refer to the *RPG-MWSC-160 Installation Manual*.

## 2. Technical Description

The MicroWave Scintillometer (MWS) RPG-MWSC-160 consists of a receiver and transmitter. It is combined with a Large Aperture Scintillometer (LAS) observing in the near infrared spectral region. Any commercially available LAS can be used. The combined system includes two transmitters and two receivers and is henceforth called OMS (Optical/Microwave Scintillometer). This chapter describes the MWS units only. For technical information on the LAS system please refer to the manufacturer's manual.

Parameter	Specification
Frequency	160.8 GHz ( $\lambda=1.86$ mm)
Radiated power	maximum power: < 25 mW, 50 dB attenuator
Antenna type	Cassegrain with 300 mm aperture
Antenna gain	52 dB
Beam width	0.45° FWHM
Detection bandwidth	10 kHz
Gain stability	$> 2.0 \times 10^{-5}$
Temperature stability	< 0.03 K (two-stage control)
Power supply	10.8-13.2 V DC
Power consumption	max. 60 W (per unit), 20 W typical (RX), 15 W typical (TX)
Output data	Level 0 <ul style="list-style-type: none"> <li>• 1 kHz digital raw data for RPG-MWSC-160 and LAS</li> <li>• housekeeping data.</li> </ul>
	Level 1 <ul style="list-style-type: none"> <li>• (co)variances of the combined OMS system.</li> </ul>
	Level 2 <ul style="list-style-type: none"> <li>• structure parameters <math>C_n^2</math></li> <li>• sensible and latent heat fluxes <math>H, L_v E</math> (with weather station)</li> </ul>
Type of installation	Line of sight TX/RX system (transmit/receive)
Baseline length	500 m to 10 km

The RPG-MWSC-160 transmitter signal originates from an RF source at 13.4 GHz. The signal is multiplied to 160.8 GHz and fed to a horn antenna. Cassegrain optics with a 300 mm main reflector form a beam with a Half Power Beam Width (HPBW) of 0.45°. After travelling through the atmosphere over a path length of up to 10 km, the signal reaches the antenna of the receiver unit. Behind the feed horn the received signal enters a sub-harmonic mixer. Here, the signal is mixed with a Local Oscillator (LO) signal that is multiplied to 79.8 GHz. The resulting Intermediate Frequency (IF) of 1200 MHz is then boosted by +20dB before it enters the detector diode (Figure 1). The signal is synchronously digitized with the analogue LAS signal and fed to the Scintillometer-PC (SP-C). The S-PC offers an Ethernet interface to set up a connection with an external Host-PC (H-PC). The H-PC is used to operate the combined OMS system:

- Measurement, setup and configuration.
- Complete data processing from digitized raw data to sensible and latent heat fluxes.
- Archiving of all data formats (see Appendix).

Once a measurement has been initialized via the H-PC, the scintillometer can be disconnected and work autonomously. Additionally, Level 1 data (signal variances, housekeeping data) and Level 2 data (e.g. heat fluxes) can be stored on the S-PC<sup>1</sup>. These data can be downloaded to the H-PC at a later stage (Section Exchanging Data Files) to reprocess all available data products (Section Fehler! Verweisquelle konnte nicht gefunden werden.). Due to the large data volume, raw data can only be stored on the H-PC.

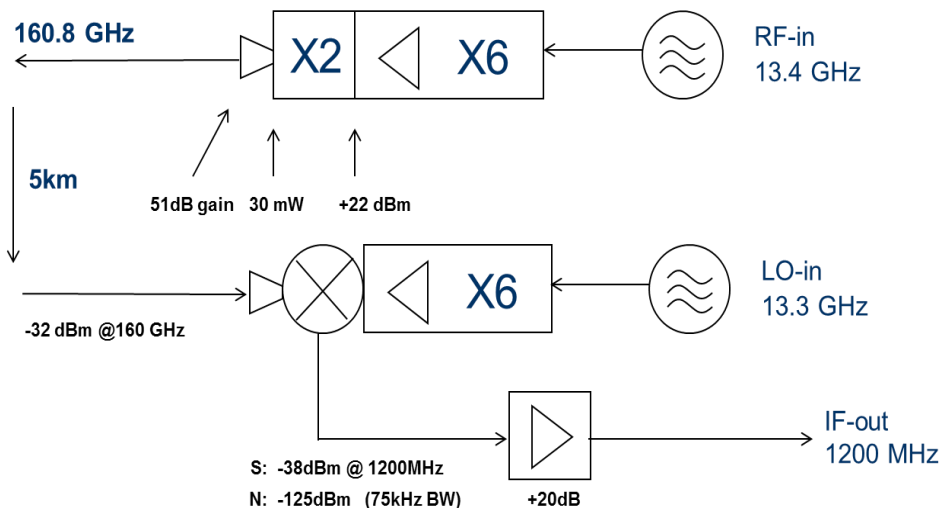


**Figure 1: Technical scheme of the RPG-MWSC-160.**

<sup>1</sup> Instruments with serial numbers 3010001-3010027 only allow the storage of Level 1 and level 2 data on the S-PC.

### 3. Software Description

The following text colour conventions are used in this software description:

- Button labels are printed in green. Example: **Cancel**
- Messages that must be answered by **Yes** or **No** are printed in light blue. Example: **Overwrite the existing file?**
- Labels are printed in grey: **UTC**
- Names of group boxes are printed in blue. Example: **Setup Handling** (in Configuration → Measurement Setup)
- Names of tabs are printed in violet. Example: **Configuration**
- Names of menus are printed in black. Example: **Configure TCP/IP Settings**
- Labels of Entry-Boxes are printed in light blue. Example: **yTL**
- When a speed button shall be clicked, this is indicated by its symbol. E.g.: 
- Hints to speed buttons are printed in brown. Example: **License Manager**
- Selections from list boxes are printed in magenta. Example: **Wageningen LAS**
- Selections from radio buttons or check boxes are printed in dark green. Example: **Raw Data (\*.RAW)**
- File names are printed in orange. Example: **MyFileName**
- Directory names are printed in dark blue. Example: **C:\RPG-MWSC\**

#### 3.1 Installation of Host Software

##### 3.1.1 Hardware Requirements for Host-PC

The hardware requirements for running the Host-PC (H-PC) software **MWSC-EXE** are the following:

- Windows® 7 operating system or higher
- 200 MB of free RAM for software execution
- LAN interface for communicating with the microwave scintillometer (MWS)
- Fibre Optics-to-LAN Converter (part of MWS delivery)

##### 3.1.2 Directories

The H- PC software can be installed in any directory and on any partition or drive. Once started, **MWSC-EXE** will automatically create sub-directories under the selected root-directory. Let us assume, this root directory is **D:\MyProgs\RPG-MWSC\**. In this case, the directory tree looks like this:

```
D:\MyProgs\RPG-MWSC
  \CONFIG
    \MCF
  \DATA
    \FILE_TRANS
    \QUICKLOOKS
  \HELP
  \LICENSE
  \LOG
  \SCINTILLOMETER PC
  \TEMP
  \TRANSLATION
```



The **RPG-MWSC**-directory contains (at least) the following files:

- **MWSC.EXE** : H-PC scintillometer software
- **NETCDF.DLL** : Dynamic link library, netCDF file format routines

These files are dynamically linked to **MWSC.EXE** during program start. If one of them is missing, the software will ask for it when started and terminate execution.

...\bCONFIG\b Here the SW stores its general configuration file **MWSC.CFG** (this is created by clicking  or when exiting the program) and the **MainFormSize.DAT** file which holds information about the current size of the application (selected by .

...\bCONFIGMCF\b Directory for storing measurement setups (Measurement Configuration File).

...\bDATA\b Suggested directory for data file storage. This directory may have any other name or may be located on a different drive. It also holds the archiving tree, if file archiving option is enabled.

...\bDATAFILE\_TRANS\b Includes data from the Automatic and User Initiated File Transfer from the S-PC to the H-PC.

...\bDATA\QUICKLOOKS\b Suggested directory for JPG or BMP quick-look graphics files.

...\bHELP\b Location for online help files. These will be included in future releases.

...\bLICENSE\b Location for license ID files. Please refer to section 'License File Manager'.

...\bLOG\b Log directory for the file access error file **FileAccessErrors.LOG**, the communication error file **CommErr.LOG**, and the TCP/IP scanning file **Get\_IP.LOG**.

...\bSCINTILOMETER\_PC\b Contains copied files from scintillometer PC.

...\bTEMP\b Directory for temporary files (for internal use only).

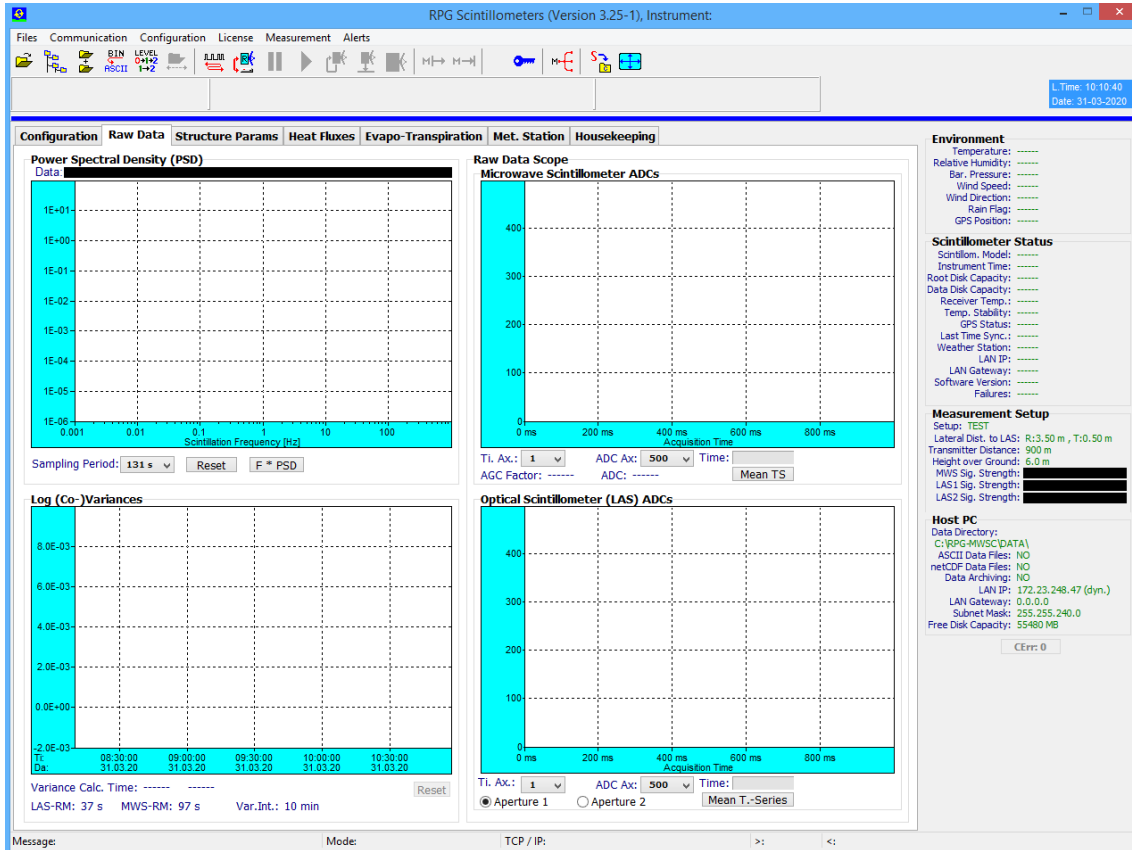
...\bTRANSLATION\b Optional translation files for adapting application to foreign languages.

On delivery, the complete installation folder is copied to a memory stick. The software can be installed by simply copying the installation folder to a PC (that fulfils the requirements described in 4.1.1) and creating a short-cut to **MWSC.EXE** for the desktop.

**Please note that the **MWSC.EXE** requires an execution as administrator (right click on executable > Properties > Compatibility > Run as administrator) in order to change system time (for GPS synchronization) and change IP settings.**

### 3.2 Getting Started

When starting the application **MWSC.EXE** (  ), the screen looks like this:



It is subdivided into different areas:

- A row of shortcut buttons on the top of the screen, allowing for a quick access to all software menus
- Another row of empty message boxes below the shortcut button row
- The graphical data display area arranged into pages with the selection tags **Configuration**, **Raw Data**, **Structure Parameters**, **Heat Fluxes**, **Surface Sensors** and **Housekeeping Data**.
- A status display on the right showing continuous information about the **Environment**, **Receiver Status**, **Measurement Status** and **Host PC**.

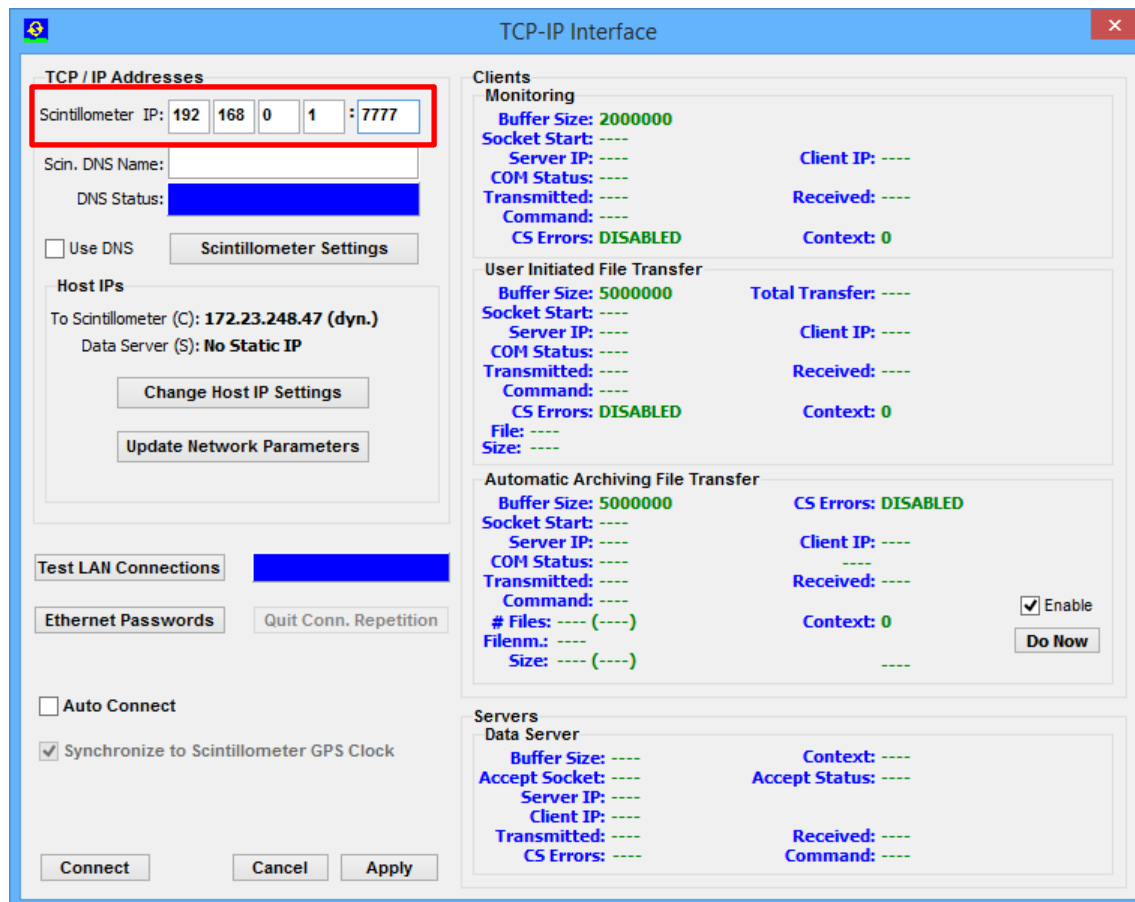
In order to run a measurement, two steps need to be taken in advance. The user must first define a measurement setup and then establish a connection to the MWS. Details about setup definitions are given in a later chapter. We first like to focus on how to connect to the embedded S-PC inside the scintillometer.

### 3.2.1 Interfacing via Ethernet

#### 3.2.1.1 Setting up IPs

The RPG-MWSC-160 scintillometer model communicates via a LAN (Ethernet) interface.

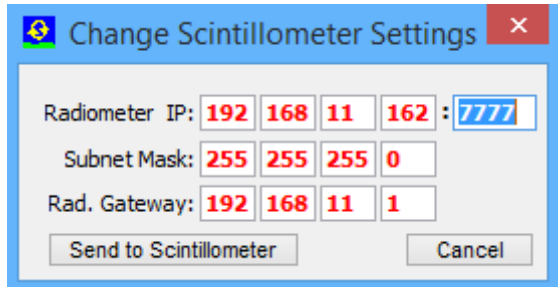
In order to establish a connection to the instrument, the user clicks on  to select the **TCP-IP Interface** menu. The configuration entry looks like this:



The Scintillometer PC (S-PC) is delivered with a fixed default IP address (default: 192.168.0.1, port no.:7777) which can be altered later. For a first connection the user needs to enter this IP to the edit fields right to **Scintillometer IP:** (see red box above). The scintillometer Gateway is set to the same address as the scintillometer IP, which is required for a 'peer-to-peer' connection between the S-PC and the H-PC. A peer-to-peer connection is an Ethernet connection between two PCs without using a network in between.

**In order to set up a peer-to-peer connection, the H-PC must have a fixed IP address as well and its gateway set to the same IP address.**

Once you are connected you may also change the scintillometer IP and gateway, e.g. when the scintillometer shall be connected to a network. For this purpose click on **Scintillometer Settings** (a new menu pops up) and edit the fields to the desired numbers:



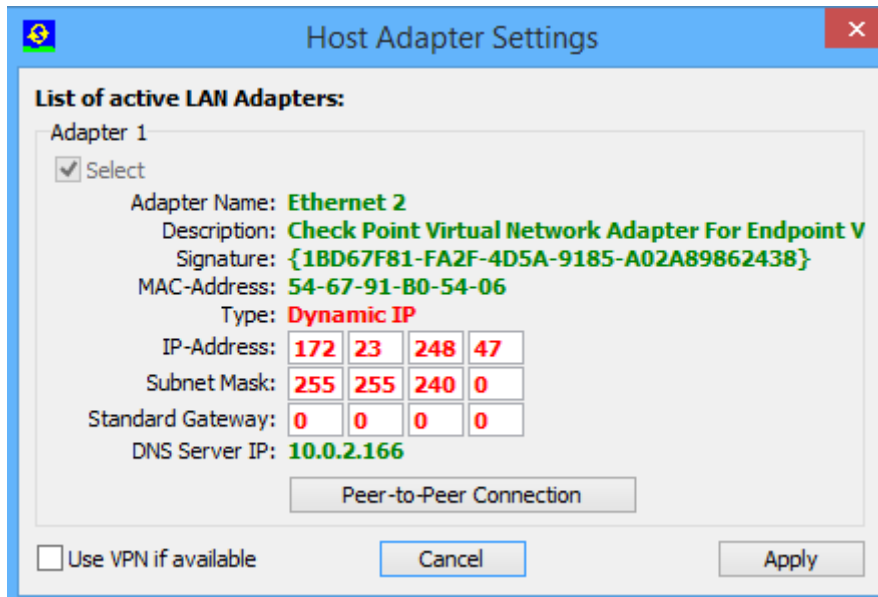
**The S-PC does not have anti malware programs installed. Please make sure to protect the S-PC, when connected to a network with internet access.**

The red IP/gateway settings are sent to the S-PC by clicking **Send to Scintillometer**. After new IPs have been successfully sent to the S-PC, it will be no longer reachable through the old IP / gateway addresses. In the case of a successful transfer of the new IP/gateway to the scintillometer, the new IP is copied to the current IP fields automatically so that the H-PC can continue its connection to the scintillometer. In case the check box is active **Auto Connect**, the H-PC will automatically re-connect to the S-PC. Otherwise, click **Connect**.

You may test the connection with **Test LAN Connections**. The H-PC will then try to get access to the S-PC via the specified IP address. If the connection is successful, 'OK' is indicated in the blue panel, otherwise 'No Connection'.

#### Example:

Consider a newly delivered scintillometer with initial IP of 192.168.0.1, gateway of 192.168.0.1 and with port address 7777. With this IP configuration the scintillometer cannot be successfully connected to a network. In order to connect to it directly in a peer-to-peer connection, the MWS communication cable must be connected **DIRECTLY** (not via a network) to the Ethernet connector of the H-PC. Without limitation of generality, let us assume the H-PC IP to be 192.168.12.27. In order to tell the H-PC to directly listen to the LAN interface (NOT via a network gateway), its gateway should also be set to 192.168.12.27 to enable a peer-to-peer connection. In order to modify the H-PC settings, click on the **Change Host IP Settings** button and the following menu shows up (with possibly different settings):



For establishing a peer-to-peer connection, select an available Ethernet Adapter and click the **Peer-to-Peer Connection** button. The gateway address will be copied from the H-PC IP address. Then click **Apply** and the H-PC will be ready to connect to the scintillometer.

Let us now assume, the user's administrator wants to connect the scintillometer to a network with the following network settings:

IP: 160.144.13.104  
Standard Gateway: 160.144.11.1  
Port Address: 6565

The way to send this new configuration to the S-PC is the following:

1. Click on **Scintillometer Settings** and edit the fields for the new scintillometer IP and scintillometer gateway and port number.

2. Then click on **Send to Scintillometer**. The settings in red are now transferred to the S-PC. If the scintillometer has successfully changed its IP / gateway / port settings, a confirmation message is displayed. After the IP / gateway / port numbers have been altered on the scintillometer, it is not possible to connect to it anymore through a peer-to-peer connection. Therefore, connect the scintillometer's communication line to the network.

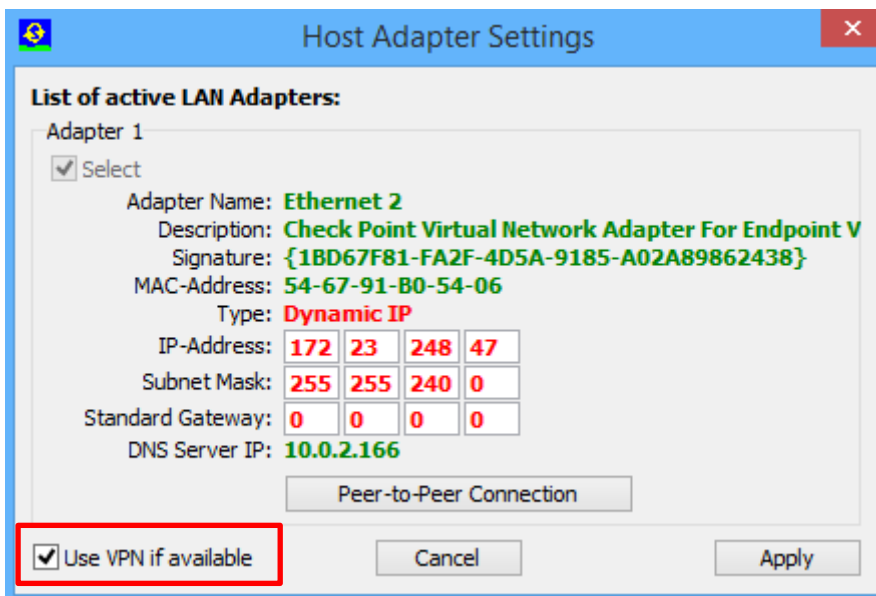
3. Let us assume, the user's administrator has reserved the following network settings for the H-PC:

IP: 160.144.13.201  
Standard Gateway: 160.144.11.1

Modify the H-PC TCP/IP settings by clicking **Change Host IP setting** and enter the new settings. Confirm your changes with **Apply**. The H-PC then needs to be connected to the network as well. Now both, the S-PC and the H-PC, are properly connected to the network with specific unique addresses and a connection between the two can be established over the network by clicking **Connect**. Click **Apply** in the **TCP-IP Interface** menu to save the new settings.

### 3.2.1.2 VPN Connections

If the H-PC is located far from the local network to which the radiometer is connected, the H-PC is typically using a VPN (Virtual Private Network) connection to the local network. This VPN connection is acting as a virtual adapter on the H-PC and can be inspected in the **Host Adapter Settings** menu (click **Change Host IP setting**).



If you are not familiar of how to set up a VPN connection to a local network on your H-PC, please contact your network administrator.

The VPN service must be started on the H-PC before it can be detected by the host SW. When checking the **Use VPN if available** box, you can ensure that the H-PC will always prefer the VPN connection over other active adapters on the system. For a long-term installation the VPN connection should be configured with re-dial option for the case that the VPN connection is interrupted. The H-PC will then automatically reconnect to the scintillometer as soon as the VPN becomes operational again.

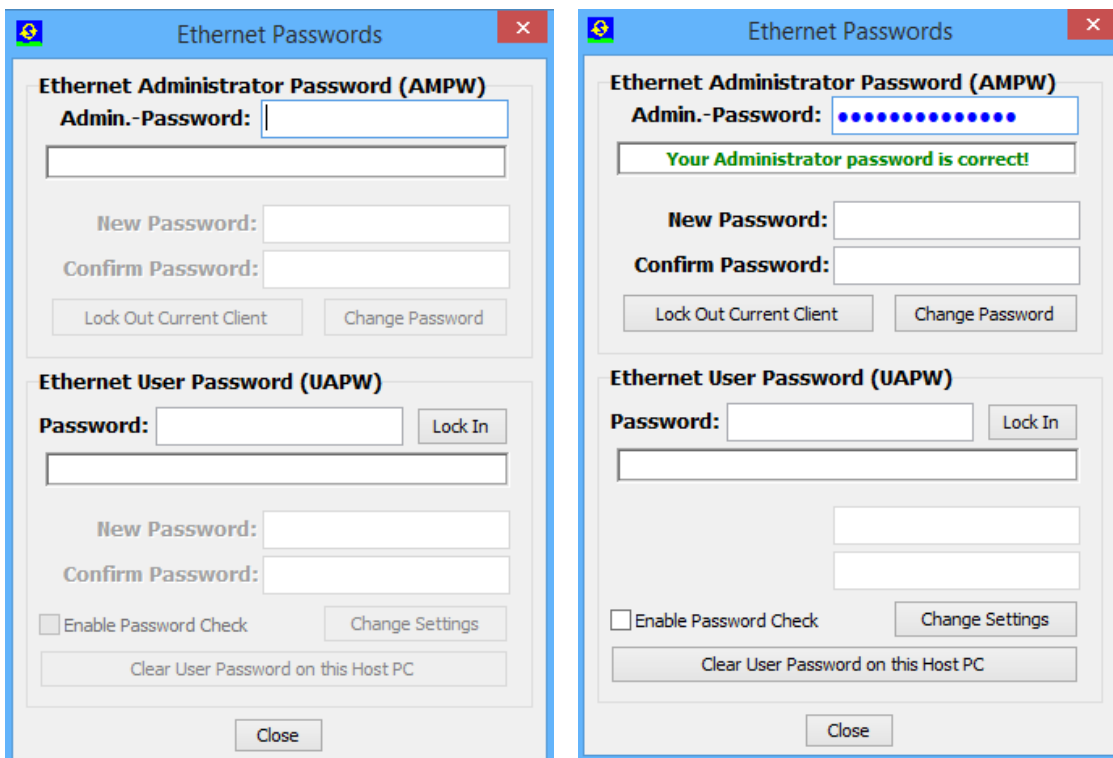
### 3.2.1.3 Multiple Clients

The S-PC connected to a H-PC is acting as a server, while the H-PC is the client. Every exchange of data packages is initiated by a H-PC request. The S-PC is permanently listening to its IP address and port for possible client requests. The H-PC is defined to be the primary client that connects to the scintillometer. The scintillometer then reserves its connection channel to this H-PC. Any other client requests from other IPs are rejected by the scintillometer and the user is notified by a pop-up message.

### 3.2.1.4 Ethernet Passwords

When the scintillometer becomes part of a network (not in a peer-to-peer connection), it acts as a server that will only allow one client (H-PC) to connect to it. In principle, any client, who uses a valid network address and who knows the scintillometer's IP address, can connect to the scintillometer. Therefore, the scintillometer is using a password control system in order to identify the access right of a particular client. This password is called a **User Access Password (UAPW)** and it is defined by a person with administrator rights, who should be a single IT person responsible for the network. Also the network administrator has a password called the **Administrator Password (AMPW)**. When clicking **Ethernet Passwords** from the TPC-IP interface menu, a new menu opens for defining such passwords.

The menu appears in the way shown below (left), if the AMPW is already defined. The fields to enter new passwords are disabled, until a valid AMPW is entered, which switches the menu to the status on the right. At scintillometer delivery, the default AMPW is '**Administrator**'. The responsible network administrator should overwrite the AMPW as soon as possible when the scintillometer has been assigned a valid IP address in a network. The network administrator is the only person who is authorized to set the UAPW and the password checking enable / disable.



A user who tries to connect to the scintillometer with a valid UAPW (**Lock In** button) will be accepted if no other client is currently present. Otherwise he will be rejected and informed about the radiometer connection being occupied. Only the Administrator has the right to interfere in an established communication between the scintillometer and a H-PC by clicking the **Lock Out Current Client** button. The Administrator client then becomes the new H-PC.



When an administrator has entered a valid AMPW, he can define a new UAPW or enable /disable password checking by the scintillometer. Once a UAPW check is enabled and the UAPW has been defined by the Administrator, a client must enter the UAPW when he connects to the scintillometer. Otherwise the access will be denied. If a client has entered the correct UAPW, the connection to the scintillometer can be established (assuming the client is the first client) and the UAPW is stored on the client's disk so that a new entry of the UAPW is not required if the client tries to connect to the scintillometer multiple times. The UAPW can be deleted from disk by **Clear User Password on this Host PC** to enforce the entry of the UAPW next time a user wants to access the scintillometer again.

The UAPW entry cannot be over-ruled by an entry of the AMPW. When the UAPW entry is requested, only the correct UAPW is accepted. An Administrator, who has forgotten the UAPW, can enter the correct AMPW and define a new UAPW or disable the password checking to get access to the S-PC.

### 3.3 Configuration

#### 3.3.1 Measurement Setup

Once the connection to the MWS is established (e.g. click ) , a measurement setup should be defined or selected before a measurement can be started. To do so, switch to the **Configuration** tag in the data display area:

The screenshot shows the 'Measurement Setup' configuration window in the RPG Scintillometers software. The window is divided into several sections:

- Measurement Setup Diagram:** A 2D plot showing the positions of transmitters (T) and receivers (R) relative to the ground. Transmitters are at zTM and zTL, and receivers are at zRM and zRL. A topography line is shown between x1 and x10. A GPS point is marked at the origin.
- Topography Table:**

	x1	x2	x3	x4	x5	x6	x7	x8	x9	x10
x [m]	0	1	2	3	4	5	6	7	8	900
z [m]	0	0	0	0	0	0	0	0	0	0
- MWSC Settings:**
  - Type: RPG-MWSC-160
  - Wavel.: 1860 µm Aperture: 0.300 m
  - Height Above Ground: zTM: 5.00 m zRM: 5.00 m
- LAS Settings:**
  - Type: Kipp & Zonen LAS Mk-II E
  - Wavel.: 0.850 µm Apt.: 0.149 m
  - Height Above Ground: zTL: 5.50 m zRL: 8.50 m
  - Y-Displacement: YTL: 0.00 m YRL: 0.00 m
- Setup Handling:**
  - Current Setup: TEST
  - New Entry Name: (empty)
  - Buttons: Add, Delete, Overwrite
- Start Trigger:**
  - Time Grid: IMMEDIATELY
- Data Storage Options:**
  - Host PC Data Files:
    - \*.RAW (checked) \*.FLX (checked) \*.VAR (checked) \*.HKD (checked)
- Filters:**
  - Manual Run. Mean: 60 s
  - Auto LAS: 37 s MWS: 97 s
  - Variance Integration: 10 min
- Environment and Host PC Status:**
  - Environment: Temperature, Relative Humidity, Bar. Pressure, Wind Speed, Wind Direction, Rain Flag, GPS Position.
  - Scintillometer Status: Scintillom. Model, Instrument Time, Root Disk Capacity, Data Disk Capacity, Receiver Temp., Temp. Stability, GPS Status, Last Time Sync., Weather Station, LAN IP, LAN Gateway, Software Version.
  - Measurement Setup: Setup: TEST, Lateral Dist. to LAS: R:3.50 m, T:0.50 m, Transmitter Distance: 900 m, Height over Ground: 6.0 m, MWS Sig. Strength, LAS1 Sig. Strength, LAS2 Sig. Strength.
  - Host PC: Data Directory: C:\RPG-MWSC\DATA, ASCII Data Files: NO, netCDF Data Files: NO, Data Archiving: NO, LAN IP: 172.23.248.47 (dyn.), LAN Gateway: 0.0.0.0, Subnet Mask: 255.255.240.0, Free Disk Capacity: 55374 MB.

The **Measurement Setup** page (see above Figure) summarizes all geometrical definitions of a measurement. The various parameters and their names are illustrated in a graphical schematic. The used coordinate system has its x-axis directed to the connecting line between transmitters and receivers with its origin at the transmitter location. The vertical direction is the z-axis and the lateral direction the y-axis. The following coordinates are defined:

- **zTL**: LAS transmitter z-coordinate [m], measured above ground level
- **zTM**: MWS transmitter z-coordinate [m], measured above ground level
- **zRL**: LAS receiver z-coordinate [m], measured above ground level
- **zRM**: MWS receiver z-coordinate [m], measured above ground level
- **yTL**: LAS lateral transmitter displacement
- **yRL**: LAS lateral receiver displacement

In this coordinate system the MWS lateral displacement is zero. In a correct setup the connecting lines of LAS receiver / transmitter and MWS receiver / transmitter must intersect somewhere along the signal path. This can be achieved by reverting the relative LAS and MWS positions on the transmitter and receiver side. For example, if the LAS and MWS are at the same altitude ( $zTL = zTM$  and  $zRL = zRM$ ), the lateral LAS displacement coordinates of transmitter and receiver must have different signs, e.g.  $yTL = -yRL$ . The relative y and z coordinates shall be measured with an accuracy of about 1 cm. In addition to the relative (ground level referenced) z-coordinates, the user defines the topography between transmitters and receivers by entering a set of 10 positions  $x[i]$  and  $z[i]$ ,  $i = 1, \dots, 10$ . **The total path length is** therefore defined as  **$x[10]$** . The topographic z-coordinates are GPS altitudes (in m). **The GPS altitudes  $z[1]$  and  $z[10]$  do not include the installation heights above ground.** If not directly measured using a handheld GPS receiver, the x and z-coordinates may also be derived from Google-maps. The accuracy of the absolute x and z coordinates shall be about 1 m.

**Note: Accurate measurements of the x, y and z-coordinates are essential for valuable heat flux observations! Particularly, when observing at short path lengths and low observation heights.**

Furthermore, a surface roughness length parameter (in [m]) can be selected from a combo box (**Surf. Roughn.:**). This parameter is needed in the calculation of the friction velocity (see Section 4.4.3). The MWS is equipped with a meteorological station providing wind speed and wind direction information. In order to derive the wind component orthogonal to the signal path, the path orientation relative to north (clockwise) is needed. The path orientation is entered in **Orient. Rel. to North (CW):**

In addition to the LAS and MWS positions, the user can select from a list of different commercially available LAS systems. While currently there is only one MWS model available (RPG-MWSC-160), the following LAS systems can be operated with the MWS:

- Scintec BLS 450
- Scintec BLS 900 (dual aperture)
- Scintec BLS 2000 (dual aperture)
- Kipp & Zonen LAS Mk-I
- Kipp & Zonen LAS Mk-II
- Kipp & Zonen X-LAS Mk-I
- Kipp & Zonen X-LAS Mk-II
- Wageningen LAS



These instruments have different wavelengths and aperture diameters. By selecting one of them from the combo box, the specifications are automatically assigned from an internal LAS data archive.

On the **Measurement Setup** page, the user also specifies which file types are stored during a measurement. The user may select different **Data Storage Options** for the S-PC and H-PC. The following file types are available:

- Raw Data Files (**\*.RAW**)  
\*.RAW data files (level 0) contain (in addition to the setup data and GPS position in the header) the surface sensor data (resolution 1 second) and the LAS and MWS detector voltages (resolution 1 ms).
- Variance Data Files (**\*.VAR**)  
\*.VAR data files (level 1) contain (in addition to the setup data and GPS position in the header) the surface sensor data (resolution 1 minute) and the variances for LAS, MWS and the co-variance of the two (resolution 1 minute). The file stores all the information to calculate heat fluxes.
- Heat Flux Data Files (**\*.FLX**)  
\*.FLX data files (level 2) contain (in addition to the setup data and GPS position in the header) the surface sensor data (resolution 1 minute), heat fluxes, and evapo-transpiration (resolution 1 minute).
- Housekeeping Data Files (**\*.HKD**)  
\*.HKD data files contain the GPS position and nine housekeeping signals (resolution 1 second).

For a detailed description of the file formats, see Appendix A.

By default, all files selected as **Host PC Data Files** are stored on in a buffer directory on the S-PC<sup>2</sup>. The buffered files automatically and regularly transferred to the H-PC. **Scint. File Backup** options do only refer to the archiving of the selected files in the same manner as defined by the **Data File Archiving** option on the H-PC (Section 3.4). Please note that the internal S-PC storage will fill up, when the **Scint. File Backup** is active a measurement is running without a connection to the H-PC. When a critical free disk space 1 GB is reached, data files will be successively deleted – starting with oldest files.

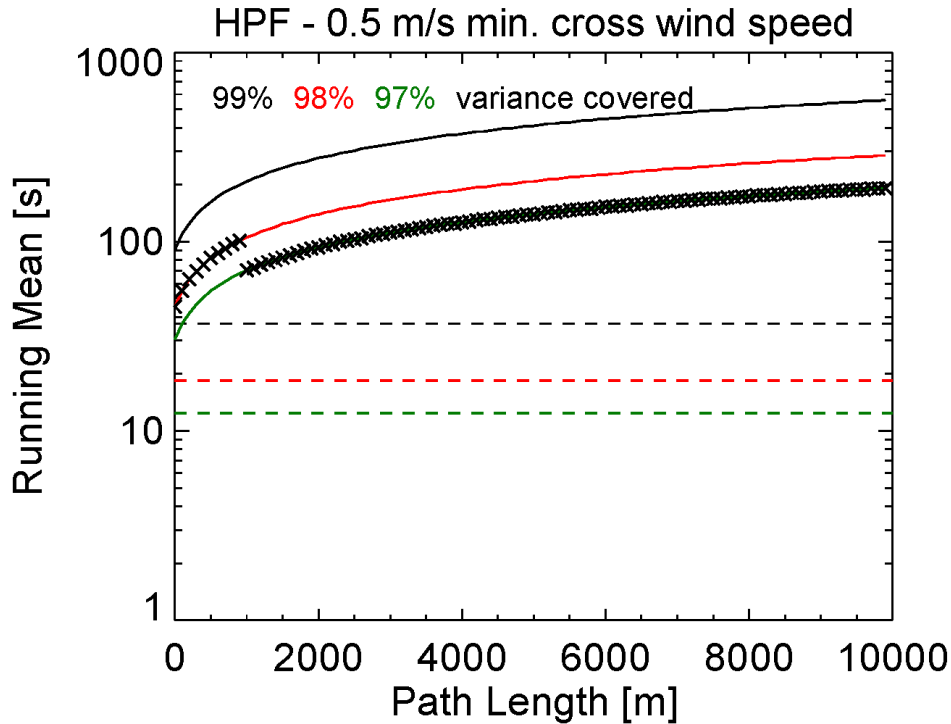
### 3.3.1.1 Filters

The group **Filters** allows for setting the running mean filters, which act as a High-Pass Filter (HPF) for the recorded RAW signals (see also Section 4.4.1). They can either be set automatically (checkbox **Auto**) or manually to values between **1 s** and **60 s**. In case **Auto** is checked, individual running mean values for LAS and MWS are read from a look-up table. The values depend on the selected path length (MWS only) and the calculated effective path height (LAS and MWS) and remain unchanged during a measurement. The look-up table distinguishes between three different **installation height** ranges, which are related to an expected minimum cross wind speed:

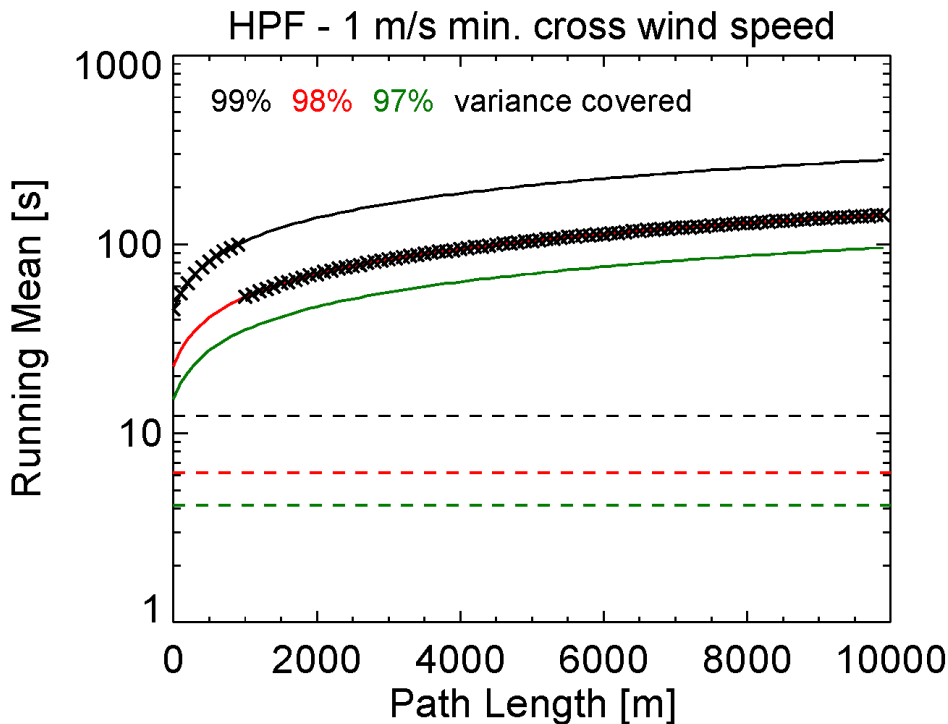
Path height range	0-10 m	11-30 m	31-100 m
Expected min. wind speed	0.5 m/s	1.0 m/s	2.0 m/s
HPF for LAS (auto filter selection)	37 s	12 s	9 s

<sup>2</sup> Instruments with serial numbers 3010001-3010027 do not create RAW-Files on the S-PC, but on the H-PC only.

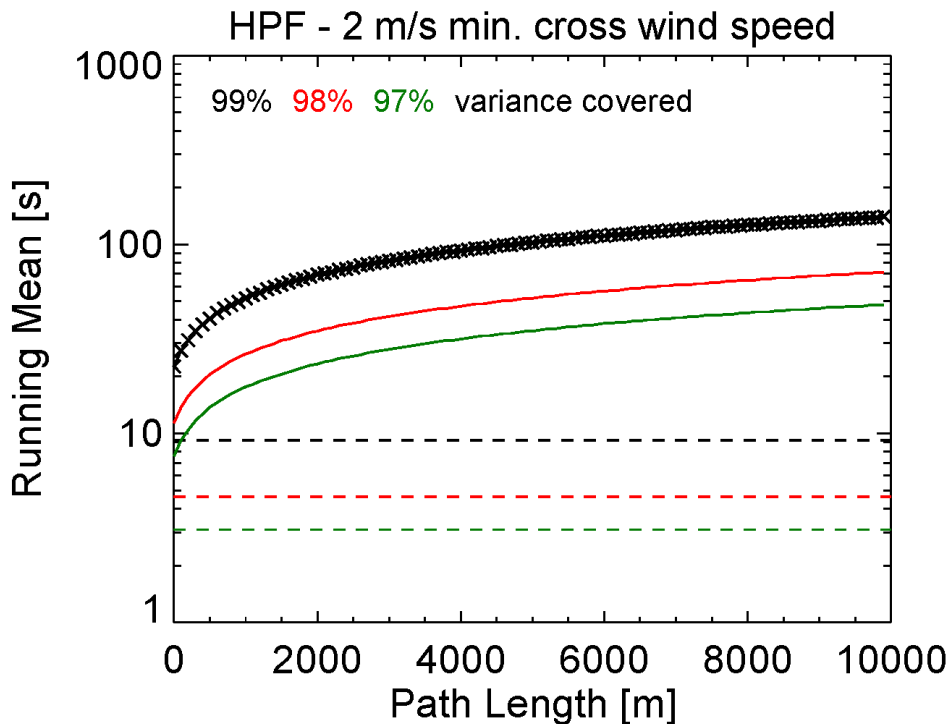
The below Figures show the selected HPF for the MWS (and the related covered variances) in dependence of the path length and height:



*High-Pass Filters (HPFs) implemented for path heights of 0-10 m via a look-up (automatic filter selection) are indicated as crosses.*



*High-Pass Filters (HPFs) implemented for path heights of 10-30 m via a look-up (automatic filter selection) are indicated as crosses.*



**High-Pass Filters (HPFs) implemented for path heights of 30-100 m via a look-up (automatic filter selection) are indicated as crosses.**

When the actual cross wind equals the expected minimum value, the scintillation spectra will be slightly cut at the lower end. The HPFs drawn from the look-up table lead to a reduced signal variance of 99%, 98% or 97% of the true variance, when observing a minimum expected wind speed. For cross wind speeds below this limit, the variance is cut by a larger percentage.

The **Variance Integration** period represents the time range on, which the signal variances are calculated (see also Section 4.4.1). The user may select periods between **1 min** and **10 min** (default 10 minutes).

After the measurement geometry has been defined, it must be stored to the setup archive. Please enter a setup name to **New Entry Name:** and click **Add**. The program then computes the spectral filter functions that are needed for later data processing. This computation takes about a few minutes (the computation progress is indicated by a progress bar), depending on the path length. When finished, the setup name is added to the combo box under **Current Setup:** and the computation results are stored in the setup archive as MCF (Measurement Configuration File). If the user selects a setup from the combo box, the computation of the spectral filter functions is not repeated, because the results have been saved to the archive. It is also possible to **Delete** or **Overwrite** setup entries.



### 3.3.2 Automatic Gain Control

During the MWSC / LAS setup, receivers and transmitters are mechanically aligned to yield maximum receiver power. Usually, the MWSC transmitter power level is set to result in a mean receiver power level of approximately 30000 ADCs (half of the full ADC range). This works fine as long as atmospheric conditions do not change dramatically during the measurement duration. In long campaigns, the system may be operated continuously for days or weeks, so that significant changes in receiver power level due to atmospheric changes are likely. The worst-case scenario occurs, when the setup is performed under relatively humid conditions with high absorption at 160 GHz (then the transmitter power is high in order to overcome atmospheric absorption) while the conditions later change to become dry. The receiver power level may then increase beyond its maximum ADC level of 65536 (16 bit).

Beginning of 2020 with the release of the “Generation 2” MWSC (RPG-MWSC-160-G2, SW-version  $\geq 3.25$ ), RPG has developed a new receiver backend which includes a programmable attenuator within the IF chain. The receiver software automatically controls its received power level by changing the total IF gain. This way, scenarios as described above can be avoided.

When connecting to a RPG-MWSC-160-G2 (or higher) instrument, the Host’s **Configuration** tag display looks like this:

(Version 3.25-1), Instrument: 0

Files Communication Configuration License Measurement Alerts

Measurement Running... LTime: 06:48:27 Date: 24-03-2020

Configuration Raw Data Structure Params Heat Fluxes Evapo-Transpiration Met. Station Housekeeping

Measurement Setup Spectral Filters & Weighting Functions <TEST> LAS Saturation Check

Diagram showing Transmitters (T) and Receivers (R) at various heights (zTM, zTL, zRL, zRM) and a Topography profile. GPS heights are shown for 10 stations (x1 to x10).

	x1	x2	x3	x4	x5	x6	x7	x8	x9	x10
x [m]	0	500	1000	1500	2000	2500	3000	3500	4000	4500
z [m]	50	50	50	50	50	50	50	50	50	50

Topography (z = GPS Heights)  
Orient. rel. to North (CV): 0° Surf. Roughn.: 0.01 m (short cut grass)  
Zero Displacement Height: 0.0 m

MWSC Type: RPG-MWSC-160  
Wavel.: 1860 μm Aperture: 0.300 m  
Height Above Ground: zTM: 25.50 m zRM: 25.50 m

LAS Type: Scintec BLS 900  
Wavel.: 0.880 μm Apt.: 0.145 m  
Height Above Ground: zTL: 25.50 m zRL: 25.50 m  
Y-Displacement: yTL: 0.50 m yRL: 0.50 m

Setup Handling  
Current Setup: TEST  
New Entry Name: [ ]  
Add Delete Overwrite

Calc. Time: ----- Cancel

Start Trigger  
Time Grid: IMMEDIATELY

Environment  
Temperature: 22.5°C / 72.5°F  
Relative Humidity: 20.7%  
Bar. Pressure: 1011.2 hPa  
Wind Speed: 0.3 km/h  
Wind Direction: 154.0° (SSE)  
Rain Flag: NOT RAINING  
GPS Position: -----

Scintillometer Status  
Scintillom. Model: RPG-MWSC-160-G2  
Instrument Time: 05:48:28, 24-03-2020  
Root Disk Capacity: 12809 MB (15266 MB)  
Data Disk Capacity: 12809 MB (15266 MB)  
Receiver Temp.: 39.3°C / 102.8°F  
Temp. Stability: 0.000 K  
GPS Status: FOUND  
Last Time Sync.: 00:00:00, 01.01.2001  
Weather Station: Vaisala WXT-520  
LAN IP: 172.23.159.145  
LAN Gateway: 0.0.0.0 (static)  
Software Version: 3.25-1  
Failures: -----

Measurement Setup  
Setup: TEST  
Lateral Dist. to LAS: R:0.50 m, T:0.50 m  
Transmitter Distance: 4500 m  
Height over Ground: 25.5 m  
MWSC Sig. Strength: [ ]  
LAS1 Sig. Strength: [ ]  
LAS2 Sig. Strength: [ ]

Host PC  
Data Directory: C:\\$VN\MWSC (32)\TRUNK\RELEASE\DATA\  
ASCII Data Files: NO  
netCDF Data Files: NO  
Data Archiving: NO  
LAN IP: 172.23.156.67 (dyn.)  
LAN Gateway: 172.23.156.1  
Subnet Mask: 255.255.255.0  
Free Disk Capacity: 281598 MB

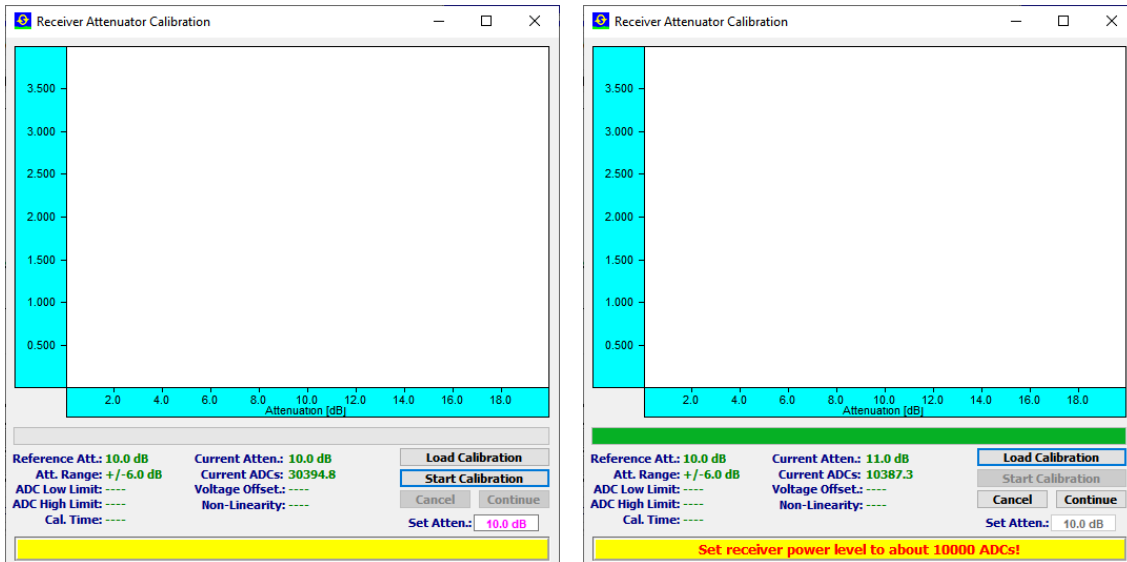
CErr: 0

Message: Mode: CONNECTED TCP / IP: GET\_DATA\_PACKAGE >13 <:12094

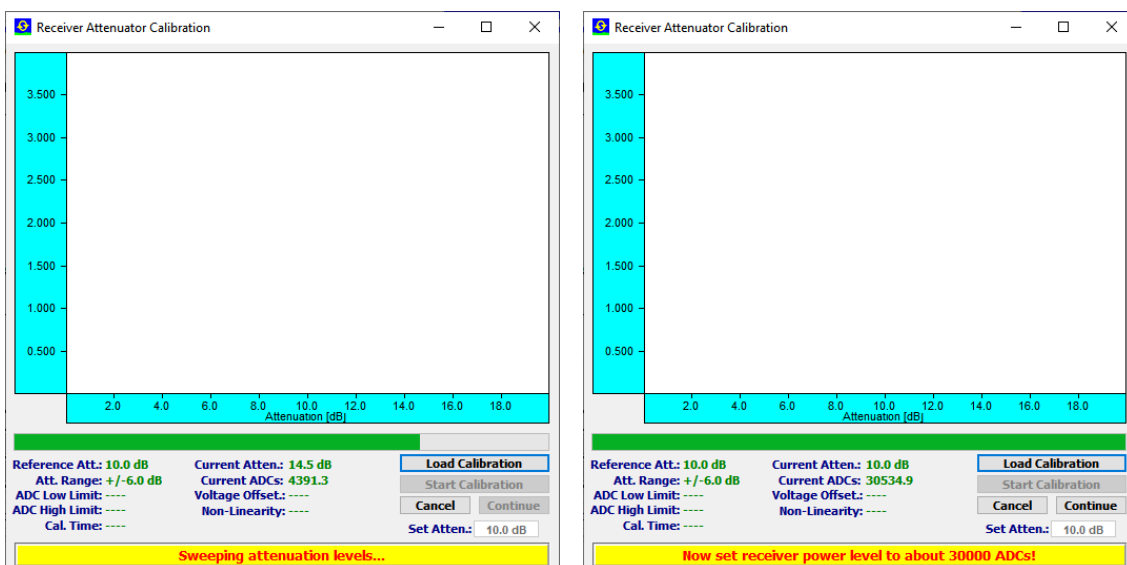
MW Receiver AGC  
 Auto Gain Control Enabled Receiver Attenuator Calibration



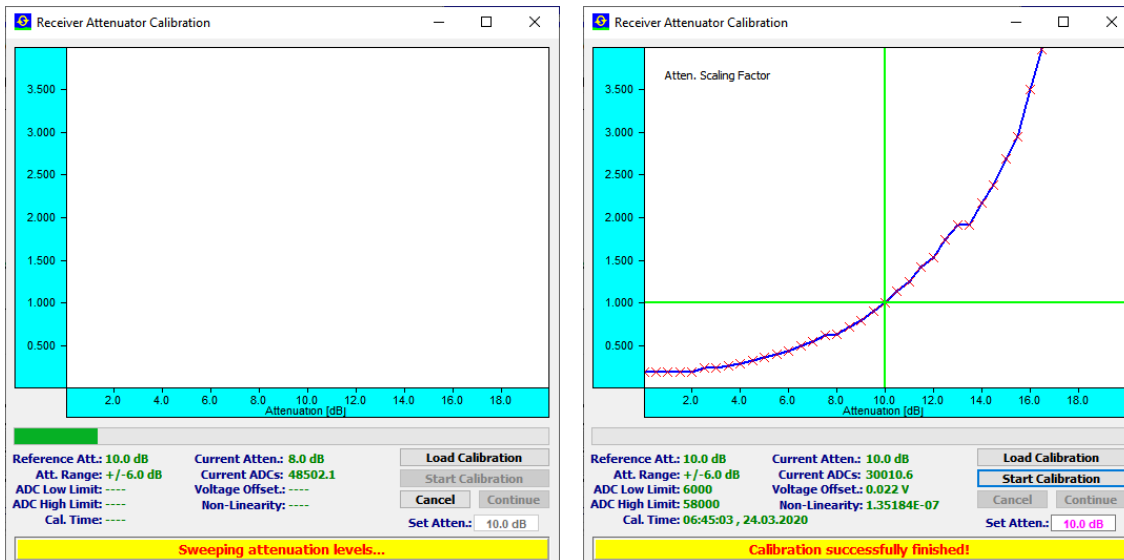
This critical calibration is executed at RPG labs before delivery, but can be repeated by the customer if receiver chain parameters have changed by aging effects. In order to enter the calibration menu click the **Receiver Attenuator Calibration** button. Then click **Start Calibration** and follow the instruction indicated in the yellow command line and adjust the transmitter power to yield about 10.000 ADCs on receiver side, indicated as “Current ADCs”.



The transmitter power needs to be very stable and not affected by atmospheric effects (e.g. scintillation). Therefore, move the transmitter as close to the receiver as possible and avoid power blocking during calibration. Then click **Continue**. The receiver now sweeps attenuation values from 0 dB to 20 dB in steps of 0.5 dB. Finally, the user is instructed to increase the transmitter power to yield about 30.000 ADCs on the receiver side.



When the transmitter power has been adjusted accordingly, click **Continue**. The receiver performs an attenuation sweep from 7 dB to 13 dB now. The attenuation sweep at higher power level is needed in order to correct for receiver non-linearity, which is unavoidable due to the high dynamic range requirements of the system.

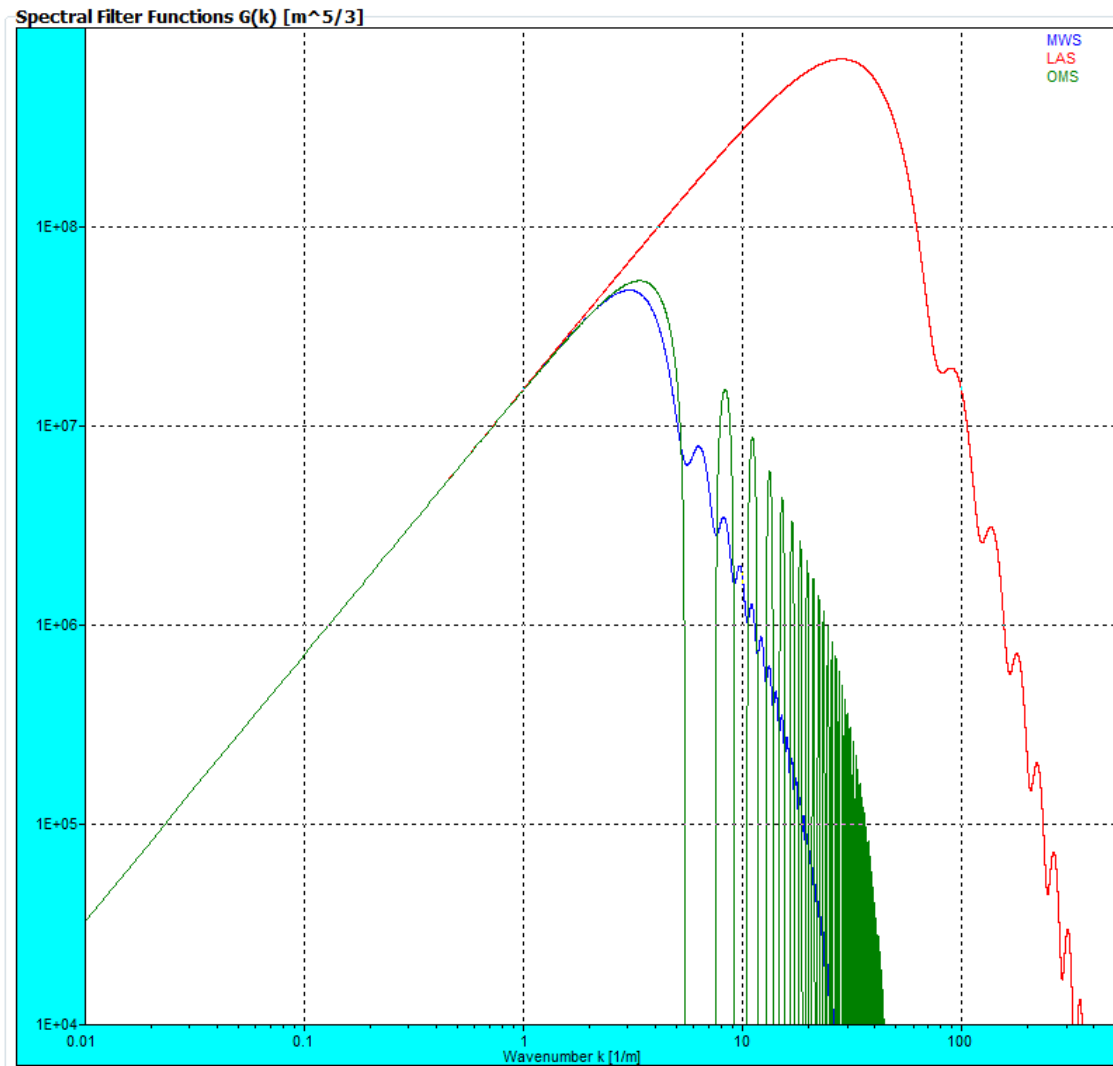


The attenuation calibration is finished and the menu can be closed. Automatic gain control is enabled/disabled during measurements by clicking the **Auto Gain Control Enabled** checkbox before a measurement is started.

### 3.3.3 Spectral Filters & Weighting Functions

For expert users, who are familiar with the theoretical background of scintillometry, the spectral filter functions are plotted on the *Spectral Filters & Weighting Functions* page for information purpose. The plot shows that the maximum of the LAS fluctuation spectrum is in the order of a few hundred wave numbers while the MWS scintillation spectrum cuts off below 30 wave numbers. In order to capture the full scintillation information, the MWS samples the LAS signal with 1 kHz sampling rate. The spectral filter function plot shows that the MWS must be more sensitive than a LAS, because its filter function peaks about one order of magnitude below the LAS filter curve. The scintillation signal level rises with increasing path length. In order to run the MWS efficiently, the minimum path length should be around 1000 m, depending on the evapo-transpiration level. The lower the evapo-transpiration, the longer is the required path length in order to achieve a sufficient signal to noise ratio.

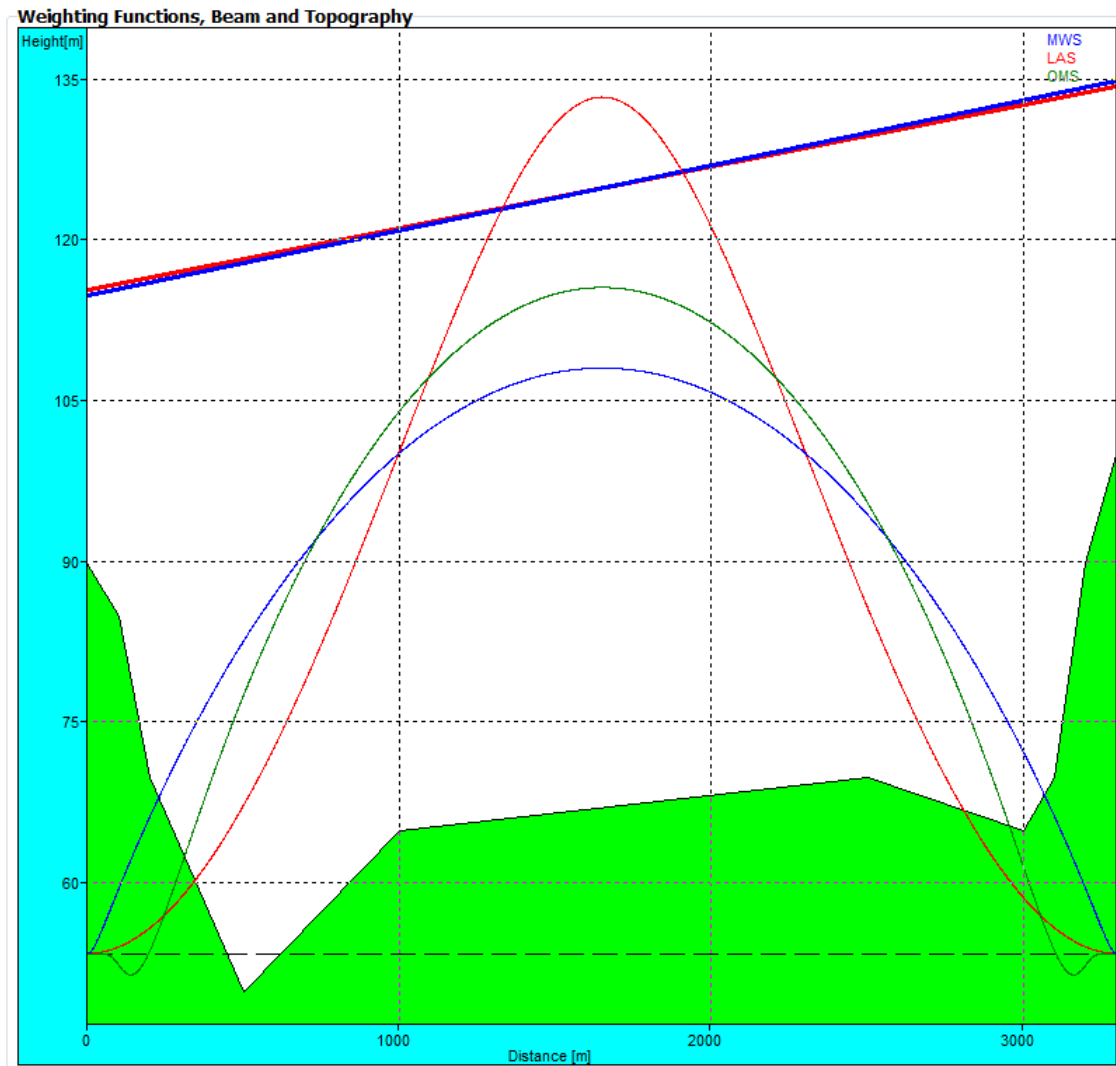
Another important parameter for the heat flux data analysis is the effective signal path height above ground. The computation of effective height requires the knowledge of the sensitivity weighting functions along the signal path. These functions are also plotted on the *Spectral Filters & Weighting Functions* page.



**Example of spectral filter functions, computed from a setup geometry (blue: MWS, red, LAS, green: Covariance OMS).**

The effective height computation is based on a convolution of the weighting functions and the distance of signal path to vertical topography coordinate along the path. The plot shows the weighting functions for MWS (blue), LAS (red) and the correlated signal (green). The topography is indicated as a green underground contour and the signal paths for LAS and MWS (tilt and location) is given as red and blue straight lines for LAS and MWS respectively.

The LAS weighting function peaks more significantly in the middle of the signal paths than the MWS while the MWS weighting function is flatter, but also peaking half way between transmitter and receiver. If the MWS and LAS signal path cross-over is not located in the middle of the signal path, the weighting function of the correlation between the two signals (in green) is distorted towards the signal cross-over point. In this case the maximum of the green curve is off-centered.

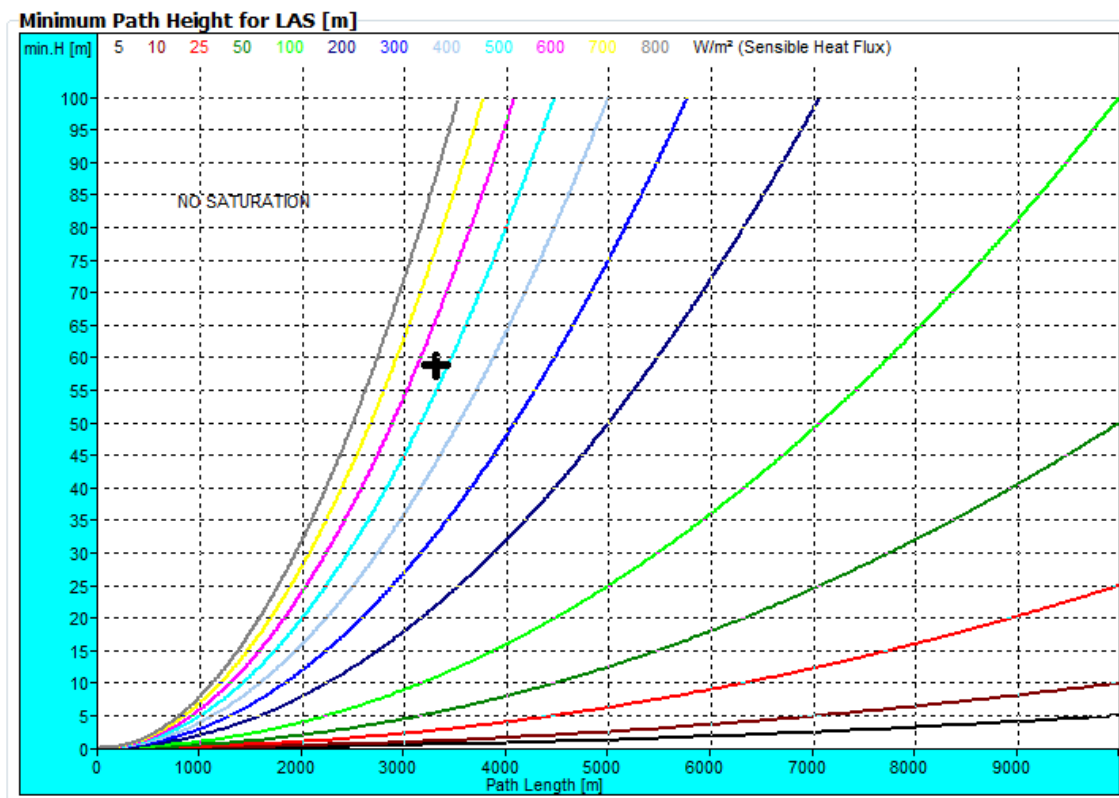


**Example of a sensitivity weighting function plot (blue: MWS, red: LAS, green: combined). Also the topography and signal paths are shown.**

### 3.3.4 LAS Saturation Check

Because the LAS is more sensitive to scintillations than the MWS, it is also more susceptible to saturation effects. For setting up the scintillometers in the field, it is essential to know when saturation may occur. Saturation becomes more likely for longer path lengths and higher heat fluxes. The user may check the diagram shown on the **LAS Saturation Check** page in order to decide about the right transmitter  $\leftrightarrow$  receiver distance and signal path height above ground.

The area to the left of the heat flux curves is the non-saturation regime. In the saturation curve plot, the current setup (effective height and path length) is indicated by a black cross. For heat flux curves right to the cross, no saturation occurs.

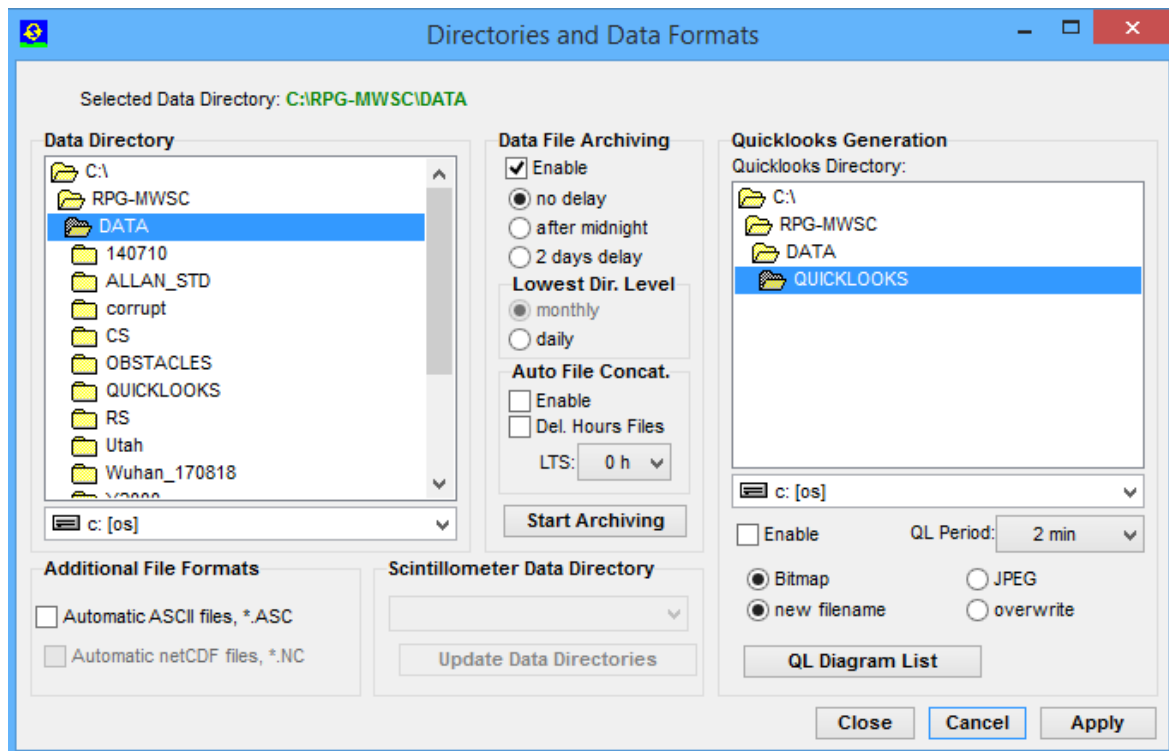


**Example of LAS saturation curves, plotted as a function of path length and minimum effective height. The black cross indicates the setup configuration. In this example, saturation would occur at sensible heat fluxes above 500 Watts/m<sup>2</sup>.**

### 3.4 Data Storage Configuration

The final step before a measurement can be started is the data file path specification.

Open the **Directories and Data Formats** menu by clicking .



**Directories and Data Formats menu, including data archiving.**

The group box on the main screen displays the data storage details. The data storage directory is selected from the directory tree shown in [Data Directory](#).

[Data File Archiving](#) is a useful feature to prevent the data directory to be filled with ten thousands of files, which may overload the operating system (Windows operating systems cannot handle more than a few 10000 files in a single directory). If **Enable** is checked, the software automatically creates sub-directories in the data directory and stores the data files according to the year, month and day of file storage. E.g. a file **08111623.VAR** would be stored in a directory **... \RPG-MWSC\Data\Y2008M11D16\**.

[Automatic File Concatenation](#) to daily files is enabled via the **Enable** check box. *Hourly files* may be deleted after concatenation (**Del. Hourly Files**). *LTS* stands for Local Time Shift. The selected time shift in hours is used localize the concatenation of hourly files. As a result, the daily files better match the diurnal cycle. Data file time stamps are not affected: They always refer to UTC.

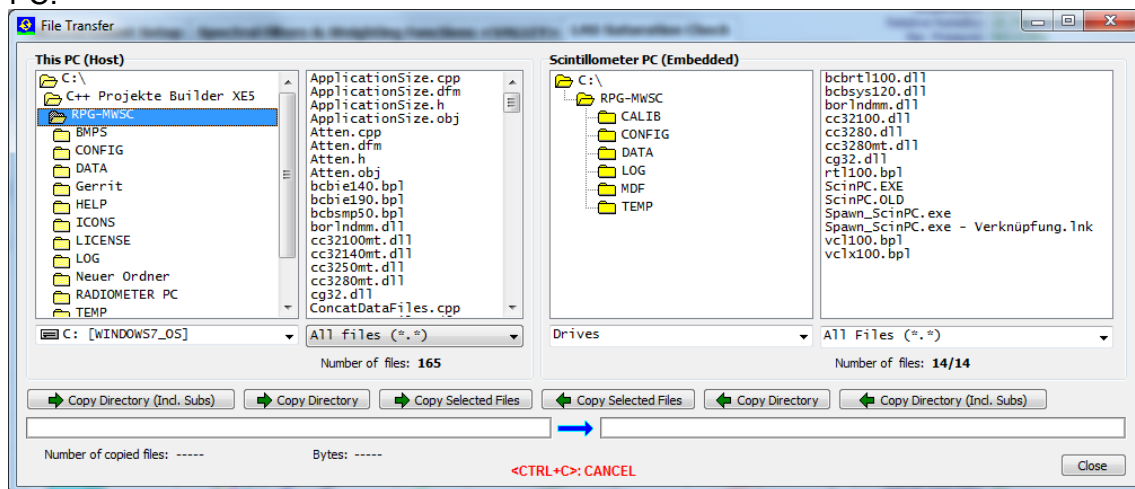
Quick-look files can be automatically created and stored to a separate directory. The file formats BMP and JPG are available. When clicking the **QL Diagram List** button, a list of graphics windows is displayed. Each of these windows can be enabled / disabled for quick-look file generation. When enabled, a certain graphics display is periodically (defined by **QL Period**) converted to a JPG or Bitmap file and stored to the quick-look directory.

Under **Additional File Formats** the user specifies, if an ASCII or netCDF version of the data files (which are in binary format by default) shall be automatically created. ASCII and / or netCDF files will then (if this option is selected) be stored to the same data directory as the binary files.

The user may use an external USB device to archive data on the MWSC receiver. By default, the system directory on the embedded Scintillometer PC (C:\DATA) is used. When an external USB drive is inserted into one of the MWSC receiver's protected service ports<sup>3</sup> (compare RPG-MWSC-160 Installation Manual), the device is automatically recognized and added to the drop-down menu within the **Scintillometer Data Directory** box. The target directory selected from the drop-down menu is transferred to the Scintillometer PC by clicking **Update Data Directories**. Temporary data files are still stored in the system directory. Data transfer to the external device will only take place during the archiving process. This means the USB-Stick may be replaced during the measurement without loss of data<sup>4</sup>.

### 3.5 Exchanging Data Files

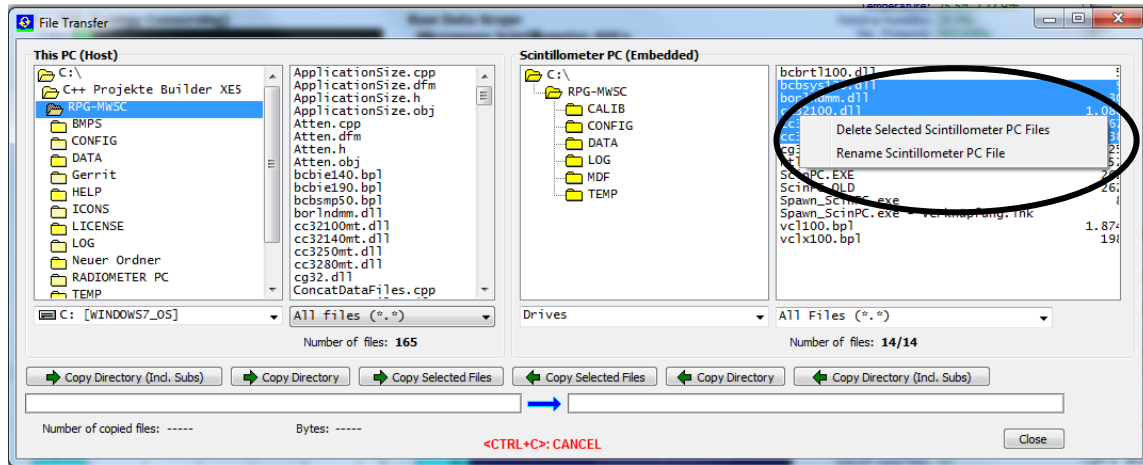
The file transfer menu is opened by clicking . It can be used to exchange files between host and scintillometer PCs. It is possible to transfer not only single files but also complete directories (including sub-directories). This feature becomes beneficial when a lot of data has to be transferred from the scintillometer's file backup to the Host PC.



<sup>3</sup> During regular operations, the protection cap has to be mounted tightly for waterproofing. This means that only miniature USB sticks, which fit underneath the protection cap, may be used.

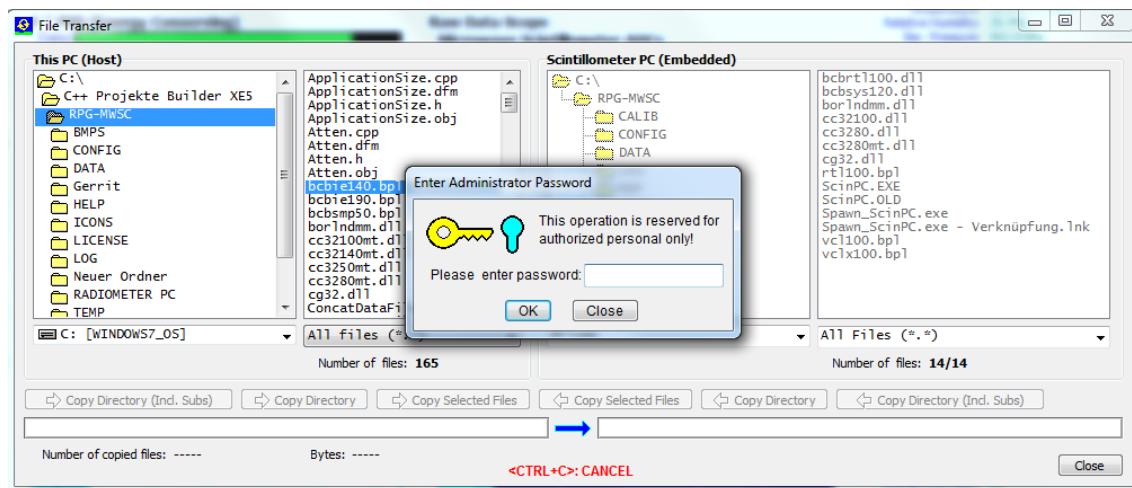
<sup>4</sup> Data loss occurs, when the external device is removed for extended time periods. The storage path may only be updated manually via the Host PC software.

Files or directories can be deleted by marking them and clicking the right mouse button:



From the displayed drop-down list the user may select '**Delete Selected Scintillometer PC Files**' or '**Rename Scintillometer PC File**'. These functions are also available for directories.

Those buttons with green arrows pointing from left to right will move files / directories from the H-PC to the R-PC and those with a green arrow pointing from right to left will move files / directories from the scintillometer to the host. If the user tries to send files to the **RPG-MWSC** directory (the system directory), a password check is initiated:



The H-PC is asking for the entry of the Administrator password (AMPW) to complete the desired action. This mechanism prevents unauthorized users to overwrite important S-PC system files.

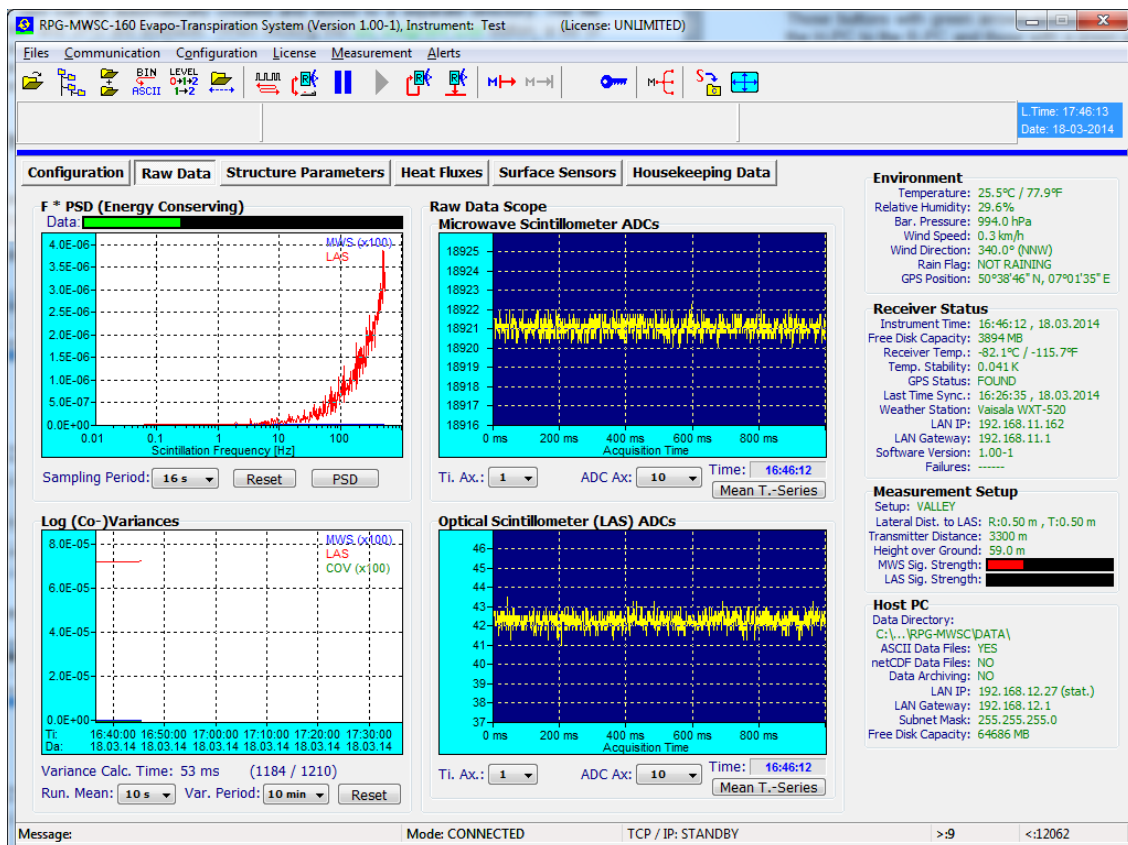
### 3.6 Starting Measurements

When the data cable is properly installed between H-PC and S-PC and the Ethernet IP settings are correctly specified according to Section 3.2.1, the host connects to the

scintillometer by clicking . The graphics data display immediately presents raw data samples like in the Figure below. The two **Raw Data Scope** displays are continuously updated by the current detector voltages of the MWS and connected LAS. The MWS not only digitizes its own microwave signal, but synchronously also the LAS analogue raw signal. The synchronisation of both time series is within 10  $\mu$ s so that the co-variance calculation is not affected over the whole fluctuation frequency band. Both time series are sampled with 1 ms sampling rate. The user may change time axis and ADC axis settings or may switch to the **Mean T.-Series** plot (mean signal time series). The scope display is useful to check the signal level from the transmitters. Also the noise performance of the receiver (without transmitter signal) may be analysed.

The power spectral density (PSD) is presented in the upper left diagram. The sampling period of the FFT can be selected between 1 s and 1048 s. The PSD informs about the fluctuation spectrum of the LAS and MWS and is a good diagnostics tool to identify artificial spectral components like 50 Hz pickup, tower vibration modes (if the LAS / MWS are mounted on a tower), etc.

In the lower left corner the LAS, MWS variances and co-variance (COV) are displayed. These parameters are calculated according to equations **Fehler! Verweisquelle konnte nicht gefunden werden.-Fehler! Verweisquelle konnte nicht gefunden werden.** and are needed as a basis for deriving heat fluxes.



**Data display after successfully connecting to the MWS.**

In this display mode, no data is stored to any data files. File storage is only performed during a running measurement. After a setup has been defined or selected and the file storage on the scintillometer and H-PC is specified, a measurement can be started with



. This command transfers the setup information to the scintillometer so that the instrument is capable of running the measurement independently without a connected host. Therefore, after initiating a measurement start, the Ethernet connection to the host may be interrupted, but the scintillometer automatically continues the measurement and stores its result in a file backup system, similar to the archiving system on the H-PC.

If the scintillometer is interrupted by a power failure, it automatically restarts the interrupted measurement after power return. If the H-PC is connecting to the S-PC while the scintillometer is running a measurement, the host automatically 'jumps' into the measurement, using the same setup as the scintillometer.

The data transfer between H-PC and S-PC can be halted any time with  and continued with . A running measurement is terminated (on both, S-PC and H-PC) by clicking .

### 3.7 The Data Processing Chain

Section **Fehler! Verweisquelle konnte nicht gefunden werden.** includes a detailed systematic summary of the mathematical procedures involved in the derivation of sensible heat and latent heat fluxes. For expert users the host software displays some of the intermediate products like the turbulence structure parameters in terms of the refractive index (Equations 30-31) or in terms of temperature and humidity **Fehler! Verweisquelle konnte nicht gefunden werden.**, and the correlation coefficients  $R_{Tq}$  (Equation 52). The experienced user may also adjust most of the parameters involved in the data processing algorithms. While the running mean filters and the variance period are set under **Configuration/Measurement Setup** (Section 3.3), the following parameters can be manually set at the bottom of the **Structure Parameters** and **Heat Fluxes** panels.

**Structure Parameters** panel:

- **Coupling Coefficients**  $A$  for conversion from  $C_n^2$  to  $C_T^2/C_q^2/C_{TQ}$ . The user is free to insert values manually or rely on the defaults.

**Heat Fluxes** panel:

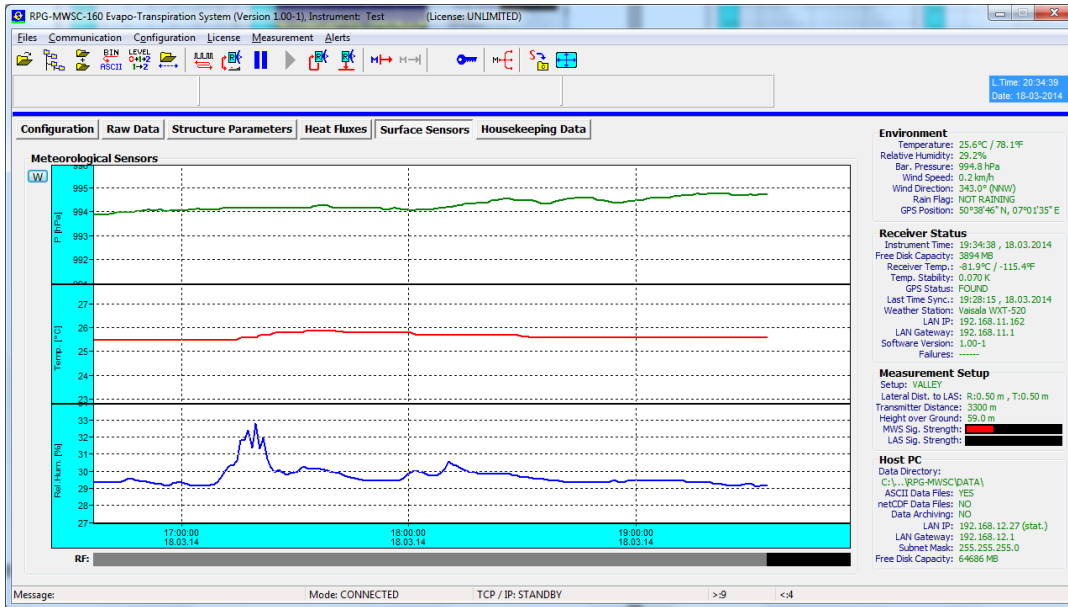
- **RTQ Handling**: Handling of correlation coefficient  $R_{Tq}$  (Section 4.4.3). The **Variable** option applies the processing as suggested by Lüdi et al. [2], where RTQ is calculated from the measured signal covariance (Equation 50). As an alternative, fixed values RTQ values during day/night the may be used<sup>5</sup>.
- **XMost Coefficients** used to link  $C_T^2/C_q^2/C_{TQ}$  with the heat fluxes via the *Monin-Obhukov Similarity Theory (MOST)* are user-selectable. Alternatively, the defaults may be used.

<sup>5</sup> Currently, this option does not use the set RTQ values (0.8 during the day and -0.6 at night) to recalculate  $C_T^2$  and  $C_q^2$  as suggested by Hill [3]. RTQ is only used to determine the fluxes' signs.

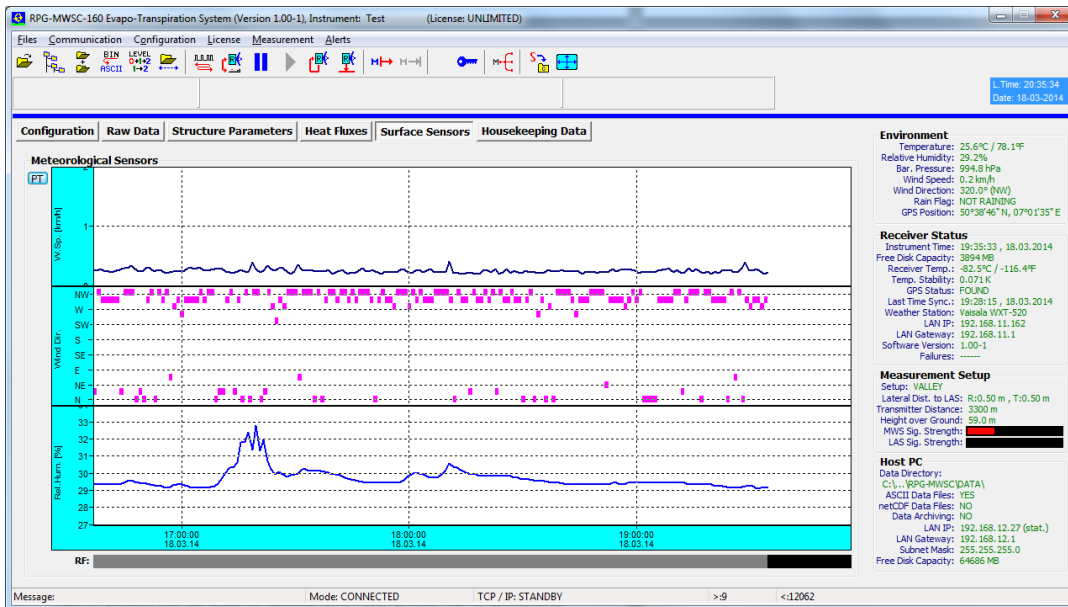




RTQ correlation coefficient (left) and heat fluxes display (right). The heat fluxes display includes markers for sunset (SS) and sunrise (SR).



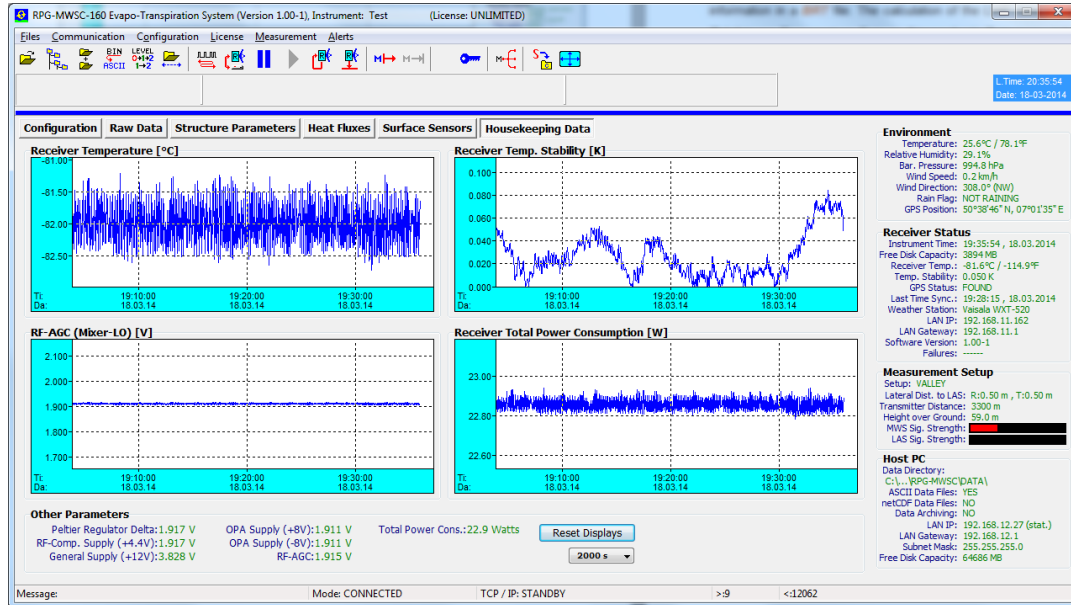
Surface sensor display: Barometric pressure, environmental temperature, relative humidity, and rain flag.



By clicking **W**, the display switches to wind speed and wind direction.



The wind speed measured by the met station is an important parameter in the flux calculation algorithm. Without wind speed there is no heat flux.



*Housekeeping data display monitoring the receiver temperature, its thermal stability, total instrument power consumption (receiver unit only), power supply voltages, PID regulator voltage and AGC receiver local oscillator power control.*

### 3.8 Data Post Processing

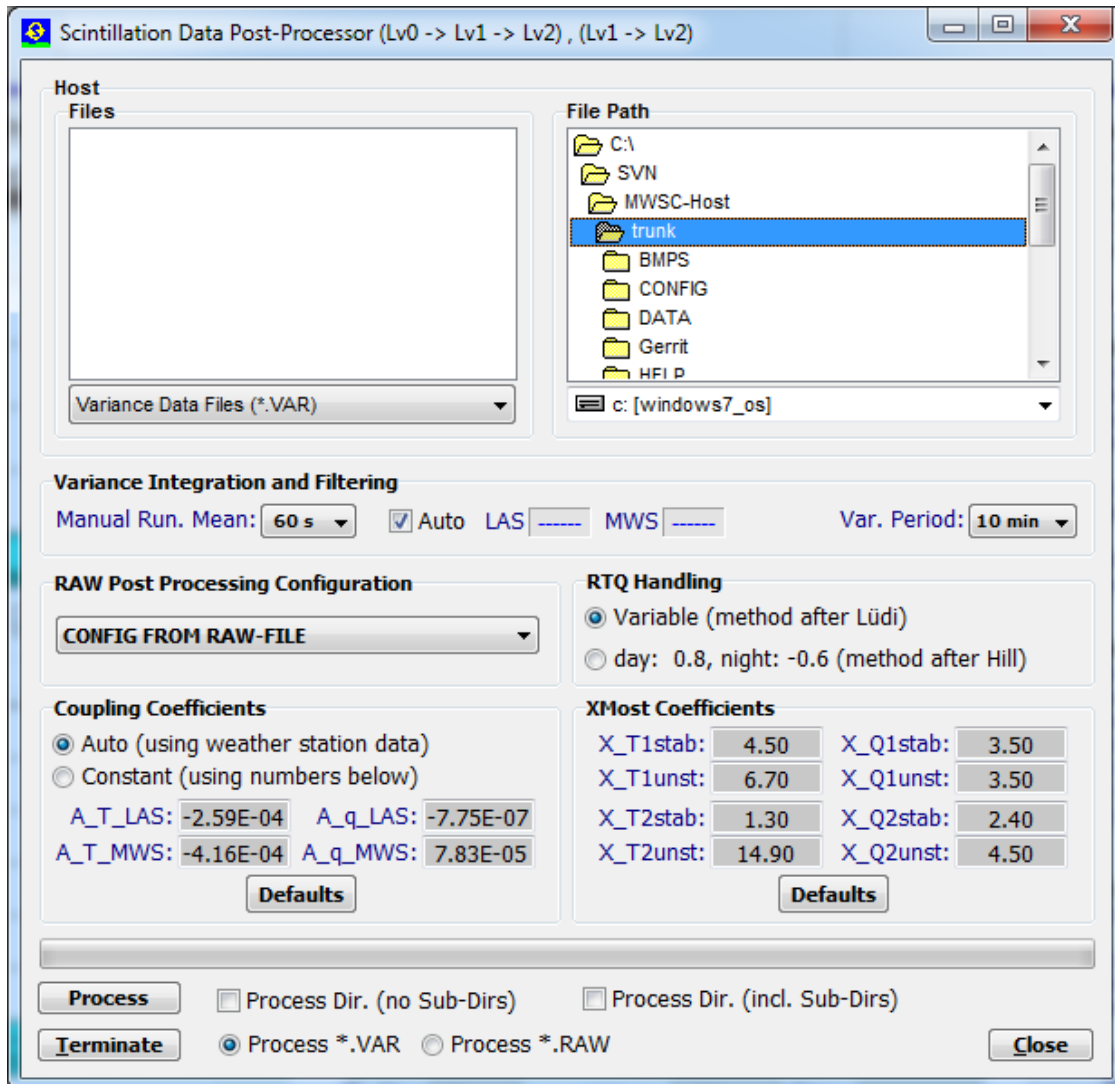
The produced data files divide into the following levels:

- Level 0: \*.RAW data files contain sufficient information to derive all other data levels (Level 1 and Level 2).
- Level 1: \*.VAR data files contain all information to derive Level 2 data.
- Level 2: \*.FLX data files are the end product files.

In general, it would be sufficient to store **raw data** alone, because all other data levels can be generated from it. The major disadvantage is the enormous file size of **approx. 670 MB / day**. For users who do not need to inspect scintillation spectra (PSDs) or who are not willing to tune variance integration and running mean time in a post processing step, will prefer to only store variance data files (\*.VAR, Level 1), which are much smaller (70 kB / day). The host software provides a post processor to create

- Level 1 and Level 2 data files from raw data files (Level 0)
- Level 2 data files from variance data files (Level 1)

The post processor is invoked by clicking . The following menu is opened:



In the upper part of the panel allows for browsing the source files or a source directory to be processed (**Files** and **File Path**). At this point is required to select the source file type (\*.VAR or \*.RAW). The box **Variance Integration and Filtering** is used to set the desired running mean and the variance periods (Section 3.3).

In case the checkbox **Auto** is not checked the running mean filter for both **LAS** and **MWS** can be set to values between **1 s** and **60 s**. The values that will be used during post-processing are shown in the **LAS** and **MWS** boxes. The variance period gives the time range that is used to calculate the signal (co-)variances. It can be set to values between **1 min** and **10 min**.

**Raw Post Processing Configuration** includes a drop-down menu that contains all stored MCF (Measurement Configuration Files). The selected setup is used for re-processing RAW data files. When **CONFIG FROM RAW-FILE** is selected, the configuration stored in the RAW file header will be used.

The **RTQ Handling**, **Coupling Coefficients**, and **XMost Coefficients** used during the post-processing are user-selectable (see Section 3.7 for details).

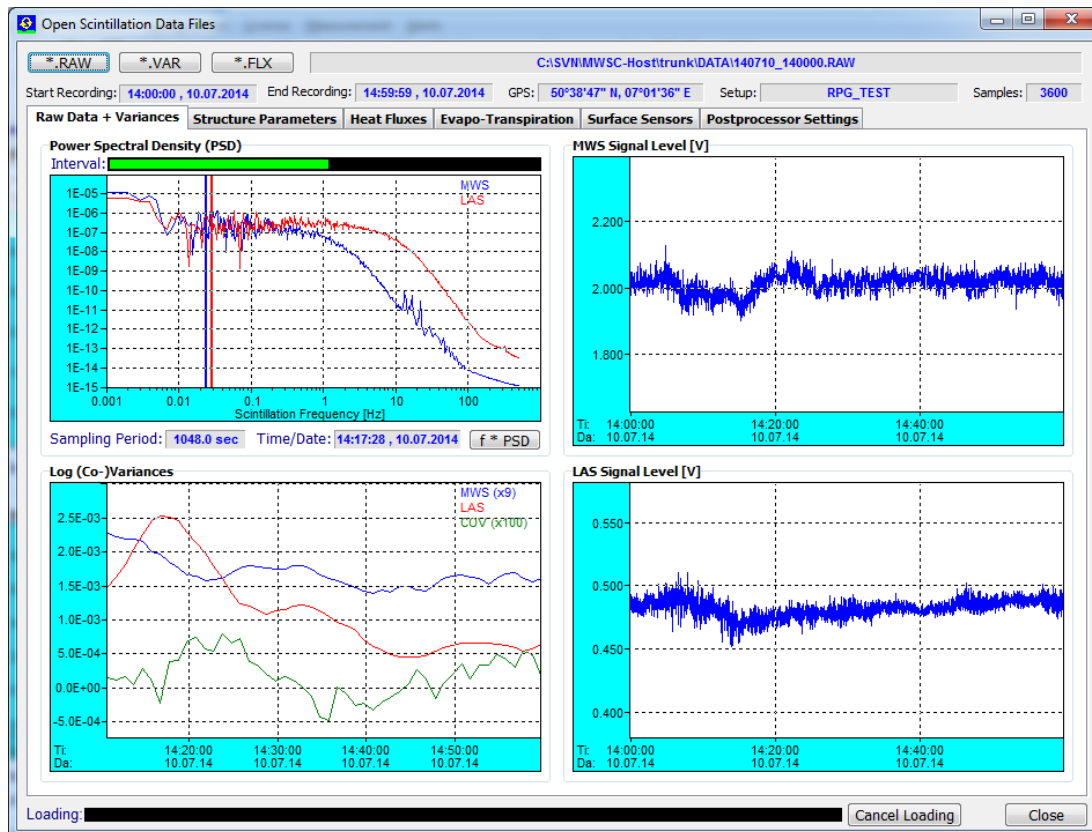
Furthermore, the user can choose whether sub-directories are included (*incl. Sub-Dirs*) or not (*no Sub-Dirs*). Finally, the post processor is started with **Process**. The processor can be terminated any time by clicking **Terminate**.

Please note that the post processor is based on the same procedures and settings as the data browser introduced in Section 3.9. Therefore, it is not possible to use both at once.

### 3.9 Inspecting Data Files

The program includes a viewer for all data file types (RAW, VAR, FLX and HKD). Click and select **Open Scintillation Data Files (\*.RAW, \*.VAR, \*.FLX)**:

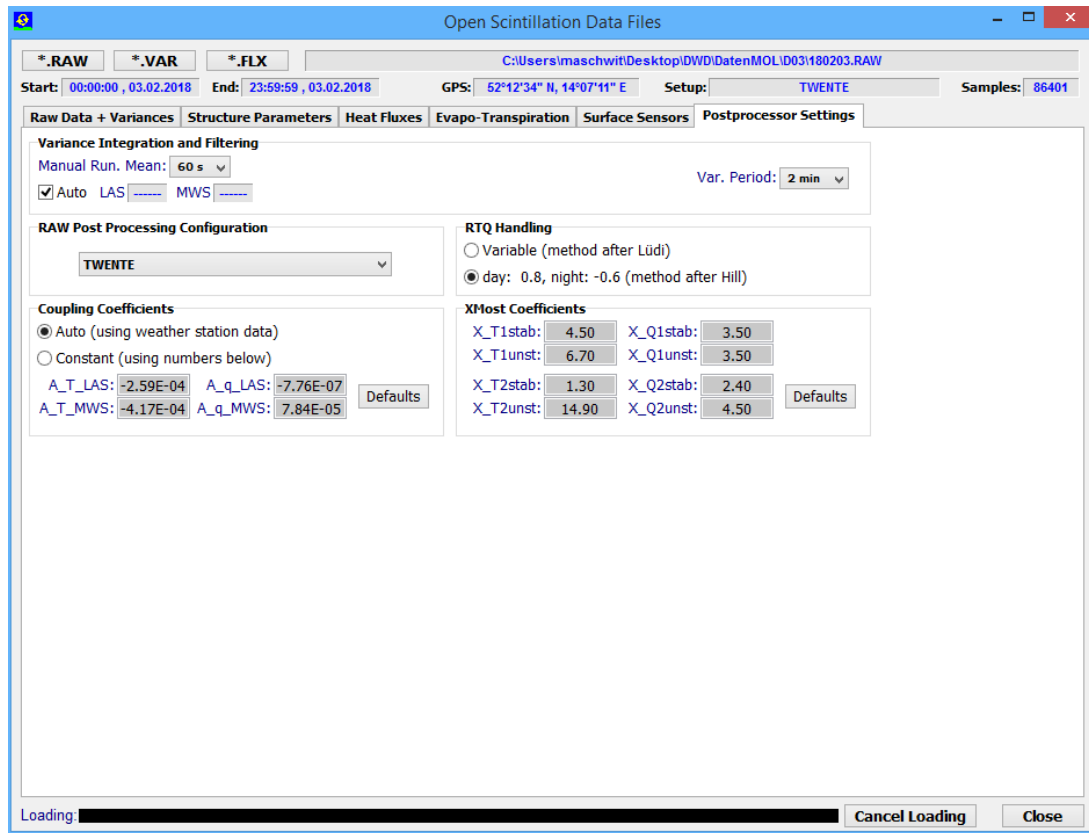
Then load one of the data types **\*.RAW**, **\*.VAR** or **\*.FLX**. VAR and FLY files will load fast, but raw data files need more processing time. The loading progress is indicated on the bottom of the menu and can be terminated (**Cancel Loading**). For example, after loading a raw data file the menu would look like the next Figure. The PSD can be inspected over the whole data set by dragging the green rectangle across the *Interval* bar. All other parameter time series like structure parameters, heat fluxes and surface sensors can be inspected. Above the graphics displays information about the file name, number of samples, start time, end time, GPS position and setup name in shown.



**Software display after opening a raw data file.**

Similar to the Postprocessor  opening of a **\*.RAW** file (L0) file will generate the signal variances (L1) and the heat fluxes (L2). Opening a **\*.VAR** file (L1) will generate the heat fluxes. All available products will fill the data displays, which are accessible via the different tabs (**Raw Data + Variances**, **Structure Parameters**, etc.). The background processing is based on the parameters set within **Postprocessor Settings** tab shown in the Figure below.

The settings equal the settings selected within the postprocessor (Section 3.8). The settings are synchronized between the two tools and only one of them can be used at once.



**Display of the Postprocessor Settings as part of the data browser.**

### 3.10 Transform Data Files to ASCII Format

The standard data file format is binary (file structures listed in Appendix A) because it is more compact than other formats. In the case that a human readable format is required,

the binary files can be transformed to ASCII. When using the  command (**Transform Data Files to ASCII Format**), a binary data file is converted to an ASCII file. The file name of the new file is the binary file name with appended '.ASC', e.g. the variance binary format file **140513.VAR** is converted to **140513.VAR.ASC**.

Beside this manual ASCII file generation, it is possible to automatically store data in ASCII format during the active measurement. See Section 3.4 for details.

Another frequently used data format is the netCDF format. The manual conversion of a binary file to a netCDF file is performed with . The file extension of the converted file is '.NC'. Automatic conversion to netCDF during measurements is activated in the **Define Directories and Data Formats** menu. As in all other post processing menus, file conversions may be performed for multiple files selected from a file box or for complete directories, with or without sub-directories.

The ASCII file post processor includes VAR, FLX, RAW and HKD file types.

### 3.11 File Concatenation

In a measurement, data files are stored in chunks of hourly files with file name convention YYMMDDHH.xxx (YY = year (two digits), MM = month, DD = day, HH = hour, xxx = file type extension (RAW, VAR, FLX or HKD)). For inspecting data, it is sometimes more convenient to overview a full day of data.

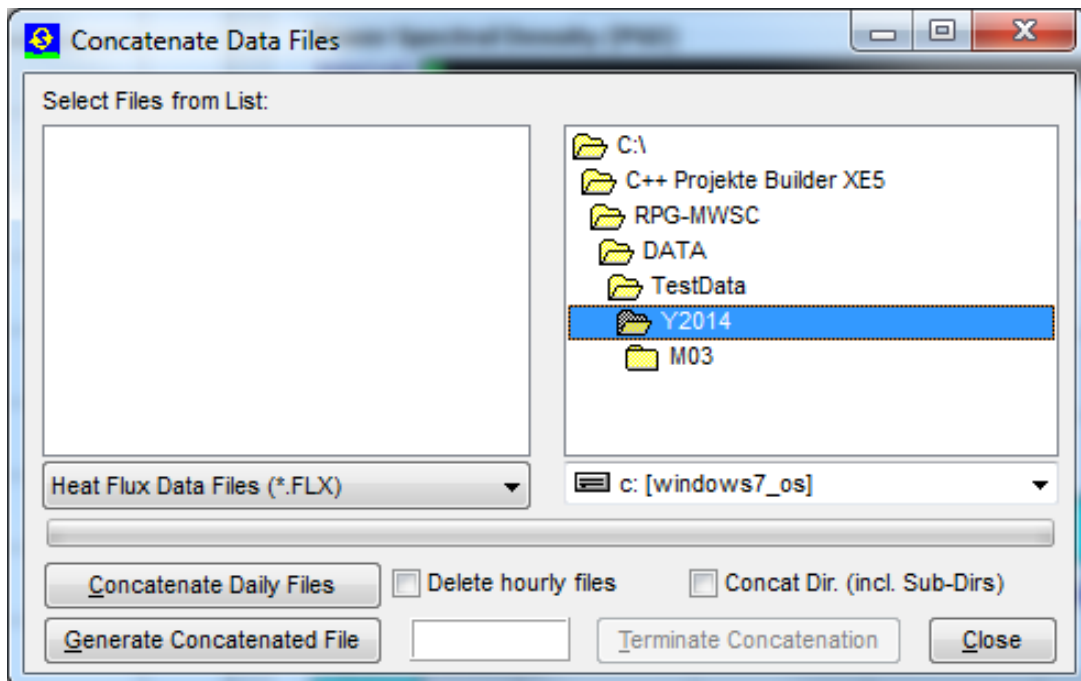
If the user enables **Auto File Concat.** within the **Directories and Data Formats** menu, the hourly files are automatically concatenated to daily files. For example, the files

**14051300.VAR, 14051301.VAR, 14051302.VAR, 14051303.VAR,...**

Are connected to a file named **140513.VAR**; of course the two digits HH for the hour are missing in this filename. The hourly files are deleted after concatenation.

It should be clear that only files of the same type can be concatenated.

If the automatic file concatenation was not activated during a measurement, this procedure can be post processed by clicking :

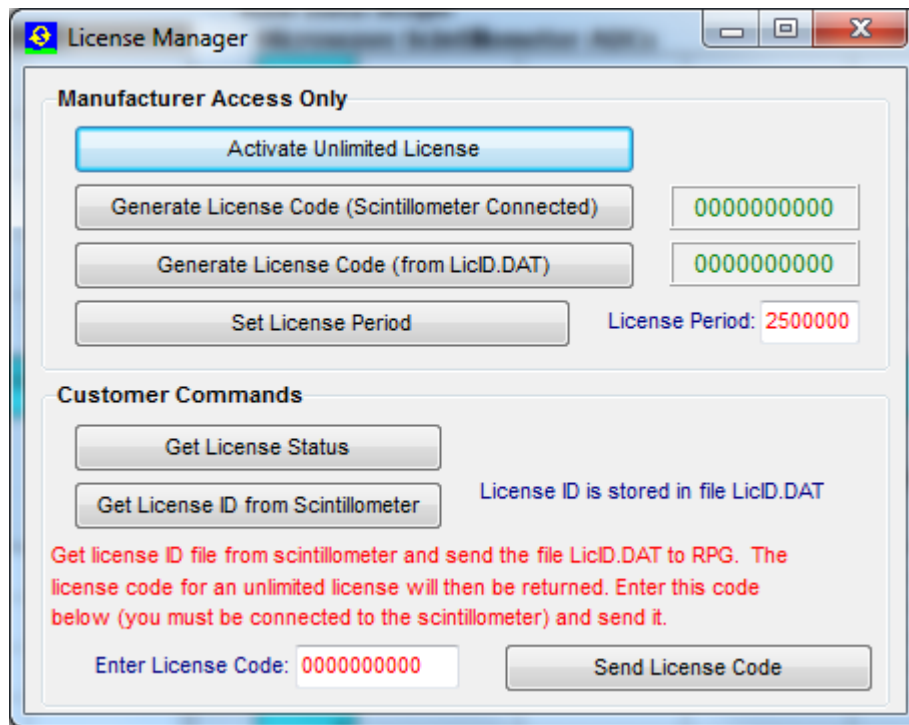


**File concatenation menu. The user may concatenate multiple files from a file list or perform the concatenation process in complete directories (all types in a row), with or without sub-directories. This enables the post processing of a complete data set, e.g. by selecting a 'year' directory (for instance Y2014) with just a few mouse clicks.**

### 3.12 The License Manager

RPG's scintillometers are delivered with a preliminary limited license of 30 days. Without activating an unlimited license, the scintillometer stops operation when the limited license is expired. The common procedure to avoid this is the following:

Invoke the **License Manager** by clicking the  button. The menu below pops up.



**License manager menu.**

The user retrieves license status information with the **Get License Status** command. The license type (limited or unlimited) as well as the expiration date and time will be displayed. In order to obtain an unlimited license, the following steps have to be performed:

1. Connect to the scintillometer and click the **Get License ID from Scintillometer** button. The license ID code is then written to the file 'LicID.DAT' stored in the license directory ...**LICENSEI** (see Section 3.1.2).
2. Send the 'LicID.DAT' file to [remotesensing-service@radiometer-physics.de](mailto:remotesensing-service@radiometer-physics.de) and you will receive the 10 digit license code via e-mail.
3. Enter the 10 digit license code into the edit box in the license manager and click **Send License Code**. The license manager will inform the user if the unlimited license installation was successful or not. If not successful, please contact RPG again.

### 3.13 Software Updates

Sometimes it is desirable to update the scintillometer and host software version, in order to add advanced features to the data processing or to correct software bugs.

The scintillometer SW is running on an embedded PC and is named **ScinPC.EXE**. This file is located in the scintillometer's root directory ...\**RPG-MWSC\**

The host SW name is **MWSC.EXE** and it is located in the application's root directory (...\**RPG-MWSC\**) on the H-PC.

For a SW update the following steps should be followed:

#### 1. Step: Save the old software versions

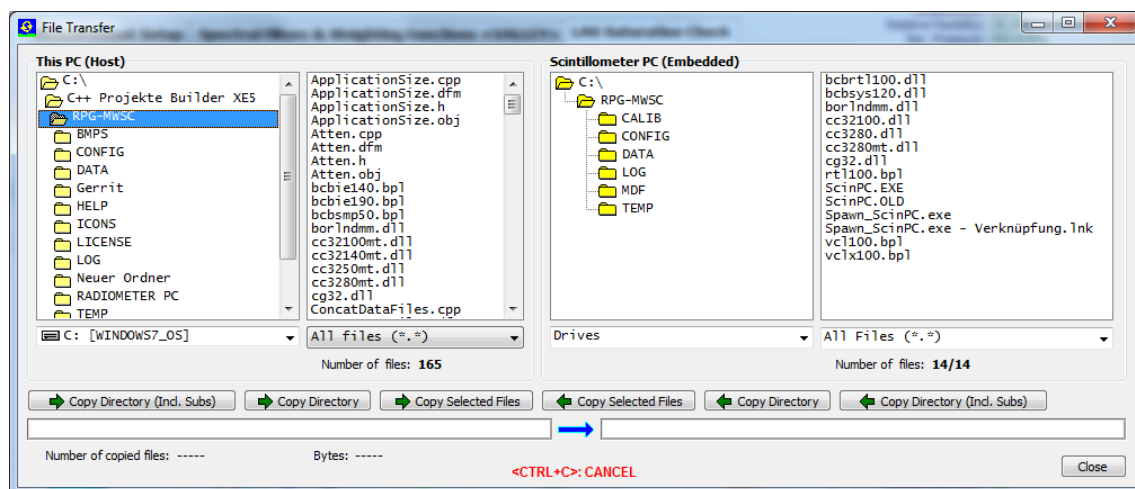
a) Create a directory to save the old software versions (e.g. **C:\MyPath\Save**).

b) Connect the H-PC to the scintillometer and enter the File Transfer Menu (↔). On the left side (H-PC, 'This PC (Host)') browse to the directory for saving the files (e.g. C:\MyPath\SAVE) and on the right side (Scintillometer) in the ...\**RPG-MWSC\** directory mark the **ScinPC.EXE** file. Then click ← **Copy Selected Files**.

c) locate the **MWSC.EXE** file in the ...\**RPG-MWSC\** directory on the H-PC and copy this file to the **C:\MyPath\Save** directory (by using the Operating System Explorer).

#### 2. Step: Overwrite the old versions by the new ones

a) Copy the new version of **ScinPC.EXE** (the S-PC software) to an arbitrary directory on your Host PC (e.g. ...\**RPG-MWSC\Scintillometer PC**). In the file transfer menu, browse to that directory. Mark the **ScinPC.EXE** file in the file list within the **This PC (Host)** box and mark the ...\**RPG-MWSC\ directory** in the **Scintillometer PC (Embedded)** box. Click the **Copy Selected Files** → button. Because you are now going to overwrite a file in the scintillometer's system directory, you must enter the Administrator password to proceed.



**File Transfer Menu**

- b) Restart the software on the S-PC to run the new **ScinPC.EXE** version ().
- c) Terminate **MWSC.EXE** on the host and overwrite it by the new version.
- d) Execute **MWSC.EXE** and reconnect to the scintillometer with .

The software upgrade is finished. You can confirm the successful upgrade by reading the software version numbers of both, the embedded S-PC (see main window, **Receiver Status** box on the right side) and the H-PC (see main window caption).

### 3.14 Automatic E-Mail Warning Messages

While a measurement is running, several events that may occur are of major interest for the user. These events could be:

- A scintillometer hardware problem
- A communication loss to the scintillometer has occurred
- The power level from transmitter is too low
- The free disk space on the scintillometer or host is insufficient

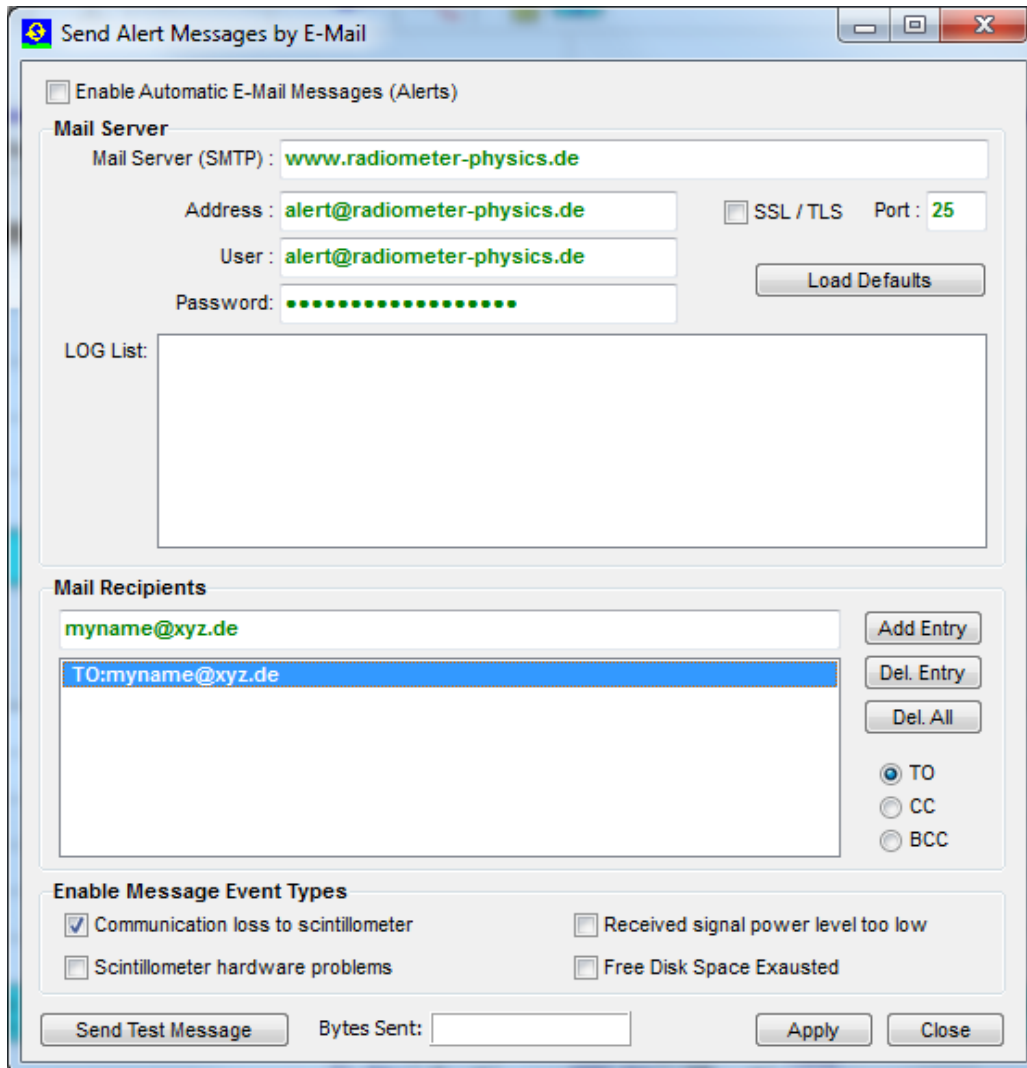
The host SW offers the possibility to send automatic e-mails to pre-defined addresses

via a built-in SMTP server. Click  to enter the SMTP server menu:

The first step is to define the SMTP server details. The user may configure a server of his choice (enter the server, a user address with user and password and the port number for the server) or simply click **Load Defaults** to use the RPG mail server for this purpose.

Then enter the address of a mail recipient as a message target and add it to the mail list (**Add Entry**). Before adding an address, the copy status may be selected (TO, CC, BCC). The message types can be enabled or disabled separately. Mail server settings, the mailing list and event types are stored permanently by clicking **Apply**.

The communication may be tested by sending a test message (**Send Test Message**). Automatic e-mails must be enabled by checking **Enable Automatic E-Mail Messages (Alerts)**.

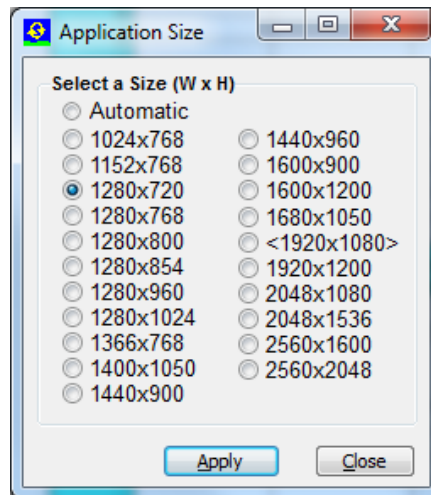


**Menu for defining automatic E-Mail warning messages.**

### 3.15 Changing the Application Size on the Screen

The host SW can scale the application to almost any common screen size. This may be useful if you want to use a beamer to display the host application in the beamer's screen

resolution and size. Click  to enter the **Application Size** menu:



The screen size in brackets <...> is the host's maximum screen size but you can select any (smaller) sizes to fit the application on other screens (like a beamer). The application sizing can be done any time, even during a running measurement.

### 3.16 Shutting Down the Scintillometer PC

Before the scintillometer is turned off (power off), it should be shut down first. This is performed by the  button. After a shutdown has been initiated, please wait for at least one minute before powering down the MWS. In case a restart of the embedded

Scintillometer PC is required click on  .

## 4. Scientific Background

### 4.1 Turbulent Fluxes in the Surface Layer

The atmospheric boundary layer is the part of the atmosphere which is directly influenced by the Earth's surface. The lowest 10% of the boundary layer are called the surface layer [5]. The surface layer is characterized by

- Turbulent mixing
- Logarithmic wind profile due to surface friction
- Constant vertical heat fluxes.

The observation of heat fluxes are needed to quantify the surface energy balance. At the surface the balance between short wave and long wave radiation leads to net transport of energy from the atmosphere to the surface. This energy surplus is balanced by turbulent sensible and latent heat fluxes towards the atmosphere and a soil heat flux into the ground (*Figure 2*).

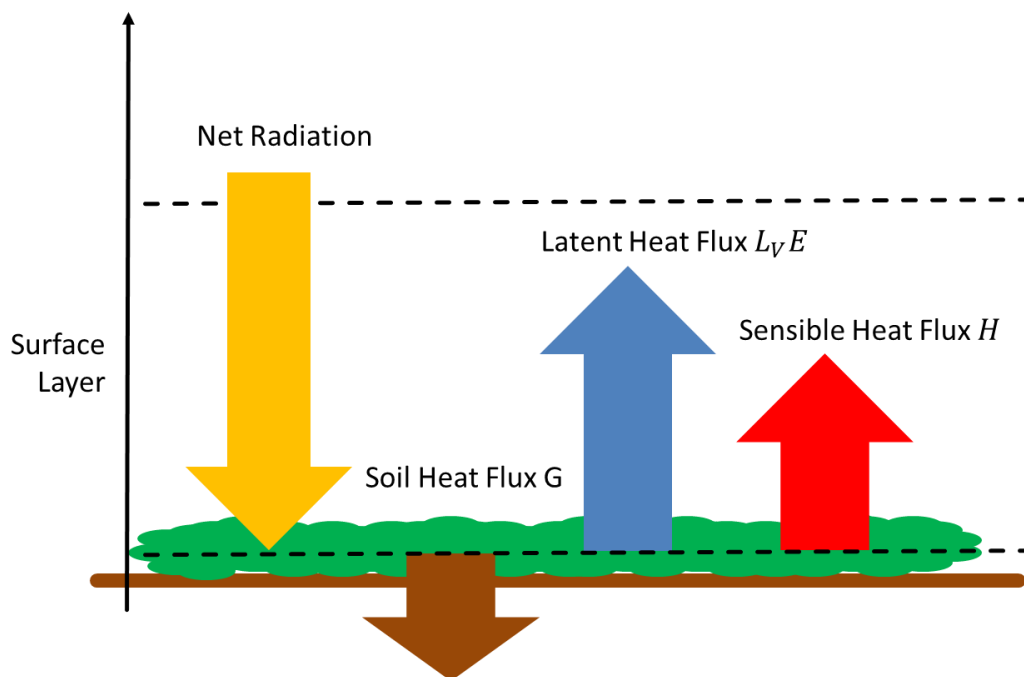


**Figure 2: Energy balance at the surface. The arrows give the local energy fluxes.**

The turbulence is driven by wind friction and radiative heating/cooling at the surface. The energy induced by these forcings lead to the creation of relatively large eddies. The size of these eddies is larger than the so called outer scale  $L_0$ . Once created, eddies repeatedly break up into smaller and smaller eddies. This process is called the energy cascade. so-called inner scale  $l_0$ . At this point, the energy of the smallest eddies is transferred into heat.  $L_0$  and  $l_0$  divide the turbulence spectrum into three regimes, the production range, the inertial sub-range and the dissipation range (*Figure 3*).

The energy cascade within in the inertial sub-range can be described by the Kolmogorov spectrum:

$$\phi_n(k) = 0.033 C_n^2 k^{-11/3}, \quad (1)$$

with the eddies' spherical wave numbers  $k = 2\pi/\lambda$  and the structure parameters  $C_n^2$ . Under the assumption of an isotropic and homogeneous turbulence field [3], the structure parameter for two points with distance  $r$  is given by:

$$C_n^2(r) = r^{-2/3} \langle [n(r, t) - n(0, t)]^2 \rangle. \quad (2)$$

$C_n^2$  characterizes the turbulent flow in the inertial sub-range. It can be derived from scintillometer measurements.

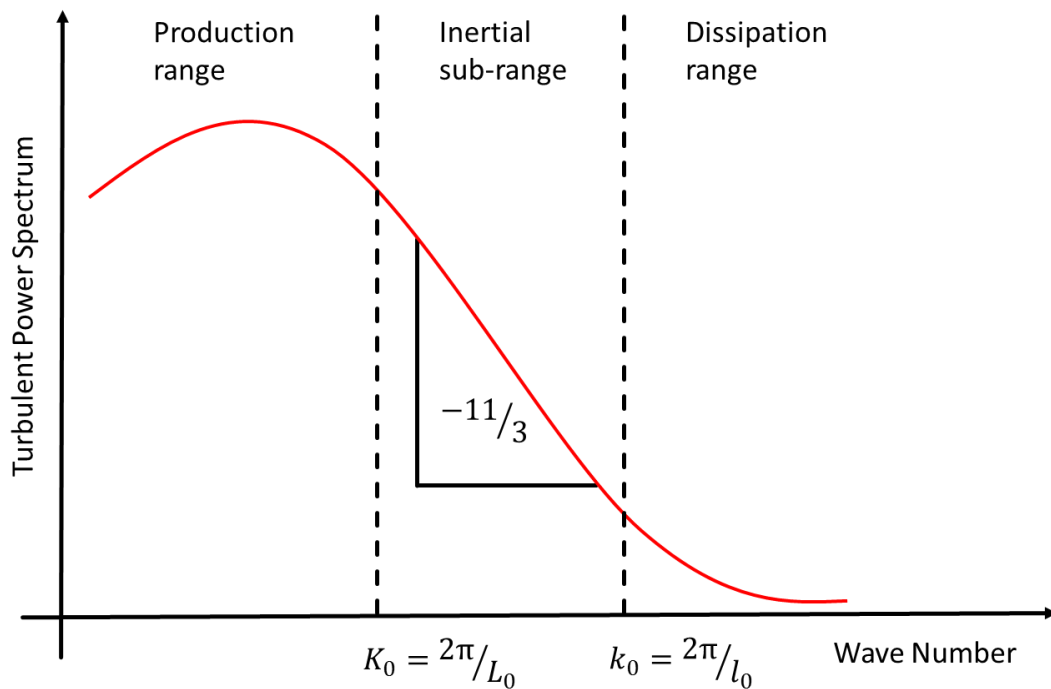


**Figure 3: Turbulent power spectrum of eddies with the inner and outer scale  $l_0$  and  $L_0$ , respectively.**

## 4.2 The Scintillation Signal

A scintillometer observing at a single wave length  $\lambda$  consists of a single transmitter (Tx) that emits a signal of constant intensity  $I_\lambda$  and a receiver (Rx) that records the signal fluctuations. The distance between the transmitter and the receiver is called the path length  $L$  (Figure 4).

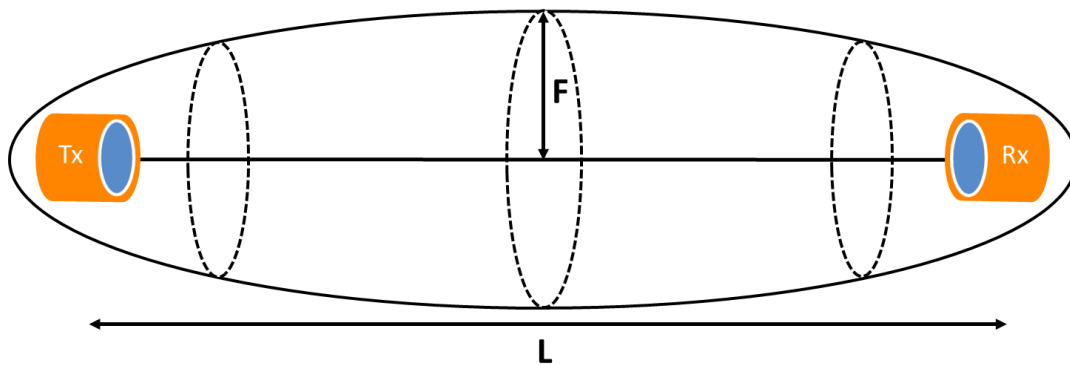


**Figure 4: Signal path  $L$  and first Fresnel zone with the maximum radius  $F$  (Fresnel length).**

The observed signal fluctuations are due to turbulent structures of the atmospheric refractive index. Under the assumption of Taylor's theorem a frozen turbulent is advected through the measurement path by the mean cross wind (Figure 5). This means that the spatial structure of the turbulent flow - expressed by the structure parameter  $C_n^2(z)$  - can be captured by recording the time series of the scintillation signal [6]. However, this is only true as long as the eddies observed by the scintillometer lie within the inertial sub-range of the turbulence spectrum.

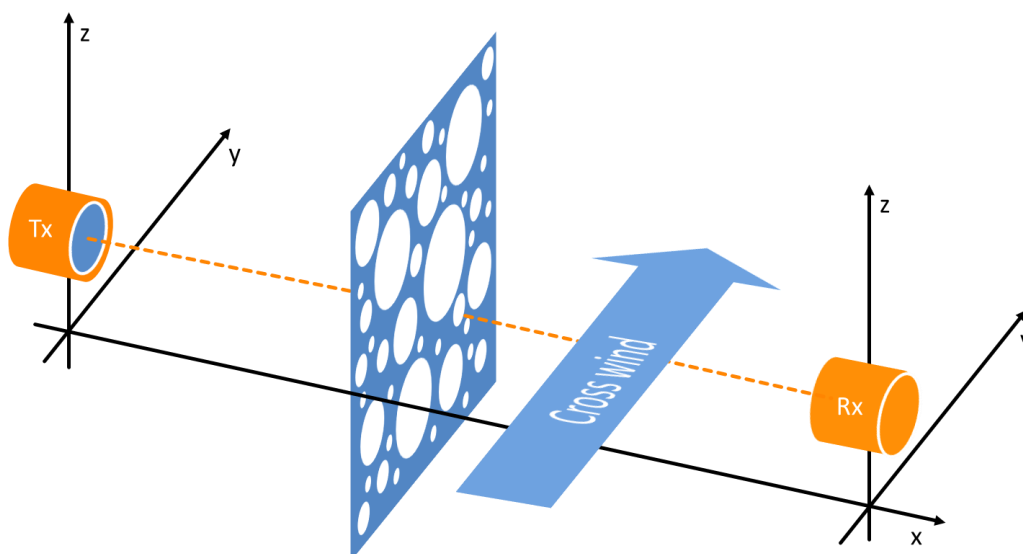


**Figure 5: Taylor's theorem – the cross wind advects the frozen turbulence field through the scintillometer beam.**

In order to validate this assumption the so-called Fresnel length, which combines wave length  $\lambda$  and  $L$ , is introduced:

$$F = \sqrt{\lambda L} . \quad (3)$$

$F$  is the maximum diameter of the first Fresnel zone (*Figure 4*). The first Fresnel zone is an ellipsoid with the transmitter and receiver units in the focal spots. It characterizes the area where most of the scintillation signal is generated. Therefore, a clean scintillation signal can only be observed when the first Fresnel zone is free of obstacles. Any signals that originate from the edges of the first Fresnel zone interfere destructively with the signal coming straight from the transmitter. As signals originating from the middle of the path dominate the total scintillation signal (*Figure 7*),  $F$  reflects the eddy size that most effectively contributes to the scintillation signal. This means that the Kolmogorov spectrum (equation (1)) can be applied for:

$$l_0 < F < L_0 . \quad (4)$$

The observed scintillation signal combines large scale effects due to refraction (eddies as focusing lenses) and diffraction (bending around eddies). At the lower of the eddy spectrum observations are constrained by the inner scale  $l_0$ . In case of  $F \ll l_0$  refraction dominates. Otherwise, diffraction is the dominating process. For microwave frequencies,  $F$  is so large that diffraction always dominates [7]. On the other end, the outer scale  $L_0$  is in the order of the observation height above the surface [8]. This means in case the path height is too small compared to the path length, outer scale effects may affect MWS measurements, because

the Fresnel length is in the same order. Also for LAS measurements at path lengths  $L > 100m$  diffraction is the dominating process ( $F \gg l_0$ ). (4) is easily met by optical scintillimeters. In case of Large Aperture Scintillometers (LAS), the inertial sub-range is more constrained by the antenna's aperture diameter  $D$  [8]:

$$20l_0 < D < 10L_0 . \quad (5)$$

This means,  $D$  has to be large enough to efficiently suppress inner scale effects. In this case, small scale turbulence is effectively averaged out across the antenna aperture (equations 18-20).

The scintillation signal is given by the variance  $\sigma_{\ln(I_\lambda)}^2$  of logarithmic intensity fluctuations. A theoretical value of the measured variance is given by the solution of the wave equation using Rytov's perturbation method. For spherical waves that propagates from a point source to a point detector through a statistically homogenous and isotropic medium it is given by [9]:

$$\sigma_{\ln(I_\lambda)}^2 = 16\pi^2 k_\lambda^2 \int_0^L dx \int_0^\infty dk k \phi(k) \sin^2 \left( \frac{x(L-x)k^2}{2k_\lambda} \right) , \quad (6)$$

where  $k_\lambda = 2\pi/\lambda$  is the spherical wave number of the observed wave length. Equation (6) relates the observed variances to the turbulence spectrum  $\phi(k)$ . All other parameters are determined by the measurement setup. Under the condition that the scintillometer measures within the inertial sub-range (equation (4)), the measured variance  $\sigma_{\ln(I_\lambda)}^2$  provides the path averaged structure parameter  $\langle C_n^2 \rangle$ .  $\langle C_n^2 \rangle$  can be derived from the variance of **logarithmic** signal Intensities  $I$  and the measurement configuration by [1]:

$$\langle C_{n,LAS} \rangle^2 = 1.12 \sigma_{\ln(I_{LAS})}^2 D^{7/3} L^{-3}, \quad (7)$$

$$\langle C_{n,MWS} \rangle^2 = 2.015 \sigma_{\ln(I_{MWS})}^2 k^{-7/6} L^{-11/6}. \quad (8)$$

### 4.3 Sensible and Latent Heat Fluxes from Scintillometry

The use of scintillometry for measurements of turbulent fluxes within the surface layer is a well-established technique. Optical scintillometers have been successfully operated for many years now.

The problem is that using optical scintillometers alone allows to determine the sensible heat flux  $H$ , but not the latent heat flux  $L_V E$  due to evapotranspiration. However,  $L_V E$  makes up an important contribution to the surface energy balance (*Figure 2*). Obviously, both components should be observed at once. The simultaneous measurement of both fluxes is provided by Eddy-Covariance (EC) stations. However, these are point measurements, which provide limited spatial representativeness and require relatively long integration times. In contrast, scintillometers provide path-integrated measurements at shorter integration times.

Like EC stations, scintillometry can provide direct measurements of the sensible heat flux  $H$  and the latent heat flux  $L_V E$  at the same time by combining an optical scintillometer with a microwave scintillometer like the RPG-MWSC-160. The combined system records time series of intensity fluctuations are simultaneously for both wave lengths. This allows the evaluation of not only the optical and microwave signal alone, but also the co-spectrum of both instruments. This allows for an independent calculation of sensible and latent heat fluxes at once [2]. The concept of the combined scintillometer systems is to ...

1. ... relate **three** measured (co)variances to **three** structure parameters of the refractive index.
2. ... use measurements of temperature and humidity to transfer the structure parameters of the refractive index to **three** structure parameters that describe the turbulent temperature and humidity field.
3. ... apply the Monin-Obukhov Similarity Theory (MOST) to the structure parameters of temperature and humidity field to estimate the sensible and latent heat flux.

In following section gives a detailed description of this the process, which his implemented in the operating software.

#### 4.4 The Data Processing Chain

This chapter describes the theoretical basis of the RPG-MWSC-160 software's (chapter 3) data processing chain: Starting with measured signal intensities and ending with the determination of sensible and latent heat fluxes  $H$  and  $L_V E$ .

In large parts the data evaluation follows the publication of Lüdi et al. (2005) [2] who introduce a method that combines a Large Aperture Scintillometer (LAS) and a MicroWave Scintillometer (MWS). The combined Optical/Microwave System (OMS) method uses the covariance system of the signal intensities measured at each wave length. This method is superior to the Two-wave-length method [3], because it does not depend on the assumption of a constant correlation between temperature and humidity fluctuations.

Figure 6 gives an overview on the complete data processing chain.

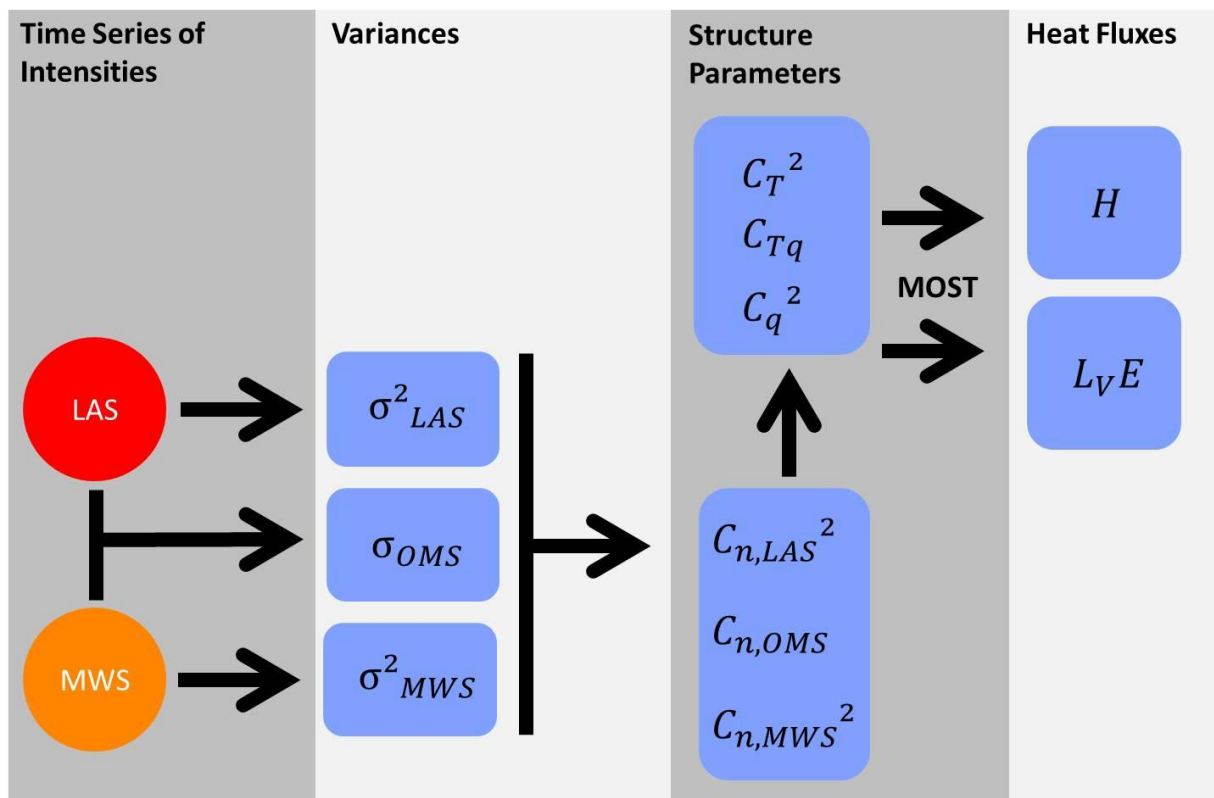


Figure 6: Scheme of RPG-MWSC-160 data processing: from signal intensities to heat fluxes.

#### 4.4.1 From Signal Variances to Structure Parameters

Both receivers of the OMS system provide a detector voltage that is proportional to the observed signal intensities. The variances over a given time interval of the **logarithmic intensities**  $\ln(I_{LAS}/I_{LAS}^0)$  and  $\ln(I_{MWS}/I_{MWS}^0)$  are:

$$\sigma_{LAS}^2 = \overline{\left( \ln \left( \frac{I_{LAS}}{I_{LAS}^0} \right) - \overline{\ln \left( \frac{I_{LAS}}{I_{LAS}^0} \right)} \right)^2} \quad (9)$$

$$\sigma_{MWS}^2 = \overline{\left( \ln \left( \frac{I_{MWS}}{I_{MWS}^0} \right) - \overline{\ln \left( \frac{I_{MWS}}{I_{MWS}^0} \right)} \right)^2} \quad (10)$$

The integration time interval (variance integration period) has to cover the whole scintillation down to frequencies of approximately 0.01Hz. The covariance of the two signals is given by:

$$\sigma_{OMS} = \overline{\left( \ln \left( \frac{I_{LAS}}{I_{LAS}^0} \right) - \overline{\ln \left( \frac{I_{LAS}}{I_{LAS}^0} \right)} \right) \left( \ln \left( \frac{I_{MWS}}{I_{MWS}^0} \right) - \overline{\ln \left( \frac{I_{MWS}}{I_{MWS}^0} \right)} \right)} \quad (11)$$

The signal levels  $I_{LAS}^0$  and  $I_{MWS}^0$  are used to scale the scintillation signals. They are provided by a running average value of the raw signal. The scaling makes the scintillation signal independent of the absolute detector level and includes acts as a high pass filter of the raw signal. The filtering effect is valuable used to exclude gain drifts and separates the scintillation signal from atmospheric absorption processes [10]. The latter aspect is particularly important for the microwave signal (water vapor absorption).

When equation (6) is applied to the OMS system, the following theoretical values for the measured (co)variances is given by [2]:

$$\sigma_{LAS}^2 = 8.448\pi^2 k_{LAS}^2 \int_0^L dx \int_0^\infty dk k^{-8/3} H_{LAS} F_{LAS} C_{n,LAS}^2, \quad (12)$$

$$\sigma_{MWS}^2 = 8.448\pi^2 k_{MWS}^2 \int_0^L dx \int_0^\infty dk k^{-8/3} H_{MWS} F_{MWS} C_{n,MWS}^2, \quad (13)$$

$$\sigma_{OMS} = 8.448\pi^2 k_{LAS} k_{MWS} \int_0^L dx \int_0^\infty dk k^{-8/3} H_{OMS} F_{OMS} J_0(k|d|) C_{n,OMS}, \quad (14)$$

with spherical wave numbers  $k = 2\pi/\lambda$ , the first order Bessel function  $J_0$ , the beam displacement  $d$  along the path  $L$ , and :

(15)

$$H_{LAS} = \left( \sin \left( \frac{\frac{x}{L}(L-x)k^2}{2 k_{LAS}} \right) \right)^2,$$

(16)

$$H_{MWS} = \left( \sin \left( \frac{\frac{x}{L}(L-x)k^2}{2 k_{MWS}} \right) \right)^2,$$

(17)

$$H_{OMS} = \sin \left( \frac{\frac{x}{L}(L-x)k^2}{2 k_{MWS}} \right) \sin \left( \frac{\frac{x}{L}(L-x)k^2}{2 k_{LAS}} \right).$$

Large aperture scintillometers (LAS) are limited in resolving turbulent structures, because signal scintillation signals from eddies smaller than the antenna's aperture cancel out each other across the aperture. This effect is assigned for by the following aperture averaging terms [2]:

(18)

$$F_{LAS} = \frac{\left( J_1 \left( 0.5kD_{LAS} \left( 1 - \frac{x}{L} \right) \right) \right)^2 \left( J_1 \left( 0.5kD_{LAS} \left( \frac{x}{L} \right) \right) \right)^2}{(0.5kD_{LAS})^4 \left( 1 - \frac{x}{L} \right)^2 \left( \frac{x}{L} \right)^2}$$

(19)

$$F_{MWS} = \frac{\left( J_1 \left( 0.5kD_{MWS} \left( 1 - \frac{x}{L} \right) \right) \right)^2 \left( J_1 \left( 0.5kD_{MWS} \left( \frac{x}{L} \right) \right) \right)^2}{(0.5kD_{MWS})^4 \left( 1 - \frac{x}{L} \right)^2 \left( \frac{x}{L} \right)^2}$$

(20)

$$F_{OMS} = \frac{J_1 \left( 0.5kD_{LAS} \left( 1 - \frac{x}{L} \right) \right) J_1 \left( 0.5kD_{LAS} \left( \frac{x}{L} \right) \right) J_1 \left( 0.5kD_{MWS} \left( 1 - \frac{x}{L} \right) \right) J_1 \left( 0.5kD_{MWS} \left( \frac{x}{L} \right) \right)}{(0.5k)^4 D_{LAS}^2 D_{MWS}^2 \left( 1 - \frac{x}{L} \right)^2 \left( \frac{x}{L} \right)^2}$$

with the antenna aperture's  $D_{LAS}$  and  $D_{MWS}$ , and the first order Bessel function  $J_1$ . For LAS systems the Fresnel length is always smaller than the antenna aperture. In this case the resolved range of resolved eddies is limited to wave numbers  $k$  larger than the aperture and  $F_{LAS}$  becomes zero. For the MWS, where the Fresnel length is larger than the aperture diameter,  $F_{MWS} = 1$  for all wave numbers.

The double integrals of equations 12-14 include the normalized spatial weighting functions:

$$W_{LAS}(x) = \int_0^{\infty} dk k^{-8/3} H_{LAS} F_{LAS} \bigg/ \int_0^L dx \int_0^{\infty} dk k^{-8/3} H_{LAS} F_{LAS} \quad (21)$$

$$W_{MWS}(x) = \int_0^{\infty} dk k^{-8/3} H_{MWS} F_{MWS} \bigg/ \int_0^L dx \int_0^{\infty} dk k^{-8/3} H_{MWS} F_{MWS} \quad (22)$$

$$W_{OMS}(x) = \int_0^{\infty} dk k^{-8/3} H_{OMS} F_{OMS} J_0(k|d(x)|) \bigg/ \int_0^L dx \int_0^{\infty} dk k^{-8/3} H_{OMS} F_{OMS} J_0(k|d(x)|) \quad (23)$$

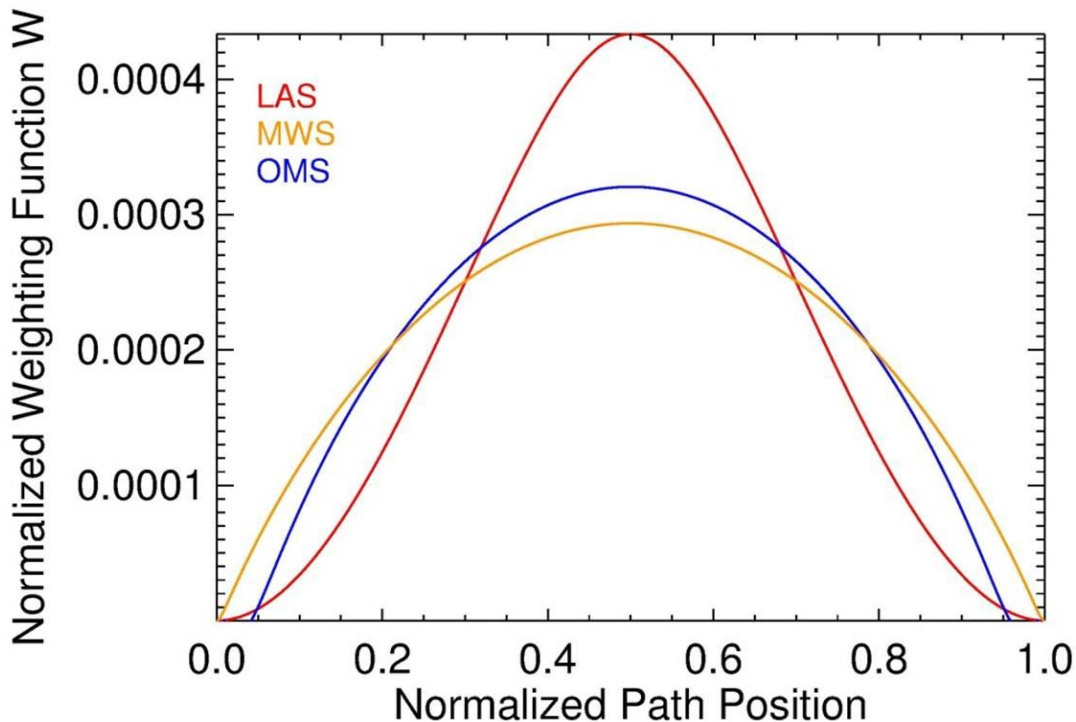


**Figure 7: Normalized path weighting functions.**

The weighting functions give the contribution of different position on the path to the total scintillation signal. For symmetric instrument setups the weighting function peak in the middle of the path (Figure 7). This reflects the fact that eddies with radii in the order of the Fresnel length (Figure 4) contribute most effectively to the scintillation signal.

Furthermore, the dependency of equations 12-14 on the wave number  $k$  can be extracted by defining the spectra filter functions [2]:

$$G_{LAS}(k) = 8.448\pi^2 k_{LAS}^2 \int_0^L dx k^{-8/3} H_{LAS} F_{LAS} \quad (24)$$

$$G_{MWS}(k) = 8.448\pi^2 k_{MWS}^2 \int_0^L dx k^{-8/3} H_{MWS} F_{MWS} \quad (25)$$

$$G_{OMS}(k) = 8.448\pi^2 k_{LAS} k_{MWS} \int_0^L dx k^{-8/3} H_{OMS} F_{OMS} J_0(k|d(x)|) \quad (26)$$

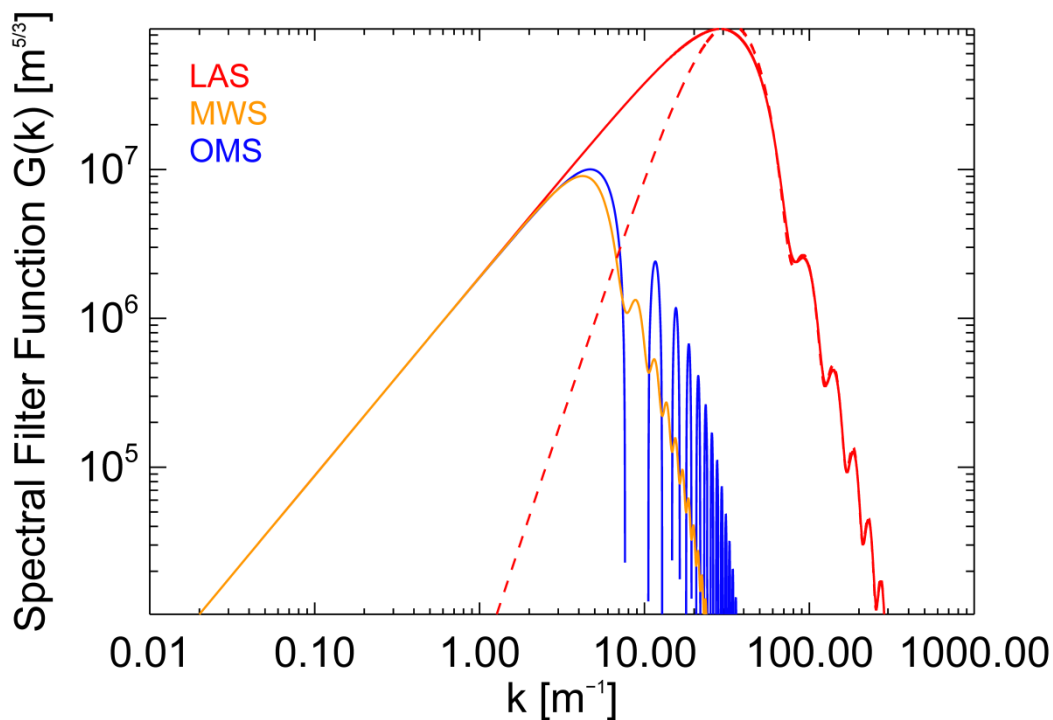


**Figure 8: The Spectral Filter functions  $G$  depend on the measurement setup ( $L = 1643 \text{ m}$ ,  $\vec{d} = (+0.4, -0.3)$ ,  $\lambda_{LAS} = 880 \text{ nm}$ ,  $\lambda_{MWS} = 1.86 \text{ mm}$ ,  $D_{LAS} = 0.145 \text{ m}$ ,  $D_{MWS} = 0.30 \text{ m}$ ).**

For path averaged structure parameters  $\langle C_{n,LAS} \rangle^2, \langle C_{n,MWS} \rangle^2, \langle C_{n,OMS} \rangle$  equations 4-6 transform to:

$$\langle C_{n,LAS} \rangle^2 = \sigma_{LAS}^2 / \int_0^{\infty} dk G_{LAS}(k) \quad (27)$$

$$\langle C_{n,MWS} \rangle^2 = \sigma_{MWS}^2 / \int_0^{\infty} dk G_{MWS}(k) \quad (28)$$

$$\langle C_{n,OMS} \rangle = \sigma_{OMS} / \int_0^{\infty} dk G_{OMS}(k) \quad (29)$$

While  $\sigma_{LAS}^2, \sigma_{MWS}^2, \sigma_{OMS}$  are provided by the scintillation measurements, the integral over G does only depend on the geometrical measurement configuration, the observed wave lengths and the antenna apertures.

#### 4.4.2 Structure Parameters of Temperature and Humidity

Once the structure parameters of the refractive index  $C_n$  have been determined, the turbulence field has to be expressed in terms of temperature and humidity, because the heat fluxes are mainly determined by fluctuations of these parameters.

$$C_{n,LAS}^2 = \frac{A_{T,LAS}^2}{\bar{T}^2} C_T^2 + 2 \frac{A_{T,LAS} A_{q,LAS}}{\bar{T} \bar{q}} C_{TQ} + \frac{A_{q,LAS}^2}{\bar{q}^2} C_q^2, \quad (30)$$

$$C_{n,MWS}^2 = \frac{A_{T,MWS}^2}{\bar{T}^2} C_T^2 + 2 \frac{A_{T,MWS} A_{q,MWS}}{\bar{T} \bar{q}} C_{TQ} + \frac{A_{q,MWS}^2}{\bar{q}^2} C_q^2, \quad (31)$$

$$C_{n,OMS} = \frac{A_{T,OMS}^2}{\bar{T}^2} C_T^2 + \frac{A_{T,LAS} A_{q,MWS} + A_{T,MWS} A_{q,LAS}}{\bar{T} \bar{q}} C_{TQ} + \frac{A_{q,OMS}^2}{\bar{q}^2} C_q^2, \quad (32)$$

where A-coefficients include the partial derivatives of the refractive index depending mainly on temperature and humidity [10] [11]. There are many different set available in the literature. Therefore, the user is able to set the coefficients by hand. The default values for  $A_{T,LAS}, A_{q,LAS}, A_{T,MWS}$ , and  $A_{q,MWS}$  used by the software are taken by from [4]

Reference	A-coefficients			
	$A_{T,LAS}$	$A_{q,LAS}$	$A_{T,MWS}$	$A_{q,MWS}$
<b>Ward et al.2013 [4] (spec.)</b>	<b><math>-2.70 \cdot 10^{-4}</math></b>	<b><math>-6.85 \cdot 10^{-7}</math></b>	<b><math>-4.13 \cdot 10^{-4}</math></b>	<b><math>7.14 \cdot 10^{-5}</math></b>
Ward et al. 2013 [4] (abs.)	$-2.71 \cdot 10^{-4}$	$-6.89 \cdot 10^{-7}$	$-3.42 \cdot 10^{-4}$	$7.18 \cdot 10^{-5}$

**Table 1: Coefficients for optical and microwave frequencies for standard atmospheric conditions ( $T = 288 \text{ K}, p = 1000 \text{ hPa}, q = 0.010 \text{ kg kg}^{-1}$ ). The software uses be coefficients based on the conservation of specific humidity (bold) instead of absolute humidity [4].**

The system of the three equations (30-32) can be solved when using an OMS system, because the combined method provides three structure parameters  $C_n$ . The corresponding coefficient matrix  $M$  is invertible when

$$\frac{A_{T,LAS} A_{q,MWS}}{A_{T,MWS} A_{q,LAS}} \neq 1,$$

and gives the solution for  $C_T^2, C_{Tq}, C_q^2$  [2] :

$$\begin{pmatrix} C_T^2 \\ C_{Tq} \\ C_q^2 \end{pmatrix} = M^{-1} \begin{pmatrix} C_{n,LAS}^2 \\ C_{n,MWS}^2 \\ C_{n,OMS} \end{pmatrix}, \quad (33)$$

with [9] [11]:

$$M^{-1} = \frac{1}{(A_{T,LAS} A_{q,MWS} - A_{T,MWS} A_{q,LAS})^2} \cdot \begin{bmatrix} A_{q,MWS}^2 / \bar{q}^2 & A_{q,LAS}^2 / \bar{q}^2 & -2 A_{q,LAS} A_{q,MWS} / \bar{T} \bar{q} \\ -A_{T,MWS} A_{q,MWS} / \bar{T} \bar{q} & -A_{T,LAS} A_{q,LAS} / \bar{T} \bar{q} & (A_{T,LAS} A_{q,MWS} + A_{T,MWS} A_{q,LAS}) / \bar{T} \bar{q} \\ A_{T,MWS}^2 / \bar{T}^2 & A_{T,LAS}^2 / \bar{T}^2 & -2 A_{T,LAS} A_{T,MWS} / \bar{T}^2 \end{bmatrix}, \quad (34)$$

#### 4.4.3 MOST– from Structure Parameters to Heat Fluxes

The Monin-Obukhov Scaling Theory (MOST) provides a relation between the structure functions and the heat fluxes for the horizontally homogenous turbulent surface layer. A central parameter of MOST is the Obukhov length  $L_{Ob}$ . For the unstable surface layer,  $L_{Ob}$  gives the negative of the height below which the turbulence is predominately generated by wind shear [13]. Above  $-L_{Ob}$  the production is dominated by buoyancy. In combination with the path height  $z = z_{eff} - d_0$  (Section 4.4.6),  $L_{Ob}$  is used to define the dimensionless stability parameter  $\zeta = z/L_{Ob}$ .  $\zeta < 0$  characterizes the unstable surface layer, while for  $\zeta \geq 0$ , the surface layer is stable. The relation between the structure parameters  $C_T^2$  and  $C_q^2$  is given by empirically determined MOST functions  $f_T(\zeta)$  and  $f_q(\zeta)$ :

$$\frac{z^{2/3} C_T^2}{T_*^2} = f_T(\zeta), \quad (35)$$

$$\frac{z^{2/3} C_q^2}{q_*^2} = f_q(\zeta), \quad (36)$$

with the scaling variables:

$$T_* = -\frac{H}{\bar{\rho} c_p u_*}, \quad (37)$$

(38)

$$q_* = -\frac{(1 - \bar{q})L_V E}{\bar{\rho} L_V u_*},$$

(39)

$$u_* = \frac{\kappa u}{\ln\left(\frac{z - d_0}{z_0}\right) - \Psi_m(\zeta) + \Psi_m(\zeta_0)}.$$

$u_*$  is the friction velocity,  $z_0$  is the roughness length and  $d_0$  is the zero displacement height.  $z_0$  and  $d_0$  are used to characterize the surface (Section Roughness Length and Zero-Displacement Height).  $\Psi_m(\zeta)$  and  $\Psi_m(\zeta_0)$  are stability corrections [6]:

$$x_m = (1 - 16 \zeta)^{1/4} \quad (40)$$

$$\Psi_m(\zeta) = 2 \ln\left(\frac{1+x_m}{2}\right) + \ln\left(\frac{1+x_m^2}{2}\right) + \operatorname{atan}(x_m) + \frac{\pi}{2} \quad (41)$$

for unstable conditions ( $\zeta < 0$ ) and

$$\Psi_m(\zeta) = 1 - (1 + 6.25 \zeta)^{4/5} \quad (42)$$

for stable conditions ( $\zeta \geq 0$ ).

The MOST functions are divided into two classes:

$$f_T(\zeta) = x_{T,1} (1 - x_{T,2} \zeta)^{-2/3}, \quad (43)$$

$$f_q(\zeta) = x_{q,1} (1 - x_{q,2} \zeta)^{-2/3} \quad (44)$$

for the unstable surface layer ( $\zeta < 0$ ) and

$$f_T(\zeta) = x_{T,1} (1 + x_{T,2} \zeta^{+2/3}), \quad (45)$$

$$f_q(\zeta) = x_{q,1} (1 + x_{q,2} \zeta^{+2/3}) \quad (46)$$

for the stable surface layer ( $\zeta \geq 0$ ).

The fit parameters  $x_{T,1}$ ,  $x_{T,2}$ ,  $x_{q,1}$  and  $x_{q,2}$  are usually determined from Eddy-covariance measurements.

Table 2 gives a short list of references, which include different parameter sets. The default values used by the operating software are taken from [14].

surface layer conditions	MOST coefficients							
	unstable				stable			
Reference	$x_{T,1}$	$x_{T,2}$	$x_{q,1}$	$x_{q,2}$	$x_{T,1}$	$x_{T,2}$	$x_{q,1}$	$x_{q,2}$
Wyngaard and Izumi 1971 [15]	4.9	7.0	-	-	4.9	2.75	-	-
Hartogensis and de Bruin [16]	-	-	-	-	4.7	1.6	-	-
<b>Li et al. 2012 [14]</b>	<b>6.7</b>	<b>14.9</b>	<b>3.5</b>	<b>4.5</b>	<b>4.5</b>	<b>1.3</b>	<b>3.5</b>	<b>2.4</b>

**Table 2: MOST coefficients from different publications. Default values of the operating software are given in bold numbers.**

The scaled variables  $T_*$ ,  $q_*$  and  $u_*$  are used to iteratively determine the sensible heat flux  $H$  and the latent heat flux  $L_V E$ . The starting point is an initial guess for  $H$  and  $L_V E$ . For known flux signs, the stability parameter  $\zeta = z/L_{Ob}$  is determined from the Obukhov length

$$L_{Ob} = \frac{u_*^2 \bar{T}}{g \kappa T_*}, \quad (47)$$

with the mean environmental temperature  $\bar{T}$ , the gravitational acceleration  $g$  and the von-Karman constant  $\kappa = 0.4$ . The iteration process converges to scales  $T_*$  and  $q_*$  that give the following fluxes:

$$H = -T_* \bar{\rho} c_p u_* , \quad (48)$$

$$L_V E = -\frac{\bar{\rho}}{(1 - \bar{q})} L_V u_* q_* . \quad (49)$$

Then mean specific humidity  $\bar{q}$  and the mean air density  $\bar{\rho}$  are determined from external in-situ measurements. However, the differentiation between stable and unstable conditions divides the flux calculations into two regimes. The stability of the surface layer is directly related to the direction of the sensible heat flux:  $\zeta$  and  $H$  are always of opposite sign. Therefore, the sign of  $H$  has to be known prior to the flux iteration. The ambiguity of the quadratic equations (37) does not allow determining the sign of  $H$  from the structure parameter  $C_T^2$ . Therefore, scintillometer measurements are often complemented by other observations to determine the flux signs. Fortunately, this is not needed when using an OMS system, because the co-spectrum provides the correlated structure parameter  $C_{Tq}$ . This allows observing the correlation coefficient

$$R_{Tq} = \frac{C_{Tq}}{\sqrt{C_T^2 C_q^2}} . \quad (50)$$

$R_{Tq}$  ranges between -1 and + 1 and gives the linear correlation between temperature and humidity fluctuations. In the classical two-wavelength method [17],  $R_{Tq}$  is set to +1 for unstable conditions and to -1 for stable conditions [3].  $R_{Tq}$  has the same sign as the product of sensible and latent heat flux  $H \cdot L_V E$  [3]. While negative sensible heat fluxes coincide with temperature inversions, negative latent heat fluxes are due to the formation of dew. Nevertheless, even when the latent heat flux becomes negative the absolute value is usually small. Therefore, RPG-MWSC's operating software assumes that the latent heat flux always has a positive sign ( $L_V E > 0$ ).

In this case,  $R_{Tq}$  unambiguously provides the sign of the sensible heat flux  $H$ . Typically, unstable conditions result in positive sensible heat fluxes during the day, while  $H$  becomes negative, when the stable surface layer is building up due to radiative cooling at night. Alternatively, strong evaporation may also lead to negative  $H$ . These cases can be identified by  $R_{Tq} < 0$  during the day.

#### 4.4.4 Signal Saturation

In weak turbulence, the measured LAS variance is proportional to the path-averaged structure parameter [18]:

$$\langle C_{n,LAS} \rangle^2 = 1.12 \sigma_{\ln(I_{LAS})}^2 D^{7/3} L^{-3}. \quad (51)$$

The proportionality is based on the single scattering approximation [1], which assumed that a wave front emitted by the transmitter is only disturbed once before reaching the receiver. This assumption breaks down, when turbulence becomes stronger [19]. As a consequence equations (12/14 are only valid for weak scattering which is limited by [19]:

$$\sigma_{\ln(I)}^2 < 0.3. \quad (52)$$

Beyond this limit – within the strong scattering regime - the signal variance is completely saturated and consequently does no longer increase with  $\langle C_{n,LAS} \rangle^2$  [20]. However, within an intermediate range the observed signals are only partially saturated. In contrast to the non-saturated signal, the variance is not proportional to the measured  $\langle C_{n,LAS} \rangle^2$  anymore, because multi-scattering effects degrade the coherence of the wave front. As a consequence, the signal contribution from eddies smaller than the Fresnel length increases [19]. For Kolmogorov turbulence (equation 1), smaller eddies contribute less to the total variance. Therefore, the observed variance starts to saturate. Following [1], the saturation free domain is further restricted by:

$$\langle C_{n,LAS} \rangle^2 < 0.193 L^{-8/3} \lambda^{2/6} D^{5/3}. \quad (53)$$

For the MWS system, which is much less affected by saturation, it is appropriate to use equation 54 alone to exclude saturation [10].

In the intermediate range the partially saturated LAS signal variance can be corrected by appending the following term to equations 12-14 [19][20]:

$$M_{ST} = \exp \left[ -48k_{LAS}^2 L \left( k\Psi(k) \left( 1 - J_0 \left( \frac{k^2 L \gamma (1-\gamma)}{k_{LAS}} \right) \right) + \int_k^\infty dk' \Psi(k') \left( 1 - J_0 \left( \frac{kk' L \gamma (1-\gamma)}{k_{LAS}} \right) \right) \right) \right], \quad (54)$$

with

$$\Psi(k) = \int_k^\infty dk' \Phi(k'). \quad (55)$$

This correction neglects the impact of the inner scale and is – following [20] - the most appropriate saturation correction. Within RPG's operating software, the correction is realized by a numerical look-up table that is automatically read during observations. The

tables have been calculated for each of the compatible LAS systems. Additionally, observations that do not meet the saturation limits (equations 54, 55) are flagged.

#### 4.4.5 Absorption Fluctuations

As stated in Section 4.4.1 the scintillation signal, can be separated from absorption fluctuations by normalizing the signal variance by a running mean value (equation 11). For the same purpose (in addition to cross wind detection) the LAS systems BLS900 and BLS2000 use a dual disk configuration. RPG-MWSC-160 fully supports this feature. RPG's data processing of the dual disk system is equivalent to the processing that is applied by Scintec (compare manufacturer's manual).

#### 4.4.6 Effective Height

When the OMS system is operated with almost constant beam heights over flat terrain without vegetation, the path height  $z$  is the average instrument height above ground. However, for slant paths and over topography, the beam height  $z_{beam}$  depends on the path position  $x$ . In this case an effective height  $z_{eff}$  shall be used (*Figure 9: Illustration of the effective height  $z_{eff}$  calculated for a slant path over topography.*).  $z_{eff}$  equals a constant observation height that reproduces the observed path averaged structure parameters  $\langle C_T \rangle^2$  and  $\langle C_q \rangle^2$  and can therefore be used to determine the fluxes  $H$  and  $L_V E$ . When the curvature effect and the stability is neglected, the effective height is calculated by [21]:

$$z_{eff} = \int_0^L dx z_{beam}(x) \cdot W(x). \quad (56)$$

$H_{eff}$  is calculated for the optical and microwave beam separately - using different weighting functions  $W_{LAS}$  and  $W_{MWS}$ . For the OMS system the average value is used:

$$z_{eff}^{OMS} = 0.5(z_{eff}^{LAS} + z_{eff}^{MWS}). \quad (57)$$

In case of dense vegetation it might be appropriate to define a zero-displacement height  $d_0$  to elevate the height reference (see Section 4.4.7 for details):

$$z = z_{eff} - d_0 \quad (58)$$

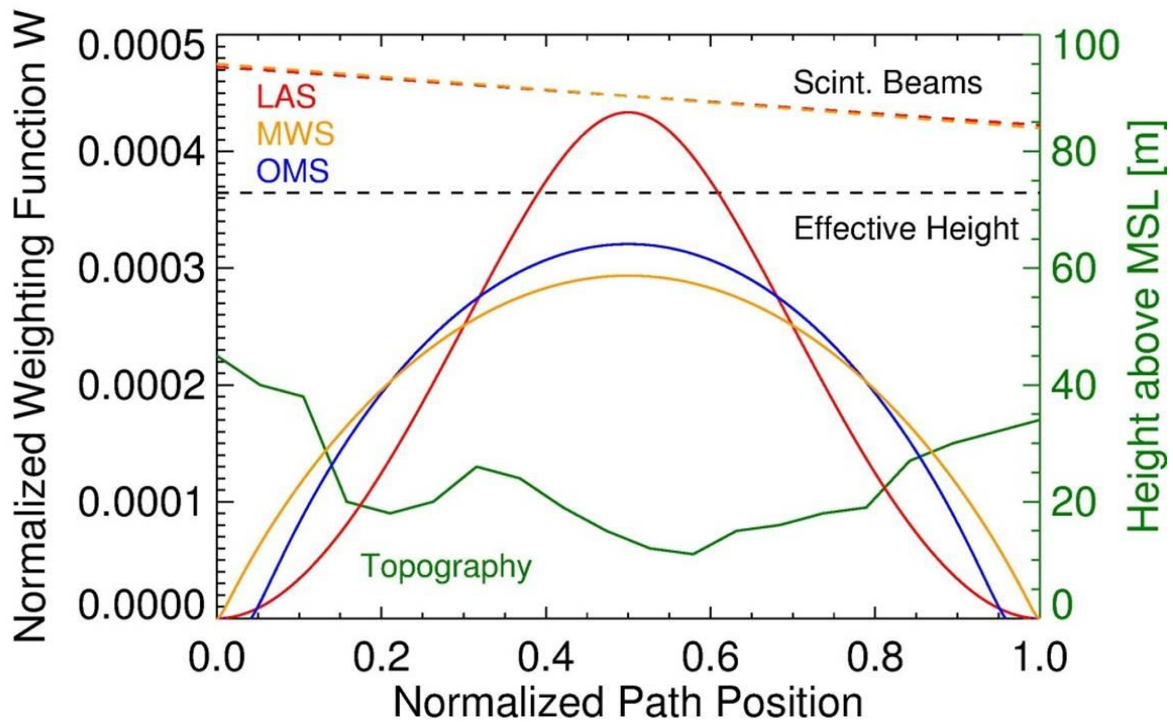


**Figure 9:** Illustration of the effective height  $z_{eff}$  calculated for a slant path over topography.

#### 4.4.7 Roughness Length and Zero-Displacement Height

When heat fluxes are derived from scintillometer measurement, it is assumed that the observations are performed within the surface layer. The surface is characterized by heat fluxes that are constant with height and a logarithmic profile of the horizontal wind speed

$$u(z) = \frac{u_*}{\kappa} \ln \left( \frac{z_{obs} - d_0}{z_0} \right), \quad (59)$$

with the wind speed observation height  $z_{obs}$  (being the installation height of the microwave receiver over ground - not the effective path height  $z_{eff}$ !), the friction velocity  $u_*$  and the von-Karman constant  $\kappa$ . The surface is described by the roughness length  $z_0$  and the zero-displacement height  $d_0$ .  $z_0 + d_0$  gives the height where the wind drops to zero due to surface friction. In case this layer is not known from wind profiler data, it has to be estimated.

The roughness of the surface is determined by the height  $H$  and distribution of roughness elements along the measurement path. The distribution is estimated by the average spacing  $X$  between the roughness elements. For  $X \gtrsim H$ , the displacement height  $d_0$  should be set to zero and landscape dependent values for  $z_0$  can be read from *Table 3*.

Terrain description	$X/H$	$z_0$ [m]
Open sea, Fetch at least 5 km		0.0002
Mud flats, snow; no vegetation, no obstacles		0.005
Open flat terrain; grass, few isolated obstacles		0.03
Low crops; occasional large obstacles	>20	0.1
High crops; scattered obstacles	15-20	0.25
Parkland, bushes; numerous obstacles	$\approx 10$	0.5
Regular large obstacle coverage (suburb, forest)		1.0
City centre with high- and low-rise buildings		>2.0

**Table 3:** Roughness length  $z_0$  for different landscapes from WMO CIMO guide [22].

However, if the roughness elements are densely packed, e.g. for observations over a dens crop field or forest, the vegetation with an average  $H_{veg}$  results in lifting the zero wind level by:

$$d_0 \approx 0.7H_{veg} . \quad (60)$$

The remaining roughness is then characterized by

$$z_0 \approx 0.1H_{veg} . \quad (61)$$

The most appropriate selection of  $z_0$  and  $d_0$  is illustrated in Figure 10: The settings for the roughness length  $d_0$  zero-displacement height  $z_0$  depend on. Apart from the friction velocity  $d_0$  is also applied to the effective height  $z_{eff}$  (Section 4.4.6).

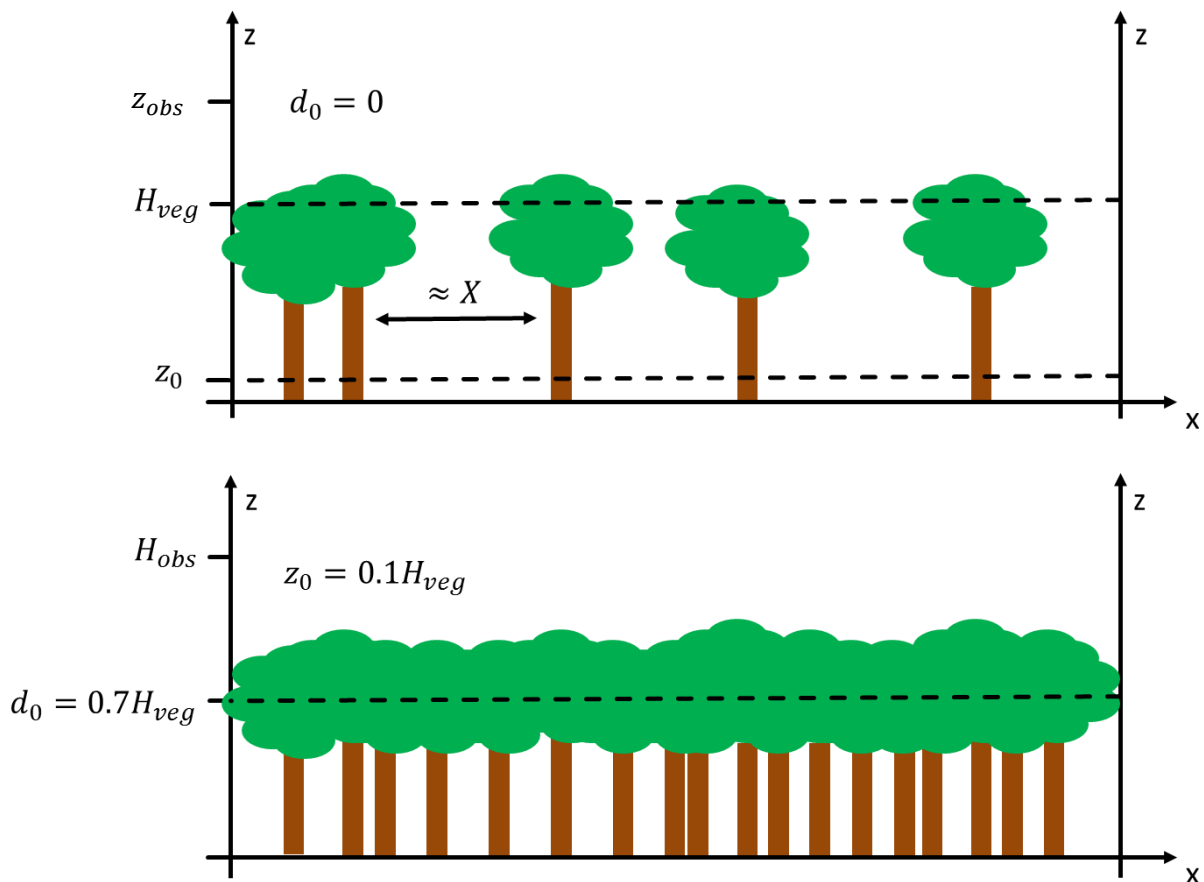


**Figure 10: The settings for the roughness length  $d_0$  zero-displacement height  $z_0$  depend on characteristic surface irregularities.  $H_{veg}$  is the vegetation height and  $z_{obs}$  is the observation height.**

#### 4.4.8 References

- [1] T. Wang, G. R. Ochs, and S. F. Clifford, "A saturation-resistant optical scintillometer to measure C2n," *J. Opt. Soc. Am.*, vol. 68, no. 3, pp. 334–338, Mar. 1978.
- [2] A. Lüdi, F. Beyrich, and C. Mätzler, "Determination of the Turbulent Temperature–Humidity Correlation from Scintillometric Measurements," *Bound.-Layer Meteorol.*, vol. 117, no. 3, pp. 525–550, Dec. 2005.
- [3] R. J. Hill, "Algorithms for Obtaining Atmospheric Surface-Layer Fluxes from Scintillation Measurements," *J Atmos Ocean Tech*, vol. 14, pp. 456–467, 1997.
- [4] H. C. Ward, J. G. Evans, O. K. Hartogensis, A. F. Moene, H. A. R. De Bruin, and C. S. B. Grimmond, "A critical revision of the estimation of the latent heat flux from two-wavelength scintillometry," *Q. J. R. Meteorol. Soc.*, p. n/a-n/a, 2013.
- [5] W. M. L. Meijninger, O. K. Hartogensis, W. Kohsiek, J. C. B. Hoedjes, R. M. Zuurbier, and H. A. R. D. Bruin, "Determination of Area-Averaged Sensible Heat Fluxes with a Large Aperture Scintillometer over a Heterogeneous Surface – Flevoland Field Experiment," *Bound.-Layer Meteorol.*, vol. 105, no. 1, pp. 37–62, Oct. 2002.
- [6] O. Hartogensis, "Exploring Scintillometry in the Stable Atmospheric Surface Layer," Wageningen, 2006.



- [7] A. J. H. van Kesteren, "Measuring water-vapour and carbon-dioxide Fluxes at Field scales with Scintillometry," Wageningen, 2012.
- [8] A. F. Moene, W. M. L. Meijninger, O. K. Hartogensis, W. Kohsiek, and H. A. R. De Bruin, "A review of the relationships describing the signal of a Large Aperture Scintillometer."
- [9] R. S. Lawrence and J. W. Strohbehm, "A survey of clear-air propagation effects relevant to optical communications," *Proc. IEEE*, vol. 58, no. 10, pp. 1523–1545, Oct. 1970.
- [10] W. M. L. Meijninger, F. Beyrich, A. Lüdi, W. Kohsiek, and H. A. R. D. Bruin, "Scintillometer-Based Turbulent Fluxes of Sensible and Latent Heat Over a Heterogeneous Land Surface – A Contribution to Litfass-2003," *Bound.-Layer Meteorol.*, vol. 121, no. 1, pp. 89–110, Oct. 2006.
- [11] E. L. Andreas, "Estimating  $C_n^2$  over snow and sea ice from meteorological data," *J. Opt. Soc. Am. A*, vol. 5, no. 4, p. 481, Apr. 1988.
- [12] E. L. Andreas, "Three-Wavelength Method of Measuring Path-Averaged Turbulent Heat Fluxes," *J. Atmospheric Ocean. Technol.*, vol. 7, no. 6, pp. 801–814, Dec. 1990.
- [13] A. M. Obukhov, "Turbulence in an atmosphere with a non-uniform temperature," *Bound.-Layer Meteorol.*, vol. 2, no. 1, pp. 7–29, Mar. 1971.
- [14] D. Li, E. Bou-Zeid, and H. A. R. De Bruin, "Monin–Obukhov Similarity Functions for the Structure Parameters of Temperature and Humidity," *Bound.-Layer Meteorol.*, vol. 145, pp. 45–67, 2012.
- [15] J. C. WYNGAARD, Y. IZUMI, and J. S. A. COLLINS, "Behavior of the Refractive-Index-Structure Parameter near the Ground," *J. Opt. Soc. Am.*, vol. 61, no. 12, pp. 1646–1650, Dezember 1971.
- [16] O. K. Hartogensis and H. A. R. D. Bruin, "Monin–Obukhov Similarity Functions of the Structure Parameter of Temperature and Turbulent Kinetic Energy Dissipation Rate in the Stable Boundary Layer," *Bound.-Layer Meteorol.*, vol. 116, no. 2, pp. 253–276, Aug. 2005.
- [17] W. Kohsiek and M. H. A. J. Herben, "Evaporation derived from optical and radio-wave scintillation," *Appl. Opt.*, vol. 22, no. 17, pp. 2566–2570, Sep. 1983.
- [18] D. L. FRIED, "Propagation of a Spherical Wave in a Turbulent Medium," *J. Opt. Soc. Am.*, vol. 57, no. 2, pp. 175–180, Feb. 1967.
- [19] S. F. Clifford, G. R. Ochs, and R. S. Lawrence, "Saturation of optical scintillation by strong turbulence," *J. Opt. Soc. Am.*, vol. 64, no. 2, pp. 148–154, Feb. 1974.
- [20] J. Kleissl, O. K. Hartogensis, and J. D. Gomez, "Test of Scintillometer Saturation Correction Methods Using Field Experimental Data," *Bound.-Layer Meteorol.*, vol. 137, no. 3, pp. 493–507, Dec. 2010.
- [21] O. K. Hartogensis, C. J. Watts, J.-C. Rodriguez, and H. A. R. De Bruin, "Derivation of an Effective Height for Scintillometers: La Poza Experiment in Northwest Mexico," *J. Hydrometeorol.*, vol. 4, no. 5, pp. 915–928, Oct. 2003.
- [22] "CIMO Guide 7th Edition," *calameo.com*. [Online]. Available: <http://www.calameo.com/books/000418449cceb3c866f47>. [Accessed: 04-Apr-2014].



## 5. Appendix A (File Formats)

### 5.1 A1a: Heat Flux Files (\*.FLX), Version 1

Variable Name	Type	# Bytes	Description
FLXCode	int	4	File ID Code (=971062)
T0 <sup>(1)</sup>	int	4	Time of first sample
N	int	4	Number of recorded samples
GPSLong	float	4	GPS Longitude
GPSLat	float	4	GPS Latitude
HeaderLen	int	4	Length of following header info in bytes
SetupStr	wide char	2*(string length +1)	null terminated wide character string (each char is coded with 2 bytes), giving the measurement setup name
MWSStr	wide char	2*(string length +1)	null terminated wide character string (each char is coded with 2 bytes), giving the MWS model used
LASStr	wide char	2*(string length +1)	null terminated wide character string (each char is coded with 2 bytes), giving the LAS model used
LASAp	double	8	LAS aperture diameter [m]
MWSAp	double	8	MWS aperture diameter [m]
LASWI	double	8	LAS wavelength [µm]
MWSWI	double	8	LAS wavelength [µm]
zTM	double	8	MWS transmitter height above ground [m]
zRM	double	8	MWS receiver height above ground [m]
zTL	double	8	LAS transmitter height above ground [m]
zRL	double	8	LAS receiver height above ground [m]
yTL	double	8	LAS transmitter lateral displacement [m]
yRL	double	8	LAS receiver lateral displacement [m]
PathOr	double	8	Orientation of signal path relative to north direction [DEG, clock wise]
SurRoughLen	double	8	Surface roughness length [m]
TopoX[]	double	8x10	Topography x-coordinate array, distance from transmitter along path, 10 points (including transmitter coord. X=0)
TopoZ[]	double	8x10	Topography z-coordinate array, GPS altitude of each topography point corresponding to TopoX[]
EffHeight	double	8	Effective height above ground for complete signal path [m]
Gint[]	double	3x8	Integrated spectral density (LAS, MWS, Covariance)
RunMean	int	4	Running mean time for variance calculation [sec]
VarPer	int	4	Variance integration period [sec]



T_1 <sup>(1)</sup>	int	4	Time of sample 1
RF_1	byte	1	Rain flag of sample 1
P_1	float	4	Barometric pressure of sample 1 [hPa]
T_1	float	4	Env. Temp. of sample 1 [K]
H_1	float	4	Rel. Hum. of sample 1 [%]
WS_1	float	4	Wind Speed of sample 1 [km/h]
WD_1	float	4	Wind Direction of sample 1 [DEG]
H_FX_1	float	4	Sensible heat flux of sample 1 [W/m <sup>2</sup> ]
Lat_FX_1	float	4	Latent heat flux of sample 1 [W/m <sup>2</sup> ]
...	...	...	...
...	...	...	...
...	...	...	...
T_N <sup>(1)</sup>	int	4	Time of sample N
RF_N	byte	1	Rain flag of sample N
P_N	float	4	Barometric pressure of sample N [hPa]
T_N	float	4	Env. Temp. of sample N [K]
H_N	float	4	Rel. Hum. of sample N [%]
WS_N	float	4	Wind Speed of sample N [km/h]
WD_N	float	4	Wind Direction of sample N [DEG]
H_FX_N	float	4	Sensible heat flux of sample N [W/m <sup>2</sup> ]
Lat_FX_N	float	4	Latent heat flux of sample N [W/m <sup>2</sup> ]

<sup>(1)</sup> The time is given as the number of seconds since 1.1.2001, 00:00:00

## 5.2 A1b: Heat Flux Files (\*.FLX), Version 2

Variable Name	Type	# Bytes	Description
FLXCode	int	4	File ID Code (=971063)
T0 <sup>(1)</sup>	int	4	Time of first sample
N	int	4	Number of recorded samples
GPSLong	float	4	GPS Longitude
GPSLat	float	4	GPS Latitude
RTQHand	char	1	RTQ handling: 0: method after Lüdi 1: method after Hill
XMost00	float	4	XMost Coefficient: XT1s
XMost01	float	4	XMost Coefficient: XQ1s
XMost02	float	4	XMost Coefficient: XT1u
XMost03	float	4	XMost Coefficient: XQ1u
XMost10	float	4	XMost Coefficient: XT2s
XMost11	float	4	XMost Coefficient: XQ2s
XMost12	float	4	XMost Coefficient: XT2u
XMost13	float	4	XMost Coefficient: XQ2u
HeaderLen	int	4	Length of following header info in bytes



SetupStr	wide char	2*(string length +1)	null terminated wide character string (each char is coded with 2 bytes), giving the measurement setup name
MWSStr	wide char	2*(string length +1)	null terminated wide character string (each char is coded with 2 bytes), giving the MWS model used
LASStr	wide char	2*(string length +1)	null terminated wide character string (each char is coded with 2 bytes), giving the LAS model used
LASAp	double	8	LAS aperture diameter [m]
MWSAp	double	8	MWS aperture diameter [m]
LASWI	double	8	LAS wavelength [µm]
MWSWI	double	8	LAS wavelength [µm]
zTM	double	8	MWS transmitter height above ground [m]
zRM	double	8	MWS receiver height above ground [m]
zTL	double	8	LAS transmitter height above ground [m]
zRL	double	8	LAS receiver height above ground [m]
yTL	double	8	LAS transmitter lateral displacement [m]
yRL	double	8	LAS receiver lateral displacement [m]
PathOr	double	8	Orientation of signal path relative to north direction [DEG, clock wise]
SurRoughLen	double	8	Surface roughness length [m]
TopoX[]	double	8x10	Topography x-coordinate array, distance from transmitter along path, 10 points (including transmitter coord. X=0)
TopoZ[]	double	8x10	Topography z-coordinate array, GPS altitude of each topography point corresponding to TopoX[]
EffHeight	double	8	Effective height above ground for complete signal path [m]
Gint[]	double	3x8	Integrated spectral density (LAS, MWS, Covariance)
RunMean[]	int	2x4	Running mean time for variance calculation [sec]
VarPer	int	4	Variance integration period [sec]
T_1 <sup>(1)</sup>	int	4	Time of sample 1
RF_1	byte	1	Rain flag of sample 1
P_1	float	4	Barometric pressure of sample 1 [hPa]
T_1	float	4	Env. Temp. of sample 1 [K]
H_1	float	4	Rel. Hum. of sample 1 [%]
WS_1	float	4	Wind Speed of sample 1 [km/h]
WD_1	float	4	Wind Direction of sample 1 [DEG]
Sat_1	char	1	Scintillometer saturation sample 1 Bit 1: LAS (1 = saturated, 0 = not sat.) Bit 2: MWS (1 = saturated, 0 = not sat.)



H_FX_1	float	4	Sensible heat flux of sample 1 [W/m <sup>2</sup> ]
Lat_FX_1	float	4	Latent heat flux of sample 1 [W/m <sup>2</sup> ]
Ev_Tr_1	float	4	Evapo-Transpiration of sample 1 [mm/h] or [Ltr/m <sup>2</sup> h]
...	...	...	...
...	...	...	...
...	...	...	...
T_N <sup>(1)</sup>	int	4	Time of sample N
RF_N	byte	1	Rain flag of sample N
P_N	float	4	Barometric pressure of sample N [hPa]
T_N	float	4	Env. Temp. of sample N [K]
H_N	float	4	Rel. Hum. of sample N [%]
WS_N	float	4	Wind Speed of sample N [km/h]
WD_N	float	4	Wind Direction of sample N [DEG]
Sat_N	char	1	Scintillometer saturation sample N Bit 1: LAS (1 = saturated, 0 = not sat.) Bit 2: MWS (1 = saturated, 0 = not sat.)
H_FX_N	float	4	Sensible heat flux of sample N [W/m <sup>2</sup> ]
Lat_FX_N	float	4	Latent heat flux of sample N [W/m <sup>2</sup> ]
Ev_Tr_N	float	4	Evapo-Transpiration of sample N [mm/h] or [Ltr/m <sup>2</sup> h]

<sup>(1)</sup> The time is given as the number of seconds since 1.1.2001, 00:00:00

### 5.3 A2: Variance-Files (\*.VAR)

Variable Name	Type	# Bytes	Description
VARCode	int	4	File ID Code (=601832)
T0 <sup>(1)</sup>	int	4	Time of first sample
N	int	4	Number of recorded samples
GPSLong	float	4	GPS Longitude
GPSLat	float	4	GPS Latitude
HeaderLen	int	4	Length of following header info in bytes
SetupStr	wide char	2*(string length +1)	null terminated wide character string (each char is coded with 2 bytes), giving the measurement setup name
MWSStr	wide char	2*(string length +1)	null terminated wide character string (each char is coded with 2 bytes), giving the MWS model used
LASStr	wide char	2*(string length +1)	null terminated wide character string (each char is coded with 2 bytes), giving the LAS model used
LASAp	double	8	LAS aperture diameter [m]
MWSAp	double	8	MWS aperture diameter [m]
LASWI	double	8	LAS wavelength [µm]
MWSWI	double	8	LAS wavelength [µm]



zTM	double	8	MWS transmitter height above ground [m]
zRM	double	8	MWS receiver height above ground [m]
zTL	double	8	LAS transmitter height above ground [m]
zRL	double	8	LAS receiver height above ground [m]
yTL	double	8	LAS transmitter lateral displacement [m]
yRL	double	8	LAS receiver lateral displacement [m]
PathOr	double	8	Orientation of signal path relative to north direction [DEG, clock wise]
SurRoughLen	double	8	Surface roughness length [m]
TopoX[]	double	8x10	Topography x-coordinate array, distance from transmitter along path, 10 points (including transmitter coord. X=0)
TopoZ[]	double	8x10	Topography z-coordinate array, GPS altitude of each topography point corresponding to TopoX[]
EffHeight	double	8	Effective height above ground for complete signal path [m]
Gint[]	double	3x8	Integrated spectral density (LAS, MWS, Covariance)
RunMean[]	int	2x4	Running mean time for variance calculation [sec]
VarPer	int	4	Variance integration period [sec]
T_1 <sup>(1)</sup>	int	4	Time of sample 1
RF_1	byte	1	Rain flag of sample 1
P_1	float	4	Barometric pressure of sample 1 [hPa]
T_1	float	4	Env. Temp. of sample 1 [K]
H_1	float	4	Rel. Hum. of sample 1 [%]
WS_1	float	4	Wind Speed of sample 1 [km/h]
WD_1	float	4	Wind Direction of sample 1 [DEG]
LAS_VAR_1	double	8	LAS variance of sample 1
MWS_VAR_1	double	8	MWS variance of sample 1
COV_VAR_1	double	8	Covariance of sample 1
...	...	...	...
...	...	...	...
...	...	...	...
T_N <sup>(1)</sup>	int	4	Time of sample N
RF_N	byte	1	Rain flag of sample N
P_N	float	4	Barometric pressure of sample N [hPa]
T_N	float	4	Env. Temp. of sample N [K]
H_N	float	4	Rel. Hum. of sample N [%]
WS_N	float	4	Wind Speed of sample N [km/h]
WD_N	float	4	Wind Direction of sample N [DEG]
LAS_VAR_N	double	8	LAS variance of sample N
MWS_VAR_N	double	8	MWS variance of sample N
COV_VAR_N	double	8	Covariance of sample N

<sup>(1)</sup> The time is given as the number of seconds since 1.1.2001, 00:00:00



### 5.4 A3: Raw Data Files (\*.RAW)

Variable Name	Type	# Bytes	Description
RAWCode	int	4	File ID Code (=294001)
T0 <sup>(1)</sup>	int	4	Time of first sample
N	int	4	Number of recorded samples
GPSLong	float	4	GPS Longitude
GPSLat	float	4	GPS Latitude
HeaderLen	int	4	Length of following header info in bytes
SetupStr	wide char	2*(string length +1)	null terminated wide character string (each char is coded with 2 bytes), giving the measurement setup name
MWSStr	wide char	2*(string length +1)	null terminated wide character string (each char is coded with 2 bytes), giving the MWS model used
LASStr	wide char	2*(string length +1)	null terminated wide character string (each char is coded with 2 bytes), giving the LAS model used
LASAp	double	8	LAS aperture diameter [m]
MWSAp	double	8	MWS aperture diameter [m]
LASWI	double	8	LAS wavelength [µm]
MWSWI	double	8	LAS wavelength [µm]
zTM	double	8	MWS transmitter height above ground [m]
zRM	double	8	MWS receiver height above ground [m]
zTL	double	8	LAS transmitter height above ground [m]
zRL	double	8	LAS receiver height above ground [m]
yTL	double	8	LAS transmitter lateral displacement [m]
yRL	double	8	LAS receiver lateral displacement [m]
PathOr	double	8	Orientation of signal path relative to north direction [DEG, clock wise]
SurRoughLen	double	8	Surface roughness length [m]
TopoX[]	double	8x10	Topography x-coordinate array, distance from transmitter along path, 10 points (including transmitter coord. X=0)
TopoZ[]	double	8x10	Topography z-coordinate array, GPS altitude of each topography point corresponding to TopoX[]
EffHeight	double	8	Effective height above ground for complete signal path [m]
Gint[]	double	3x8	Integrated spectral density (LAS, MWS, Covariance)
RunMean[]	int	2x4	Running mean time for variance calculation [sec] (has no effect here)
VarPer	int	4	Variance integration period [sec] (has no effect here)
DualAp	char	1	Dual aperture flag. 1: dual aperture, 0: single aperture



T_1 <sup>(1)</sup>	int	4	Time of sample 1
RF_1	byte	1	Rain flag of sample 1
P_1	float	4	Barometric pressure of sample 1 [hPa]
T_1	float	4	Env. Temp. of sample 1 [K]
H_1	float	4	Rel. Hum. of sample 1 [%]
WS_1	float	4	Wind Speed of sample 1 [km/h]
WD_1	float	4	Wind Direction of sample 1 [DEG]
LAS1[ ]_1	float	1000x4	Array of 1000 LAS voltage samples in 1 ms resolution of sample 1 (aperture 1)
LAS2[ ]_1 <sup>(2)</sup>	float	1000x4	Array of 1000 LAS voltage samples in 1 ms resolution of sample 1 (aperture 2)
MWS [ ]_1	float	1000x4	Array of 1000 MWS voltage samples in 1 ms resolution of sample 1
...	...	...	...
...	...	...	...
...	...	...	...
T_N <sup>(1)</sup>	int	4	Time of sample N
RF_N	byte	1	Rain flag of sample N
P_N	float	4	Barometric pressure of sample N [hPa]
T_N	float	4	Env. Temp. of sample N [K]
H_N	float	4	Rel. Hum. of sample N [%]
WS_N	float	4	Wind Speed of sample N [km/h]
WD_N	float	4	Wind Direction of sample N [DEG]
LAS1[ ]_N	float	1000x4	Array of 1000 LAS voltage samples in 1 ms resolution of sample N
LAS2[ ]_N <sup>(2)</sup>	float	1000x4	Array of 1000 LAS voltage samples in 1 ms resolution of sample N (aperture 2)
MWS [ ]_N	float	1000x4	Array of 1000 MWS voltage samples in 1 ms resolution of sample N

<sup>(1)</sup> The time is given as the number of seconds since 1.1.2001, 00:00:00

<sup>(2)</sup> only if 'DualAp' = 1

## 5.5 A4: Housekeeping Data Files (\*.HKD)

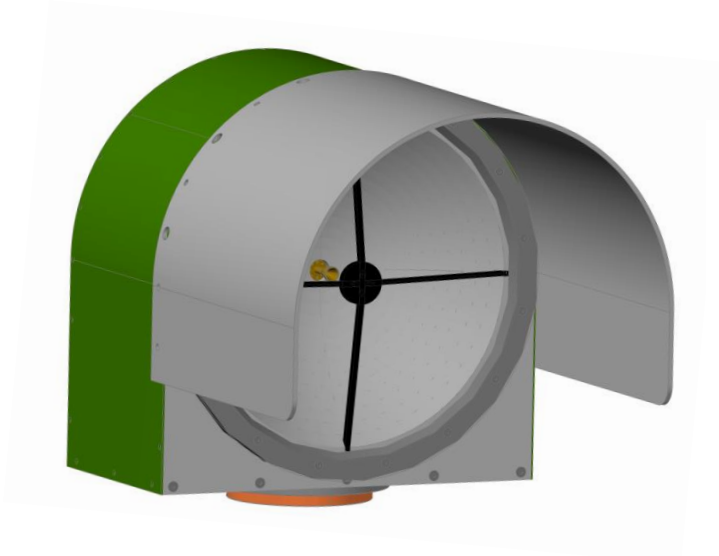
Variable Name	Type	# Bytes	Description
HKDCode	int	4	File ID Code (=5093871)
T0 <sup>(1)</sup>	int	4	Time of first sample
N	int	4	Number of recorded samples
GPSLong	float	4	GPS Longitude
GPSLat	float	4	GPS Latitude
HeaderLen	int	4	Length of following header info in bytes (here zero)
T_1 <sup>(1)</sup>	int	4	Time of sample 1
AGC_1	float	4	AGC voltage [V] (receiver LO) of sample 1
Pow_1	float	4	Total power consumption [W] of sample 1



PID_1	float	4	PID regulator voltage [V] of sample 1
Trec_1	float	4	Receiver temperature [K] of sample 1
RFV_1	float	4	RF supply voltage [V] of sample 1, 4.4V
OPA1_1	float	4	OPA1 voltage [V] of sample 1, +8V
OPA2_1	float	4	OPA1 voltage [V] of sample 1, -8V
GSV_1	float	4	General supply voltage [V] of sample 1, +12V
Stab_1	float	4	Thermal receiver stability [K] of sample 1
...	...	...	...
...	...	...	...
...	...	...	...
T_N <sup>(1)</sup>	int	4	Time of sample N
AGC_N	float	4	AGC voltage [V] (receiver LO) of sample N
Pow_N	float	4	Total power consumption [W] of sample N
PID_N	float	4	PID regulator voltage [V] of sample N
Trec_N	float	4	Receiver temperature [K] of sample N
RFV_N	float	4	RF supply voltage [V] of sample N, 4.4V
OPA1_N	float	4	OPA1 voltage [V] of sample N, +8V
OPA2_N	float	4	OPA1 voltage [V] of sample N, -8V
GSV_N	float	4	General supply voltage [V] of sample N, +12V

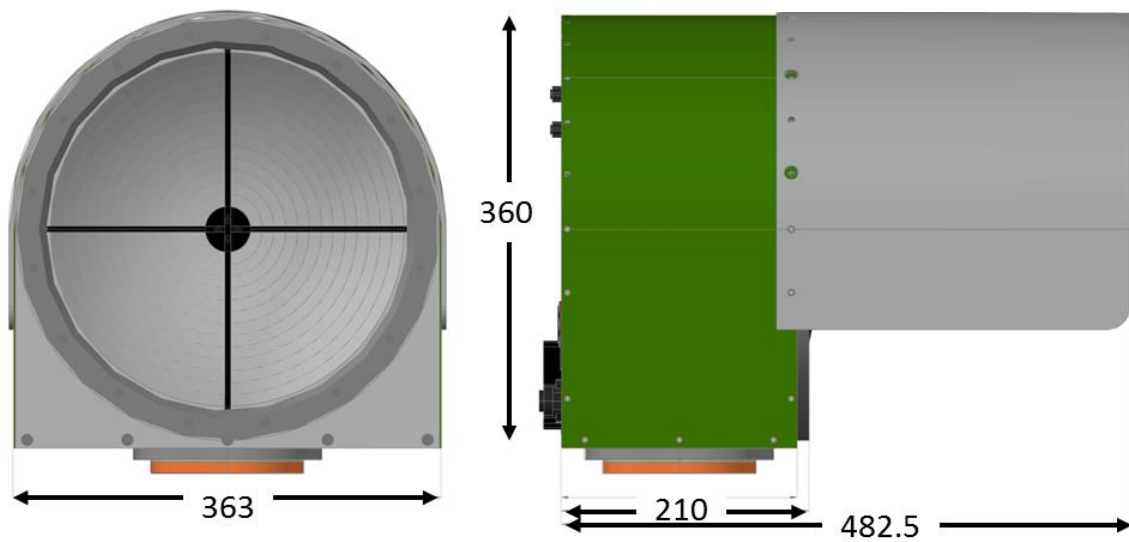
<sup>(1)</sup> The time is given as the number of seconds since 1.1.2001, 00:00:00

## 6. Appendix B (Instrument Dimensions)



**Total weights:**

- Receiver: **12 kg**  
(including weather station)
- Transmitter: **10 kg**



in mm